Ministry for Primary Industries
Manatū Ahu Matua

The potential impact of ocean acidification on deep-sea corals and fisheries habitat in New Zealand waters

D. Tracey
H. Bostock
K. Currie
S. Mikaloff-Fletcher
M. Williams
M. Hadfield
H. Neil
C. Guy
V. Cummings

New Zealand Government

Growing and Protecting New Zealand

Requests for further copies should be directed to:

Publications Logistics Officer
Ministry for Primary Industries
PO Box 2526
WELLINGTON 6140

Email: brand@mpi.govt.nz
Telephone: 0800 00 83 33
Facsimile: 04-894 0300

This publication is also available on the Ministry for Primary Industries websites at:
http://www.mpi.govt.nz/news-resources/publications.aspx
http://fs.fish.govt.nz go to Document library/Research reports

© Crown Copyright - Ministry for Primary Industries

TABLE OF CONTENTS

EXECUTIVE SUMMARY

Substantial shifts in the chemistry of the oceans driven by anthropogenic CO_2 have occurred in recent times resulting in a significant decrease in seawater pH and an increase in the average ocean acidity. This phenomenon termed ocean acidification (OA) causes the reduction of seawater carbonate concentrations and there is evidence to show that it will have a significant effect on organisms that have calcium carbonate shells and exoskeletons such as corals and the diverse fauna associated with them, including fish and fish populations. This research project aimed to provide some baseline data on the influence of carbonate availability on the current deep-sea coral distribution and associated fisheries habitat in New Zealand waters, in order to determine whether these important deep-sea habitat forming carbonate organisms may be affected by future ocean acidification.

This two year project addressed several different components of OA including describing the spatial and depth distributions of selected habitat forming deep-sea corals, analysing the carbonate mineralogy of the corals, improving maps of the carbonate concentrations and the aragonite and calcite saturation states for the South West Pacific, and comparing these data with both present day carbonate chemistry and published future OA predictions for the region. A literature review was undertaken to determine the most appropriate tools to age deepsea corals to measure the effects of OA and other stressors onthis group, and a feasibility study to keep deepsea corals alive in aquaria was carried out. Each of these project activities are addressed in separate chapters in this report.

The branching stony coral species (Order: Scleractinia) *Goniocorella dumosa*, *Solenosmilia variabilis*, *Enallopsammia rostrata*, *Madrepora oculata*, and the endemic *Oculina virgosa*, and the gorgonian corals (Order: Alcyonacea) *Keratoisis* spp., *Lepidisis* spp., *Paragorgia* spp. and *Primnoa* sp., data show an overall broad spatial distribution, but individual species display regional and depth variations. Peak depth distributions are at around 800–1000 m for most of the species and genera listed above, but *G. dumosa*, *E. rostrata*, and *Lepidisis* spp. show bimodal distributions with a second shallower peak at 400–600 m and *O. virgosa* occurs primarily in shallow depths (0–200 m).

The mineralogy of the study corals was analysed. The five branching scleractinian coral skeletons are aragonitic, while the gorgonian corals *Keratoisis* spp., *Lepidisis* spp. and *Paragorgia* spp. have high magnesium (Mg) calcite skeletons (8–11 mol% $MgCO_3$). The high Mg content of the calcite increases the solubility of the coral carbonate skeleton. The gorgonian *Primnoa sp.* is a bimineralic species, with a skeleton made up of a number of different layers of both aragonite and Mg calcite.

To improve our knowledge of the ocean carbonate concentrations for the New Zealand region a multiple linear regression (MLR) was developed between the carbonate parameters and hydrographic data at a few stations. These algorithms were then used with ocean climatologies to provide detailed maps of the carbonate saturation horizons for aragonite and calcite (ASH and CSH respectively). Saturation horizons are the depth at which these carbonate minerals start to dissolve. The ASH was found to sit between 1000 and 1250 m water depth in the New Zealand EEZ, while the CSH sits between 2800 and 3100 m. Opportunistic water sampling was undertaken on NIWA voyages to measure alkalinity and dissolved inorganic carbon (DIC) within the New Zealand EEZ to ground truth these new detailed maps of ASH and CSH.

As well as the uptake of anthropogenic CO_2 from the atmosphere, OA in surface waters can also be exacerbated by the upwelling of old, high DIC waters. To test whether this was likely in the New Zealand region the Regional Ocean Models (ROMS) were coupled to the Pelagic Interaction Scheme for Carbon and Ecosystem Studies (PISCES) ocean biogeochemistry model to investigate the mean, amplitude and standard deviation of DIC at four key fishery depths: 200 m, 500 m, 750 m and 1250

m. We found no evidence of physically induced amplification of ocean acidification in the New Zealand EEZ from upwelling.

The deep-sea coral distribution data were compared with current and predicted ASH for 2100. Results show that about 90% of the scleractinian and 83% of the gorgonian corals in the New Zealand region are currently living in above the ASH. This suggests that the carbonate saturation state has a strong control on the depth distribution of both groups of these habitat-forming corals. Global climate models in New Zealand waters suggest that the ASH will shoal dramatically to 600 m by the end of the 21st Century and this will significantly reduce the habitat available for these deep-sea corals. Only the continental shelf, the top of Chatham Rise, small regions of the Campbell Plateau and the Kermadec and Macquarie Ridge seamounts will remain above the ASH, and so potentially represent the only areas that will still support deepsea corals. Areas below the predicted ASH at end of century may be important fisheries areas and the information in this study suggests where future refugia might be for certain species which in turn can inform potential protected area decisions.

A literature review determined the most appropriate tools to age, and measure the effects of OA on habitat-forming, deep-sea corals, summarised growth and longevity data for corals in the region, and recommended growth studies to help define calcification rates that may be non-linear and affected by several environmental and physiological factors. Calcification rates are indicated to decrease with increasing age, with longer term calcification rate studies suggesting that deepsea corals are able to maintain constant calcification rates until a dissolution threshold, or critical tipping point, is reached. Opportunistic at-sea sampling of live corals was undertaken and the corals were kept alive in the aquaria for several months, indicating the feasibility of undertaking these kind of manipulative experiments on deep-sea corals in the laboratory.

This work provides some baseline data of the potential impact OA may have on deepsea habitat forming corals. We recommend future research to further understand the effects on different coral species and the impacts on deep water fisheries. These include the need to further investigate the relationship between deep-sea corals and fisheries, investigate variations in coral mineralogy composition, and continue to carry out water sampling for alkalinity and DIC to improve our carbonate maps of the New Zealand region. The new improved global climate model predictions for OA can help to identify potential refugia for deep-sea corals. In-aquaria, multiple stressor experiments to determine how these deep-sea corals might tolerate and respond to future climate change are required.

This Final Report presents results for the June 2013 reporting requirements, Contract Milestones 3, 6, 9. Project title: Ocean Acidification in Fisheries Habitat. The project objectives are consistent with the Fisheries Resources goal in the Ministry of Fisheries Strategic Research Directions document. Specifically the research addresses Strategic Directions 5 and 7 for BTMR 2007-2102 (5) *'To determine the effects of climate change and increased ocean acidification on marine biodiversity'*.

Chapter 1: INTRODUCTION

Atmospheric CO_2 concentrations have increased substantially since the industrial revolution and approximately 25–30% of anthropogenic CO_2 emissions have been absorbed by the world's oceans (Canadell et al. 2007; Gruber et al. 2009). This has resulted in a significant decrease in seawater pH over this same time period, and as a result the average ocean acidity is now 30% higher than in the 1700s (Feely et al. 2008). This phenomenon, termed 'ocean acidification', represents a potential risk to the functioning of New Zealand's marine ecosystems and the services that those ecosystems provide, including the support of nationally important fisheries.

Changes in the ocean's acidity is expected to affect the structure and function of a wide variety of fauna and flora (e.g., Fabry et al. 2008). Organisms may be impacted by changes in the availability of seawater carbonate required for development and maintenance of skeletal structures (e.g., Doney et al. 2009;

Riebesell et al. 2000), and their acid-base balance, and thus physiological functions such as respiration, circulation, and metabolism, are also likely to be affected (e.g., Fabry et al. 2008).

1.1   The Ocean Carbonate System

Atmospheric CO_2 equilibrates with the surface waters via air-sea gas exchange. Once the CO_2 is dissolved in the surface waters it reacts with the water to form carbonic acid (H_2CO_3), which then dissociates – losing hydrogen ions (H^+) – to form bicarbonate (HCO_3^-) and carbonate (CO_3^{2-}) ions. Adding more CO_2 to the seawater increases the concentrations of HCO_3^- and H^+, the latter resulting in a decrease in pH ($pH=-log_{10}[H^+]$), and concentrations of CO_3^{2-}. The surface ocean pH has decreased by 0.1 since preindustrial times and carbonate ions have decreased by 20%. Global ocean carbon models project that the pH will decrease by 0.3–0.4 by the end of the century and CO_3^{2-} by 50% (Orr et al. 2005).

Many marine organisms use calcium carbonate ($CaCO_3$) to build their skeletons. The majority of these organisms are thought to use the CO_3^{2-} to build these (although some have recently been found to use HCO_3^- or a combination of the two). Declining CO_3^{2-} concentrations and saturation states will make it harder for these organisms to secrete and maintain their skeletons.

Saturation states are dependent on the solubility of the mineral, which varies with temperature, salinity, pressure and the mineral phase. There are three main calcium carbonate ($CaCO_3$) minerals found in nature: calcite, aragonite and high Mg calcite. Aragonite is 50% more soluble than calcite (Mucci 1983), while high Mg calcite solubility is dependent on the amount of Mg (Walter & Morse 1984). As Ca^{2+} is fairly constant in the oceans and directly proportional to salinity, the saturation state (Ω) is controlled by the amount of CO_3^{2-}. The CO_3^{2-} concentration cannot be measured directly in the seawater (at least not yet), but it can be calculated from measurements of total alkalinity and dissolved inorganic carbon (DIC).

If $\Omega>1$, the ocean is supersaturated with respect to the mineral, and if $\Omega<1$, then the water is undersaturated and the mineral will start to dissolve. The depth at which $\Omega=1$ is termed the saturation horizon. The aragonite saturation horizon (ASH) is significantly shallower than the calcite saturation horizon (CSH), due to the increased solubility of aragonite.

Carbonate is more soluble at lower temperatures and higher pressures, and thus high latitudes and deep waters are likely to be significantly affected by future ocean acidification (Orr et al. 2005; Doney et al. 2009). Cold, deep waters also have lower CO_3^{2-} concentrations, and consequently, in areas of upwelling of such waters OA could be exacerbated (Feely et al. 2008).

1.2   Deepsea habitat-forming corals

Deepsea corals are found most commonly between about 200 and 2000 m water depth and at temperatures between 4°C and 12°C (Freiwald et al. 2004). However, *Lophelia* and other cold-water coral groups (e.g., *Desmophyllum* and *Primnoa*) have been observed as shallow as 2 metres in the fjords when environmental conditions are favourable, and with some frequency in waters less than 200 metres deep (Etnoyer & Morgan 2005; Grange et al. 1981; Häussermann & Försterra 2007). The dark and calm fiord environment allow many marine species which are usually restricted to deep water (more than l00 m) to flourish in shallow water (less than 50 m) More than 10 000 deepsea and or cold water species are known worldwide (Roberts et al. 2009).

The New Zealand region supports a very diverse coral fauna (Cairns 1995; Cairns 2012), with the majority of records being the calcifying, framework-forming reef corals (scleractinians, or branching stony corals from the families Caryophylliidae, Dendrophyllidae and Oculinidae). Deepwater stony corals are widely distributed throughout the New Zealand region (Cairns 1995; Tracey et al. 2011a).

The New Zealand fiords support deep-water emergent species including antipatharian black corals and stylasterid hydrocorals (e.g., *Errina* spp.), (Grange et al. 1981; 1985).

Some stony coral species produce 3-dimensional matrix colonies that form 'reef', 'mound' or 'thicket' structures, and thus provide biogenic habitat on slope margins, ridges and seamounts (Mortensen & Buhl-Mortensen 2004; Auster et al. 2005; Reveillaud et al. 2008; Roberts et al. 2008; Henry & Roberts 2008; Rogers et al. 2007; Wheeler et al. 2007). These structures can be large (e.g., 14 km long x 35 m high; Sula Ridge *Lophelia pertusa*; Huehnerbach et al. 2007), and are often associated with high concentrations of fish and invertebrates (McCloskey 1970; Jensen & Frederikson 1992 ; Husebø et al. 2002; Costello et al. 2005; Stone 2006; Moore et al. 2008; Soffker, et al. 2011).

Gorgonian corals are also an abundant calcifying group represented in the New Zealand region and include: bubblegum corals (Paragorgidae), primnoid sea fan, sea whip corals (Primnoidae), and bamboo corals (Isididae), as well as stylasterid hydrocorals (Hydroida). All of these groups, along with the black corals (Antipatharia), are protected under the New Zealand Department of Conservation Wildlife Act 2010 (amendment of Schedule 7A of the Wildlife Act 1953). The Order Gorgonacea has recently been revised and all gorgonians are now in the Order Alcyonacea. Gorgonians, like certain stony corals, have tree-like forms (Cairns 2012), and are also important habitat forming species (Buhl-Mortensen & Mortensen 2005).

The spatial variability of the protected deepsea corals is reasonably well known for the New Zealand region (Tracey et al. 2011a &b; Baird et al. 2013). Depth and location relative to a seamount are consistently identified as important factors influencing the probability of occurrence of five species of branching stony corals (in Order Scleractinia) in the New Zealand region (Tracey et al. 2011a). Tracey et al. (2011b) analysed the distribution of nine groups of protected corals based on bycatch records from observed trawl effort for 2007–10. Most coral catches were from 800–1200 m. Estimated catches were highest where fishing effort took place on features such as seamounts on the Chatham Rise, West Norfolk Ridge in northwestern waters of the EEZ, east of the Pukaki Rise, and on the Macquarie Ridge. Baird et al. (2013) further added to the knowledge of the distribution of protected corals by using data from research sampling and commercial fishing effort where observers had been present. Distributions of the protected corals within the EEZ were mapped by their structural differences and the potential biogenic habitat that they provide ("tree-like" e.g., bubblegum corals; "reef-like", e.g. the stony branching corals, "solitary small" e.g., the scleractinian cup corals, and "whip-like", e.g., bamboo coral *Lepidisis* spp.).

1.3   Deep-water fisheries and coral habitat

It is widely recognised that there is need for information on the interaction between fish and deep-sea coral habitats in order to assist in ecosystem-based management in the deep sea (e.g., Clark & Dunn 2012), and some initiatives are helping to address this understanding (see European Union project CoralFISH (http://ec.europa.eu/research/environment/pdf/project_summaries/fp7/marine_environment/coralfish.pdf).

Deepsea fish are seen on, or in close proximity to, stony and other habitat forming corals (Purser et al. 2013) such as members of the gorgonian group, using them as a refuge or shelter and feeding on corals or animals associated with them. Large aggregations of commercial species can occur above seamounts that support high coral densities, but direct linkages between the fish and corals are often uncertain. Some recent work has described associations of commercial fish species with essential habitat. Over a two year period, Fosså et al. (2012) looked at the associations and functional links between tusk (*Brosme brosme*), a fish of the ling family, and cold-water coral and sponge habitats. In both years, the catch per unit of effort (CPUE) of tusk was highest in the most complex habitat (high density of cold-water corals and sponges) and lowest in the unstructured sea-bed habitat on the adjacent continental plain. However, the variability of CPUE in replicate lines and plots was high and

no statistically significant differences in tusk abundance in different habitats were found. Tusk is a top predator and is potentially energetically linked to the coral reefs where there are enhanced feeding possibilities due to a higher abundance of the squat lobster (*Munida sarsii*), its main prey item.

D'Onghia et al. (2010) found that adult rockfish and sea bream use coral banks in an area of the Mediterranean as a refuge, with higher abundance of large-sized fish. However, more striking were the densities of juvenile deep-water shark, hake, blue whiting, cod and rockfish species, which all appear to use the coral as a nursery ground. Off Ireland, a small cod (*Guttigadus*) was observed in greater abundance over complex coral grounds than adjacent flat areas (Soffker et al. 2011), a similar result to that reported by Fosså et al. (2012). Some fish species also showed higher abundance levels over the reef areas. Baillon et al. (2012) reported hundreds of fish larvae amongst soft corals and sea pens collected from deep waters off Newfoundland, showing that corals provide a nursery for these fish larvae. Biber et al. (2013) found no overall statistically significant difference in fish abundance and biomass in coral framework habitats compared to non-coral areas, however, the relationship between fish and coral framework actually varied among fish species and study site (Biber et al. 2013), highlighting the need for more investigation.

1.4 Risk to protected corals from New Zealand fisheries

Information on the distribution of corals within New Zealand waters comes from dedicated sampling during biodiversity surveys, opportunistic sampling from other research surveys including trawl surveys, and observed commercial fishing. The latter fishery-dependent information reported by government observers has improved in recent years since the use of invertebrate guides and the introduction in October 2007 of added data collection directed at benthic bycatch, including corals.

Protected coral catches in the New Zealand region that are monitored on commercial vessels have been summarised by Ramm (2012 a b), Tracey et al. (2011a), Baird et al. (2013). Areas where deep sea corals species are at highest risk of interactions with commercial fishing gear have been identified and mapped and the likely coral distributions using predictive models presented (Baird et al. 2013). This research showed that the fisheries that pose the most risk to protected corals are the deep water trawl fisheries for species such as orange roughy (*Hoplostethus atlanticus*), black oreo (*Allocyttus niger*), smooth oreo (*Pseudocyttus maculatus*), black cardinalfish (*Epigonus telescopus*), and alfonsino (*Beryx* spp.). In shallower waters, scampi (*Metanephrops challengeri*) trawl fisheries in 300–500 m appear to pose the greatest risk to corals in all of the protected Orders. Bottom long-line fisheries pose a risk to those corals that have a branching or bushy structure. Set-net fisheries may pose a risk in areas of hard substrate.

1.5   Ocean acidification and deepsea corals

Coral structures are often fragile and hence vulnerable to both physical disturbance with recovery from physical damage appearing to be slow (e.g., Clark & Rowden 2009; Williams et al. 2010), and also potentially susceptible to ocean warming and ocean acidification. In the latter case, the expected changes in seawater concentrations of the available carbonate ions required for coral skeleton generation are predicted to affect coral distribution by impacting their calcification ability (Caldeira & Wickett 2003; Turley et al. 2007; Maier et al. 2009), and potentially on their health and survival through skeleton dissolution (Fine & Tchernov 2007) and effects on physiological processes (Buckley & Szmant 2004; Naumann et al. 2013). The strong dependency of coral distribution on the availability of aragonite and calcite is noteworthy. Hence a reduction in the availability of carbonate ions through acidification of the oceans will potentially limit the ability of stony and gorgonian corals to form their hard skeletons and, therefore, affect the amount of suitable biogenic habitat they provide for other marine organisms, including fish.

The aragonite saturation horizon (ASH) is considered to be a primary control on the global spatial and depth distributions of habitat-building scleractinian corals, with 95% found in depths above the ASH (Guinotte et al. 2006). In the North Atlantic, the ASH is more than 2000 m deep and scleractinians are found down to these depths, forming extensive reefs in some regions (Huehnerbach et al. 2007). In comparison, surveys in the North Pacific, where the ASH is very shallow (100–200 m), have not found any evidence of extensive deep-sea scleractinian reefs (Guinotte et al. 2006). Instead the North Pacific, is dominated by habitat-forming, deep-sea gorgonian corals (Bryan & Metaxas 2006; Yesson et al. 2012). Understanding deep-sea coral mineralogy is key to assessing their susceptibility to ocean acidification, with aragonitic and high Mg calcite (8–12mol% $MgCO_3$) corals likely to be the most vulnerable.

Given the present evidence of acidification of the oceans, undersaturation of seawater carbonate concentrations has significant implications for the global distribution of deep-sea corals and coral reefs (Turley et al. 2007; Royal Society 2005) and the diverse fauna associated with them. Carbonate saturation horizons have already shoaled over the last century (Feely et al. 2004) and global ocean carbon models suggest that they will continue to shoal significantly by 2100 (Orr et al. 2005). For example, seamounts along the south coast of Australia which are covered by cold-water reefs, comprising the branching scleractinian coral *S. variabilis,* and support high biodiversity, will become undersaturated with respect to aragonite under a "business-as-usual" scenario for CO_2 emissions (IPCC 2007) in the next 50–100 years (Poloczanka et al. 2007). This undersaturation will potentially cause the disappearance of many of these deep-sea reefs. A more recent study in the South Australian region, which combines models for ocean acidification and temperature changes, suggests that there will be little, if any, suitable habitat for the *S. variabilis* remaining by 2100 (Ron Thresher (CSIRO), pers. comm.) Global habitat models of Tittensor et al. (2010) predict that suitable deep-sea coral habitat will be particularly reduced in the New Zealand region.

1.6   Purpose

Little is known about the impacts of ocean acidification on cold water (deep sea) coral-associated fish and other species (Turley et al. 2007). Given the importance of the association between coral habitat and some of New Zealand's key deep water fisheries (e.g., orange roughy, black oreo, smooth oreo, and black cardinalfish; Baird et al. 2013), determining the relationships between the present distributions of key habitat-forming species with respect to current and predicted ASH and CSH is paramount to assessing both the vulnerability of deepsea corals to future change as well as the potential impact of OA in general on New Zealand's deep sea biodiversity.

Objectives

To assess the risks of ocean acidification to deep-sea corals and deep-water fishery habitat.

Specific Objectives:

1. To determine the carbonate mineralogy of selected deep-sea corals found in the New Zealand region.

2. To assess the distribution of deep-sea coral species in the New Zealand region relative to improved knowledge of current and predicted aragonite (ASH) and calcite saturation horizons (CSH), assessment of potential locations vulnerable to deep-water upwelling and areas of key deep-water fishery habitat.

3. Through a literature search and analysis, determine the most appropriate tools to age and measure the effects of ocean acidification on deep-sea, habitat-forming corals, and recommend the best approach for future assessments of the direct effects of changes in ocean pH on these key fauna.

The project has strong synergies with several research streams and was completed with support from other biodiversity, ecosystem, and oceanographic research programmes supported not only by MPI but by the Department of Conservation (DOC), the Ministry of Business Innovation and Employment (MBIE), and NIWA core funding. There are a large number of recommendations for future work to help understand and help manage the impacts of climate change, in general, and ocean acidification, in particular

Chapter 2: CORAL SPECIES DISTRIBUTION

Di Tracey, Helen Bostock (NIWA)

2.1. Coral species

The selected deep-sea coral groups in this study are listed in Table 2.1, and comprise five species of the reef-like scleractinian stony branching corals (Figure 2.1) and members of the gorgonian tree-like coral group (Figure 2.2). Both these groups build their skeletons out of calcium carbonate and are potentially vulnerable to future ocean acidification (Section 3). The protected coral dataset produced by Baird et al. (2013) for the EEZ (7731 records), was used to map the distributions of the scleractinian and gorgonian coral species selected for this study.

Table 2.1: Deep-sea coral species selected for the study.

Order	Family	Genera and species
Scleractinia (stony branching corals)	Caryophyllidae	*Goniocorella dumosa*
	Caryophyllidae	*Solenosmilia variabilis*
	Dendrophyllidae	*Enallopsammia rostrata*
	Oculinidae	*Madrepora oculata*
	Oculinidae	*Oculina virgosa*
Alyconacea (gorgonian corals)	Isididae	*Keratoisis* spp.
	Isididae	*Lepidisis* spp.
	Paragorgidae	*Paragorgia* spp.
	Primnoidae	*Primnoa sp.*

Figure 2.1: Scleractinian stony branching coral study species (Top L to R) *Goniocorella dumosa*, *Solenosmilia variabilis*, *Enallopsammia rostrata*, **(Bottom L to R)** *Madrepora oculata*, **and the endemic** *Oculina virgosa*.

Figure 2.2: Gorgonian coral study species (Top L to R) *Keratoisis* **spp.,** *Lepidisis* **spp. (bamboo corals) (Bottom L to R)** *Paragorgia* **spp. (bubblegum coral) and** *Primnoa sp*. **(Primnoid sea fan).**

2.2   Association of fisheries with deep sea corals

In the New Zealand region, there have been no studies to quantify the association of fish species with biogenic habitat such as the 3-D habitat forming stony branching corals (Order: Scleractinia). However a strong correlation exists between the location of commercially important deep-sea fish species, habitat forming corals, and seamounts (e.g., Clark 1999; Tracey et al. 2011a; Baird et al. 2013). New Zealand's major deep-sea fisheries include orange roughy, black oreo, smooth oreo, and black cardinalfish. These species tend to be abundant on seamounts (Clark & O'Driscoll 2003), which also host high densities of scleractinian stony and some gorgonian corals (Clark & Tittensor 2010; Tracey et al. 2011a). This association between deep-sea corals and fishes has not been directly attributed to the use of the corals as habitat by the fish species. Nevertheless, seamounts tend to be areas of high food availability due to the dynamic oceanographic environment, and coral habitat on seamounts is also used by a variety of invertebrates which may themselves be a food source for the fish (Buhl-Mortensen & Mortensen 2005; Stone 2006; Moore et al. 2008). Consequently, any impact on the distribution and abundance of coral habitat may have implications for New Zealand's biodiversity and potentially on our key deep-sea fisheries.

We define deep-water fisheries as those located at depths greater than 700 m and based on the management (fish stock) boundaries and main fisheries catches for deep-sea fish, such as orange roughy and oreos, in the New Zealand EEZ. (Anderson & Dunn 2007; Anderson 2011). Several of the fisheries are associated with seamounts and other underwater topographical features where deep-sea corals are often (but not always) located. The regions do not strictly link to the Ministry of Primary Industries (MPI) distinct Fisheries Management Areas (FMAs), nor to the species specific Quota Management Areas (QMAs) which are different for each species (Ministry for Primary Industries 2012), but instead were chosen due to their distinct oceanography and because they encompass the major deep-sea fishery areas for orange roughy, smooth oreo, black oreo and black cardinal fish – there is also some overlap with particular fishery QMA areas for hoki (*Macruronus novaezelandiae*), scampi and other middle depth species that have a maximum depth of more than 700 m.

2.3   Distribution of key habitat forming corals

The first component of Specific Objective 2 was "To assess the distribution of deep-sea coral species in the New Zealand region". This section focuses on the distribution of the main deep-sea habitat forming coral species, updating previous work by Sanchez (2005), Consalvey et al. (2006), and uses the recent distribution data described in Tracey et al. (2011a b) and Baird et al. (2013). There is specific focus on the depth distribution of these deep-sea corals, which is critical to answer the second part of Objective 2 which is a comparison with the carbonate saturation horizons.

The stony branching coral species are widely distributed throughout the New Zealand region. One species is the endemic *O. virgosa*, and the remaining species are found globally, with the exception of *G. dumosa*, which has a New Zealand and Indo-Pacific distribution (Roberts et al. 2008).

The gorgonian corals used in this study are only identified to genera as bubblegum corals are difficult to tell apart without expert identification, and some species of the genera *Keratoisis* and *Lepidisis* have major taxonomic problems that need resolving (Watling et al. 2011).These gorgonian genera are found throughout the world's oceans (Yesson et al. 2012) and are widely distributed in New Zealand (Sanchez 2005; Tracey et al. 2011b; Baird et al. 2013).

2.4 Methods to map study species distributions

2.4.1 Data

Data used to produce the updated branching stony coral and gorgonian coral plots for this report originate from several sources: appendix 1 from Tracey et al. (2011a), where information from historical records and 'grey literature' reports were compiled along with coral records from unpublished fisheries research trawl (*trawl* database), commercial by-catch (*cod* database), and biodiversity research surveys; more recent biodiversity survey research data; observer data that have been collected and ground-truthed to genera and species level since 2007 (Tracey et al. 2011b) and recent trawl survey data. Baird et al. (2013) compiled these data as part of a Project DOC12303 / POP2011-06 to produce a groomed protected coral dataset

2.5 Results

2.5.1 Distribution of scleractinian stony branching corals in the New Zealand region

Overall, the scleractinian corals are well distributed throughout the New Zealand region, although limited numbers have been recorded on the Challenger Plateau (Figure 2.3). As also seen in Tracey et al. (2011a), most stony branching corals occur along the edge of the plateau regions and continental shelf, and on the seamounts. The majority of the corals are found shallower than 1200 m depth, with less than 8% found below this depth.
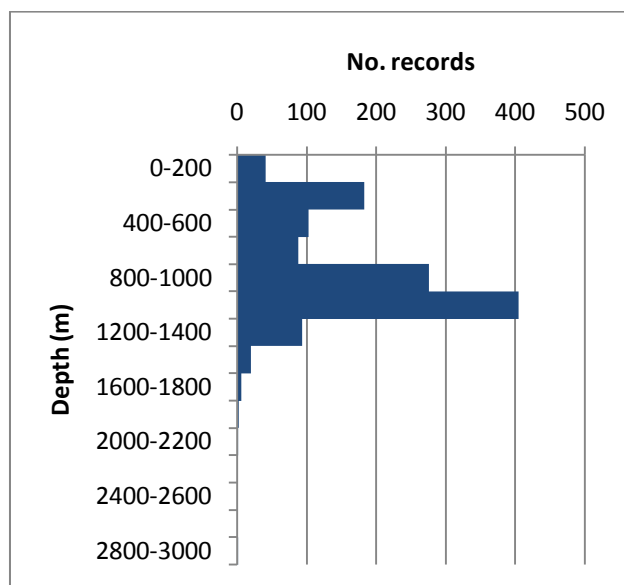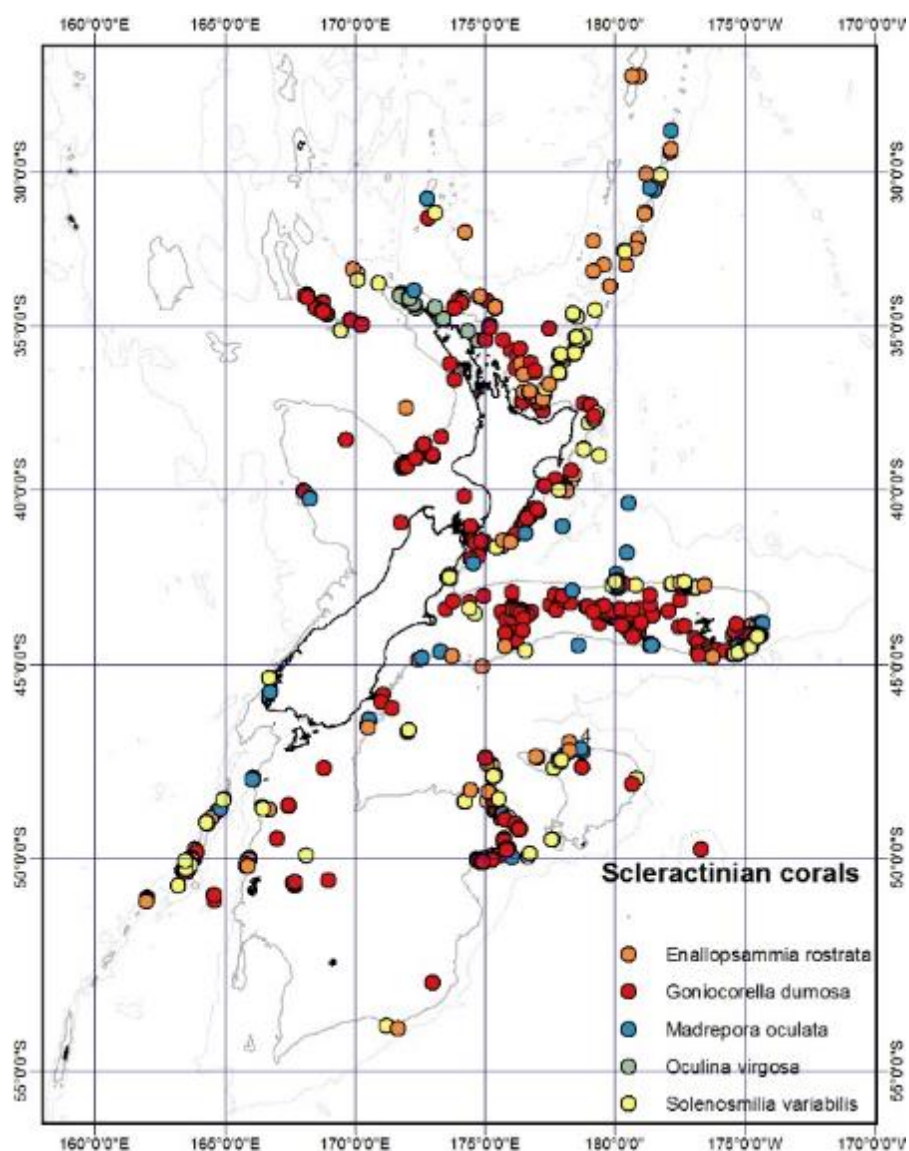
Figure 2.3: Distribution and depth data of all records of the five species of scleractinian stony branching corals. Bathymetric contours are 1250 m (dark grey) and 3000 m (light grey).

Each species of stony branching coral has a slightly different regional distribution both spatially and by depth. *S. variabilis* (n=333) occur throughout the region although they are relatively rare on the Challenger Plateau (Figure 2.4). There is a well-defined peak in depth distribution for this species, with 85% of records from between 800 and 1400 m (Figure 2.4) and an average depth of about 1000 m.

Enallopsammia rostrata has fewer records (n=159), and is found along the edge of the continental shelf and on seamounts (Figure 2.5). This species has a broader and slightly shallower depth distribution with 80% found between 600 and 1200 m and also a small peak at 200–400 m (Figure 2.5), with an average depth of 860 m.

Madrepora oculata (n=152) is similarly distributed to *S. variabilis* and *E. rostrata* (Figure 2.6), although *M. oculata* is found shallower than the other two species, with 63% found between 800 and 1200 m, and with as many as 30% of the records found shallower than 800 m (Figure 2.6). The average depth of this species for the New Zealand region is 820 m.

Goniocorella dumosa is the most commonly occurring of the stony branching corals with over 540 records mapped. This species has a very different distribution to the previous three corals, with a significant proportion of the records from the tops of plateaus and rises – particularly from the Chatham Rise (Figure 2.7). The depth distribution for *G. dumosa* is distinctly bimodal. Approximately 50% of the records are from the 800–1200 m depth, with the other 50% shallower than 800 m and a peak in the 200–600 m depth range (Figure 2.7). The latter is due to the large number that were collected along the top of the Chatham Rise.
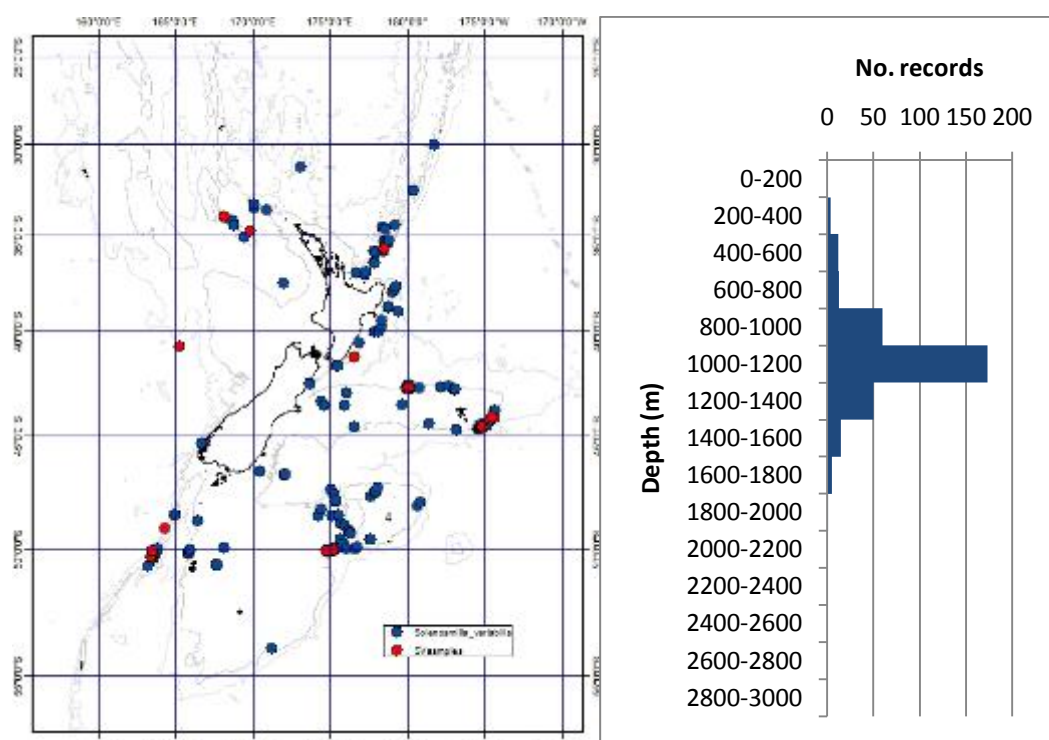
Figure 2.4: Distribution and depth data for *Solenosmilia variabilis* in the New Zealand region. Red dots show the samples used for the mineralogy and trace element analyses (see Section 3).

Figure 2.5: Distribution and depth data for *Enallopsammia rostrata* in the New Zealand region. Red dots show the samples used for the mineralogy and trace element analyses (see Section 3).

Figure 2.6: Distribution and depth data for *Madrepora oculata* in the New Zealand region. Red dots show the samples used for the mineralogy and trace element analyses (see Section 3).

Figure 2.7: Distribution and depth data for *Goniocorella dumosa* in the New Zealand region. Red dots show the samples used for the mineralogy and trace element analyses (see Section 3).

There are few records of the endemic species *O. virgosa* (n=32). It is predominantly found to the north of New Zealand, although there has been one record from the Fiordland coast and a couple from southern part of the east coast of the North Island and northeast of the South Island (Figure 2.8). The depth distribution is predominantly in the 0–200 m range, although two records have been collected from 1000–1200 m (Figure 2.8).

Figure 2.8: Distribution and depth data for *Oculina virgosa* in the New Zealand region. Red dots show the samples used for the mineralogy and trace element analyses.

2.5.2 Distribution of gorgonian corals

The gorgonian corals are also widely distributed in the New Zealand region, although again there are few records from the Challenger Plateau. Most of the study species are found shallower than 1400 m (Figure 2.9), with only 2% found deeper than this. They have been found down to depths of 3200–3400 m in the New Zealand region.

The distribution of the gorgonain coral genera does vary within the region. *Keratoisis* spp. is the most commonly recorded gorgonian (n=333). This genus is broadly distributed along the edge of the continental shelf and on seamounts (Figure 2.10). There is a distinctive depth distribution with a peak between 800 and 1200 m with 67% of records and an average depth of 955 m. 93% of the records are shallower than 1400 m, but one record is from about 3400 m.

While considerably fewer records of *Lepidisis* spp. have been recorded (n=104), this genera is predominantly found to the north and east of New Zealand (Figure 2.11). There are two distinct peaks in the depth distribution: one between 800 and 1200 m with 63% of the records, and a second smaller peak between 400 and 600 m with 16% of the records. Fewer than 2% have been recorded shallower than 200 m while fewer than 5% are found deeper than 1400 m.
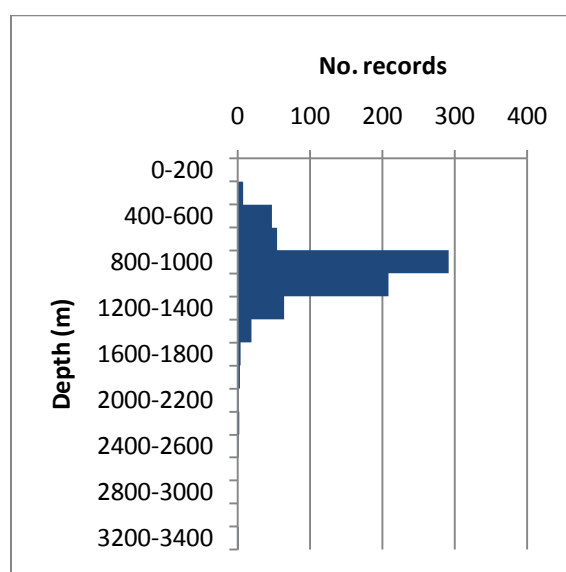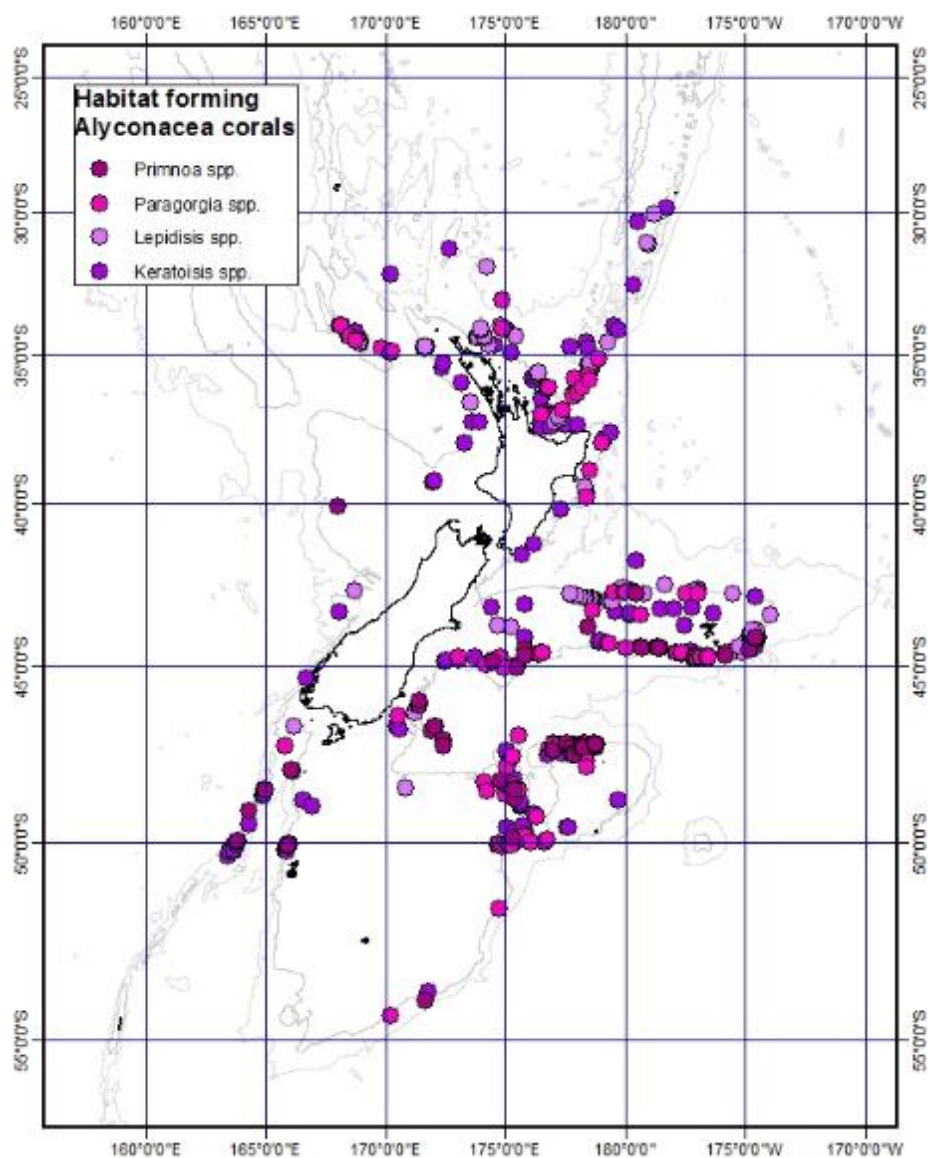
Figure 2.9: Distribution and depth data for the gorgonian coral study species (bamboo (*Keratoisis* and *Lepidisis* spp) , bubblegum (*Paragorgia* spp.), and sea fans corals (*Primnoa sp.*).
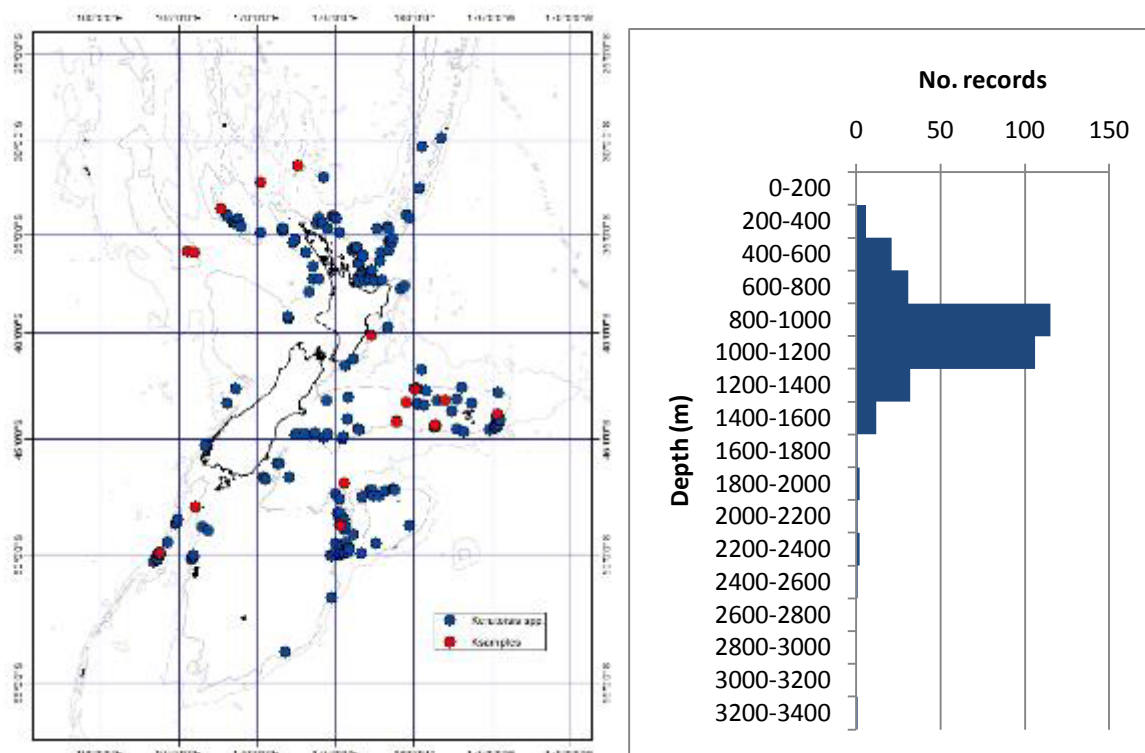
Figure 2.10: Distribution and depth data for *Keratoisis* spp. in the New Zealand region. Red dots show the samples used for the mineralogy and trace element analyses (see Section 3)
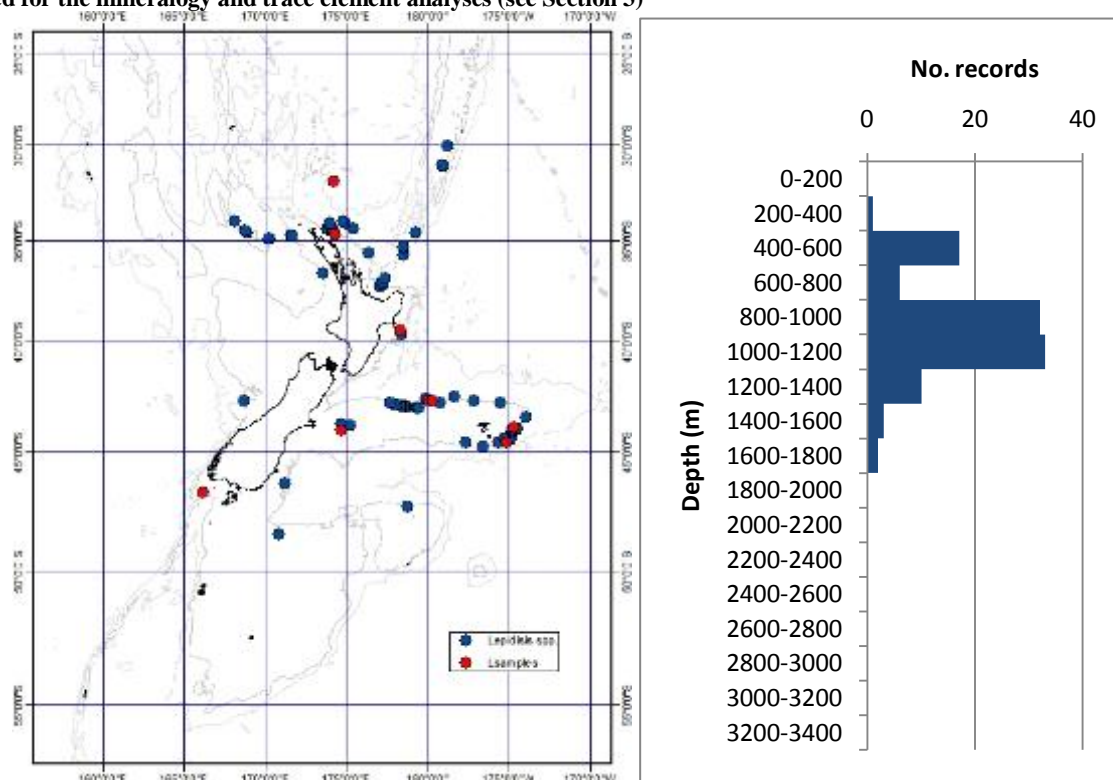
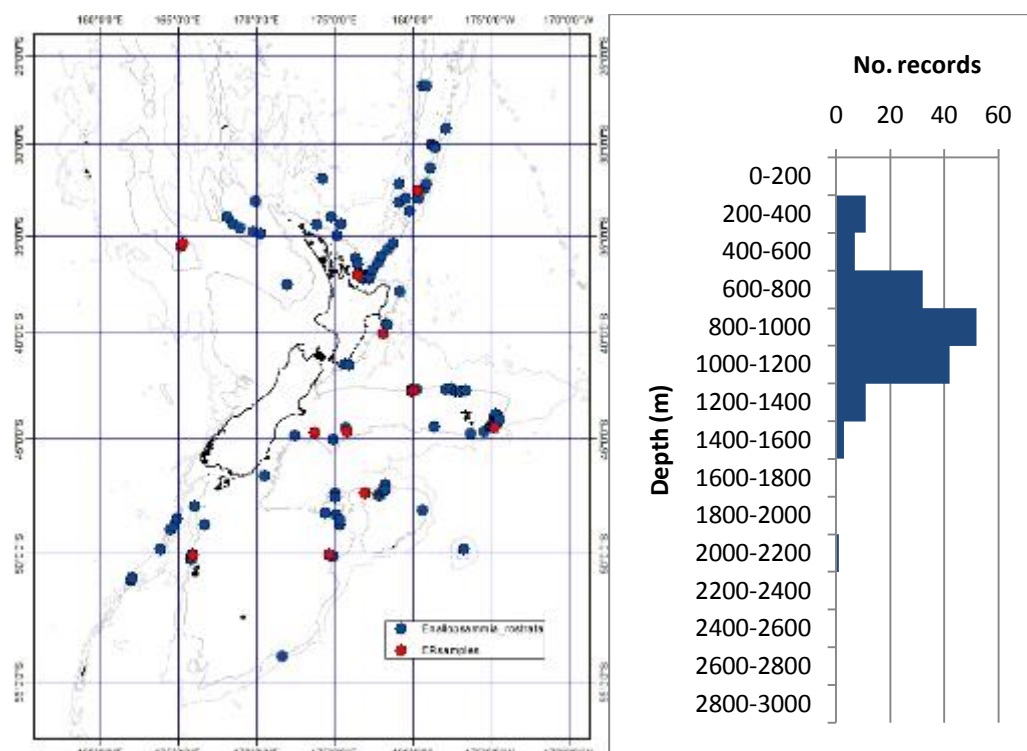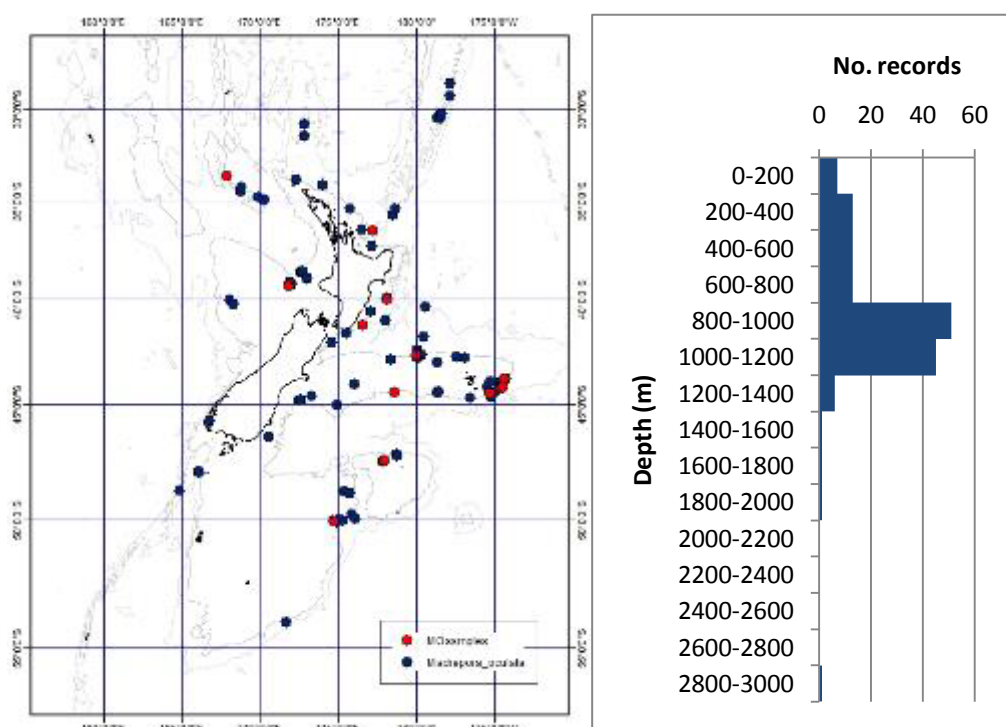**Figure 2.11: Distribution and depth data for *Lepidisis* spp. in the New Zealand region. Red dots show the samples used for the mineralogy and trace element analyses (see Section 3).**
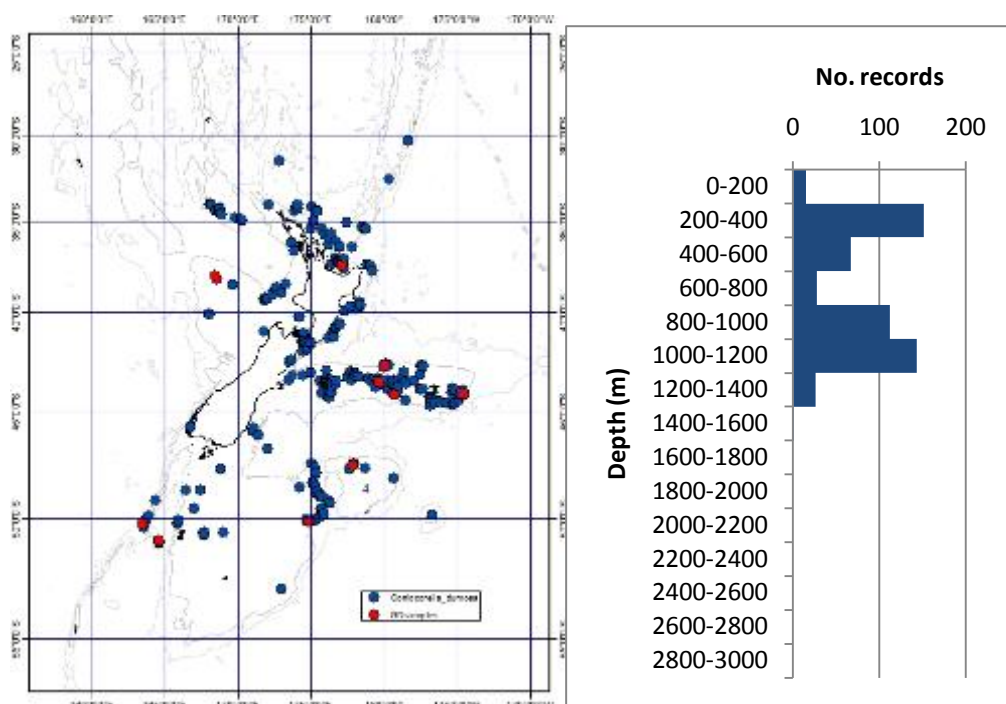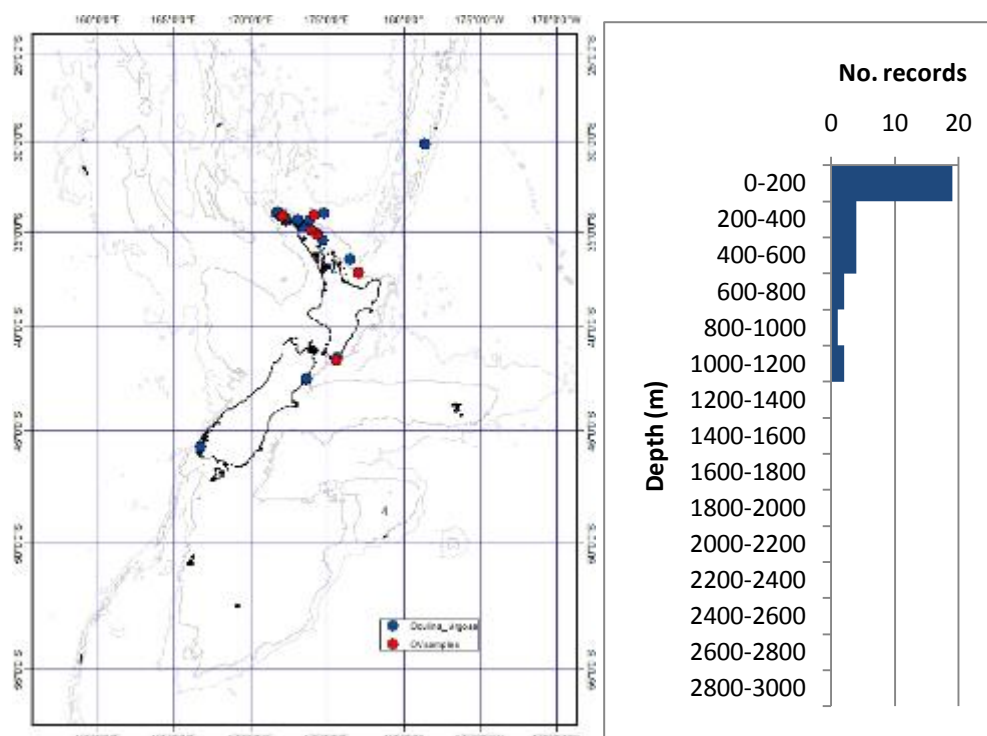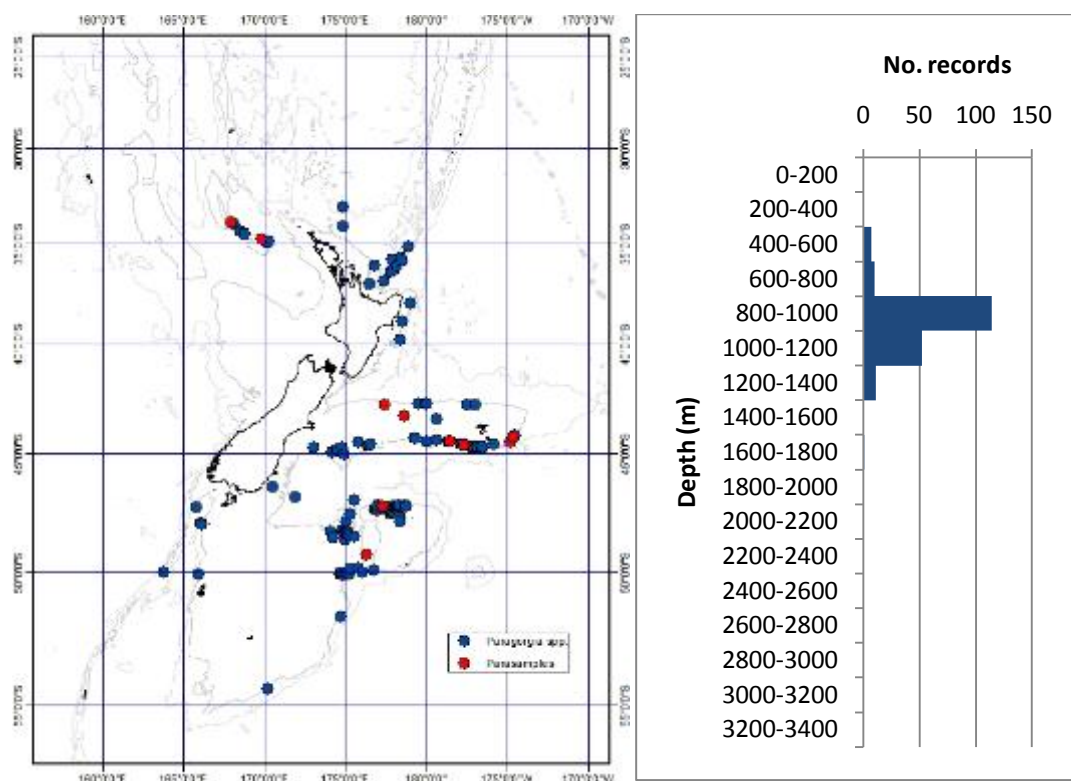
Figure 2.12: Distribution and depth data for *Paragorgia* spp. in the New Zealand region. Red dots show the samples used for the mineralogy and trace element analyses (see Section 3).

Paragorgia spp. (bubblegum corals) are the second most common gorgonian coral found in the New Zealand region (n=195), although no records occur from the Challenger Plateau (Figure 2.12). Bubblegum corals are located predominantly along the continental shelf, although some have been found on seamounts. It has a very distinct depth distribution with 85% of records from 800–1200 m depth. None have been recorded shallower than 400 m and there is only one record from deeper than 1400 m.

The gorgonian sea fan *Primnoa sp.* is the least common of the selected study species (n=72). This species is located primarily south of the Chatham Rise and extends into the Campbell Plateau region (Figure 2.13). No records occur shallower than 400 m, and there is a distinct peak in the depth distribution at 800–1000 m. 80% of the records are from 800–1400 m, with fewer than 7% deeper than 1400 m.
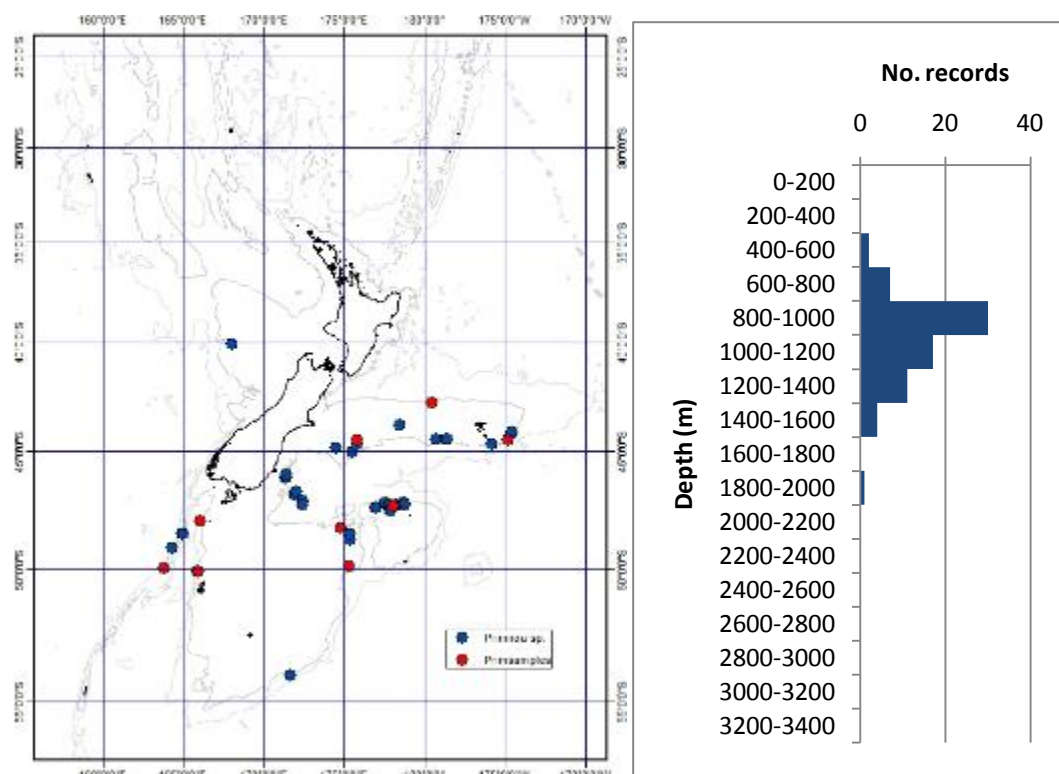
Figure 2.13: Distribution and depth data for *Primnoa sp*. in the New Zealand region. Red dots show the samples used for the mineralogy and trace element analyses.

There are clearly some differences in the distribution of these habitat-forming, deep-sea corals throughout the New Zealand region. The highest numbers are found between 800 and 1200 m, with some species such as *G. dumosa* having a second peak at 400–600 m depth. The endemic species *O. virgosa* is an anomaly with the majority of records found shallower than 400 m. *Primnoa sp*. have the highest number of occurrences deeper than 1400 m. Very few deep-water corals have been collected from the Challenger Plateau to the west of New Zealand. This could be due to a lack of sampling or different environmental factors (Tracey et al. 2011b). Several corals show spatial preferences; *O. virgosa* and *Lepidisis* spp. are found in the north, while *Primnoa sp*. are found predominantly south of Chatham Rise. These distinct distributions suggest that various environmental factors are controlling the locations of different species that are found in the New Zealand region. The important environmental variables seen in the studies by Tracey et al. (2011a) and Baird et al. (2013 for both stony coral species and gorgonians included depth, proximity to a seamount, tidal current speed, particulate organic carbon flux, and primary production. However, in both of these studies, the ocean chemistry data layers were unavailable for the predictive modelling.

2.5.3 Potential of deep-sea corals present in shallower depths

There is a need to continue to collect coral data and update regional datasets to ensure a more complete understanding of the spatial distribution of corals – by depth and location and within location. Data from shallower regions need to be included in the dataset and unsampled areas studied as in the future the corals with shallower distribution modes may potentially be very important species due to their broader tolerances of environmental conditions. Improved knowledge of the spatial variability of corals within specific areas, e.g., where the various species are present in shallower depths, in Benthic Protected Areas or on the top of the Chatham Rise, is required. Certain branching stony corals and sea fan species may continue to thrive in certain areas under changing environmental conditions and the potential refugia where these corals may thrive, need to be defined. This could provide managers with options to close areas of high density coral regions where associated fisheries and invertebrate habitats exist. Overall, the continued data collection and analyses of habitat and

fisheries distributions will help improve our understanding of the association between deep-sea corals and deep-water fisheries.

Chapter 3: DEEP-SEA CORAL CARBONATE MINERALOGY

Helen Bostock, Di Tracey (NIWA), Gavin Dunbar, Monica Handler, Joel Baker (Victoria University Wellington), Abigail Smith, Marc Riedi (University of Otago)

This section covers a part of Specific Objective 1 - to determine the carbonate mineralogy of selected deep-sea corals found in the New Zealand region.

3.1   Carbonate mineralogy

Three calcium carbonate mineral phases commonly occur in nature: aragonite, low magnesium (Mg) calcite and high Mg calcite (over 8 mol% $MgCO_3$; Andersson et al. 2008). Aragonite is a less stable carbonate polymorph and is 50% more soluble than low Mg calcite (Mucci 1983), while high Mg calcite containing 8–12mol% $MgCO_3$ has equal or greater solubility than aragonite (Walter & Morse 1984; Bischoff et al. 1987; Morse et al. 2006).

The carbonate mineralogy of marine organisms has been studied for over 150 years (Silliman 1846). In the early days, the composition of the skeletal material was determined using wet chemical analyses (Forchammer 1852; Damour 1852; Hobgom 1894; Nichols 1906; Butschli 1908) and staining (Meigen 1903). Clarke & Wheeler (1917) noted a correlation between chemistry and mineralogy, and the influence of water temperature. In the 1950s, the development of X-ray diffraction techniques and more comprehensive global sampling significantly improved our knowledge of which organisms produced which calcium carbonate mineral or minerals (Chave 1954). However, our current knowledge of the mineralogy of many deep marine taxa is still extremely limited. All previous work describing deep-sea coral mineralogy is summarized in Table 3.1. Note that only one study analysed samples from the New Zealand region (Cairns & Macintyre 1992).

It is important that we understand the mineralogy of these deep-sea organisms. Although the surface waters of the world's oceans are currently supersaturated in terms of carbonate ion concentration $[CO_3^{2-}]$ with respect to all polymorphs of calcium carbonate (Feely et al. 2004; Andersson et al. 2008), saturation states decrease with increasing mineral solubility, decreasing temperature, and increasing pressure/depth. Thus many of these deep-sea corals already live in waters with low carbonate ion concentrations, which are likely to be reduced further by ocean acidification (Guinotte et al. 2006).

Table 3.1: Summary of previous studies on coral mineralogy.

Order	Species	Mineralogy	Reference
Scleractinia	Tropical	Aragonite	Clarke & Wheeler 1917; Chave 1954; Milliman 1974
	Solenosmilia variabilis, Enallopsammia rostrata, Desmophyllum dianthus, Caryophyllia diomedeae	Aragonite	Milliman 1974; Thresher et al. 2011
Alcyonacea (previously Gorgonacea)	Numerous shallow and deep species.	Mg calcite and aragonite and apatite, many bi-mineralic	Bayer & Macintyre 2001
	Isididae – numerous species	Mg calcite	Clarke & Wheeler 1917; Chave 1954; Milliman 1974
	Paragorgia spp.	Mg calcite (14–15 mol% $MgCO_3$)	Thresher et al. 2011
	Chrysogorgia spp.	Mg calcite (19 mol% $MgCO_3$) and aragonite	Thresher et al. 2011
	Keratoisis spp.	Mg calcite (8 mol% $MgCO_3$)	Thresher et al. 2011
	Primnoisis spp.	Mg calcite (10 mol% $MgCO_3$)	Thresher et al. 2011
	Lepidisis spp.	Mg calcite (10 mol% $MgCO_3$)	Thresher et al. 2011
	Narella spp.	Aragonite (axis), Mg calcite (spicules) (10 mol% $MgCO_3$)	Thresher et al. 2011
	Isidella spp.	Mg calcite (11 mol% $MgCO_3$)	Thresher et al. 2011
	Thourella spp.	Mg calcite (8 mol% $MgCO_3$) and aragonite	Thresher et al. 2011
	Corallium spp.	Mg calcite (10 mol% $MgCO_3$)	Clarke & Wheeler 1917; Weinbauer et al. 2000; Thresher et al. 2011
Stylasteridae	Numerous species	Aragonite and Mg calcite, some bi-mineralogy	Cairns & Mcintyre 1992; Thresher et al. 2011

3.2.   Methods

3.2.1. Sample selection

Specimens of the stony branching and gorgonian corals were obtained from the National Invertebrate Collection (NIC) at NIWA. Only the most recent growing tips of the coral colony were used for this study and samples were visually inspected to check for evidence of organic tissue and also that the stony coral samples were not coated in manganese (an indicator of having been dead for some time before collection).

To encompass spatial variability, coral specimens were selected from each of the eight regions within the New Zealand EEZ, and reflect areas which are influenced by different water masses (see Section 4). The first six of these regions support areas of key deep-water fisheries (Figure 3.1).Where possible, specimens were analysed from the minimum and maximum depth in each of these regions. The regions were:

1.   East Coast North Island
2.   North Chatham Rise
3.   A - Southeast Chatham Rise, B – Southwest Chatham Rise
4.   Northeast Campbell Plateau
5.   Puysegur Bank and Macquarie Ridge
6.   Challenger Plateau
7.   Northland – not a major fishery
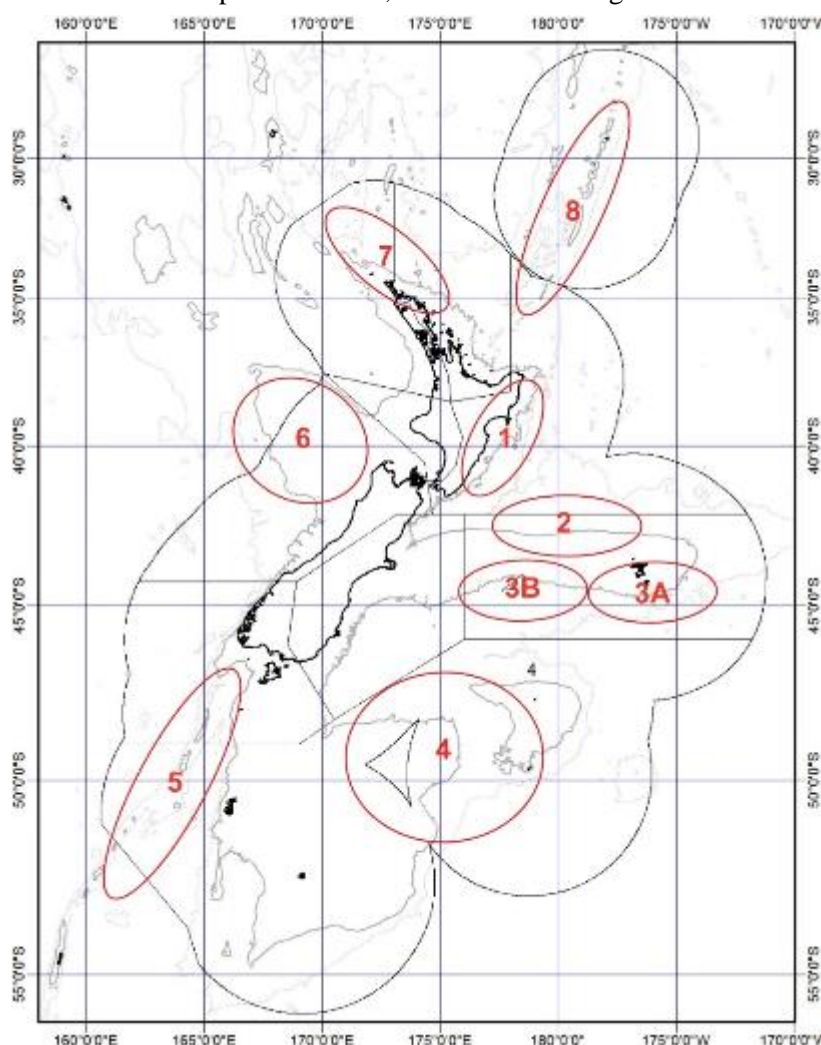8.   Kermadecs – protected area, no bottom trawling.

Figure 3.1: Map of the nine Fishery Management Areas (FMAs) with the eight regions chosen for this project overlain and numbered in red.

The justification for the broad coverage of sample selection was to help determine whether environmental factors (for example, temperature, depth/pressure, water mass type) have any control on the mineralogy and % Mg within the Mg calcite. A total of 90 samples across all the species/genera of the key New Zealand habitat forming species listed in Table 2.1 were sampled (Appendix 1). The location of the selected samples is plotted on the distribution maps presented in Section 2.2 (Figures 2.3–2.13).

Epibenthic sleds or trawls can cover a depth range of several hundred metres and the corals could have been collected at any depth during the trawl. We have assigned the average depth for each station and compared these depths with temperature (taken from the World Ocean Atlas 2009) and carbonate saturation states (see Section 4).

3.2.2. X-ray diffraction (XRD) analyses

Each of the samples was analysed to determine their carbonate mineralogy using X-ray diffraction (XRD). Samples for XRD were prepared by slicing through the body of the coral to create a flat surface with a 5 cm diameter diamond cutting wheel. The flat slices were mounted on "blu-tac" adhesive and analysed using a Panalytical X'Pert Pro x-ray diffractometer running at 45 KV and 40 mA. Each sample was scanned across an angular range of 5 to 70º 2 Theta with a step size of 0.013º 2 Theta. Mineral phase(s) present in the resulting scans were identified using Panalytical's "Highscore" search-match software. Additional specimens of *Primnoa* sp. were disarticulated into morphological components, powdered with halite, and analysed using XRD at the University of Otago.

3.2.3. Trace element analyses

Trace element analyses were carried out using Inductively Coupled Plasma Mass Spectrometry (ICP-MS). The important aspect of the trace element analyses is to ascertain the magnesium content of the high Mg calcite corals –the gorgonians. The higher the Mg content the more susceptible these organisms will be to future ocean acidification. Other trace element data were obtained as part of the analytical process, including Strontium (Sr). High concentrations of Sr are incorporated into aragonite, but not calcite – due to the differences in the crystal structure. Therefore, by also measuring Sr, we can independently check the XRD results. The concentration of Mg in high Mg calcite and the Sr in aragonite are potentially also controlled by other environmental factors such as temperature (Chave 1954; Gagan et al. 1998).

Whole coral samples were each placed into a 30 mL shot glass container and filled with ultrapure (more than 18.2 MΩ) water before being transferred into an ultra-sonic bath for 270 min. Every 10 minutes the approximately 30 mL of ultrapure water was discarded and a fresh volume added to remove loose external organic debris from the coral samples. The corals were then placed into an oven for 24 hours at 40˚C to evaporate all water. Samples were then individually crushed into a homogenous powder using a mortar and pestle (cleaned in between samples with 6 M HCl) and collected using weighing paper before being returned into 30 mL shot glass containers and sealed with Parafilm.

To ensure that external organic debris was removed from all coral samples, so as not to compromise the validity of the analysis, a series of tests were conducted. We tested several cleaning processes (Appendix 1) all of which underwent the initial sample cleaning step described above. Following the results of these tests, 3% H_2O_2 was chosen for chemical pre-treatment. Typically 50 mg of the powdered sample was weighed into a pre-cleaned centrifuge tube. The samples were then cleaned in 2 mL of 3% H_2O_2 before being digested in 6 mL of 1 M HNO_3 and left to digest for 1 hour before being centrifuged at 5000 rpm for 5 min. A 3 mL aliquot of this solution was then diluted with 3 mL of Milli-Q water before being analysed in solution mode on the ICP-MS. A synthetic coral standard was created by mixing selected certified single-element solution standards in proportions comparable to

the samples and measured after every 5 samples. Samples and standards were measured with 90 second acquisitions following 60 second background measurements to measure instrumental noise.

Raw trace element data were background-subtracted using the Iolite software package. A two standard deviation outlier rejection was used for all baselines and integrations. Background-corrected data were converted to trace element/Ca ratios in a spreadsheet, using interpolated bracketing standards, and converted to mmol/mol ratios. Two standard error (SE) uncertainties in the standards and samples calculated using Iolite were propagated through the data reduction, and were typically less than ± 3% (2SE). External reproducibility was checked using duplicate analyses and was typically better than 10% and 5% (2 standard deviations for Mg/Ca and Sr/Ca respectively).

3.3 Results

3.3.1. XRD

The XRD results from this study provided similar data to previous studies found in the literature. The Scleractinian corals were all aragonitic, while most of the gorgonian corals were Mg calcite (Table 3.2). The exception to this was *Primnoa* sp., which was determined to be bimineralic, with both aragonite and Mg calcite layers (see Appendix 2 for details). Examples of the aragonite and Mg calcite plots from the XRD trace analyses are shown in Figure 3.2. The examples are for a stony branching coral (*G. dumosa*) and a gorgonian bamboo coral (*Keratoisis* spp.)

Table 3.2: XRD results for the stony branching and gorgonian corals.

Order	Species or Genera	Mineralogy
Scleractinia (stony corals)	*Solenosmilia variabilis*	Aragonite
	Oculina virgosa	Aragonite
	Goniocorella dumosa	Aragonite
	Enallopsammia rostrata	Aragonite
	Madrepora oculata	Aragonite
Alyconacea (gorgonian corals)	*Paragorgia* spp.	Mg calcite
	Lepidisis spp.	Mg calcite
	Keratoisis spp.	Mg calcite
	Primnoa sp.	Mg calcite/Aragonite
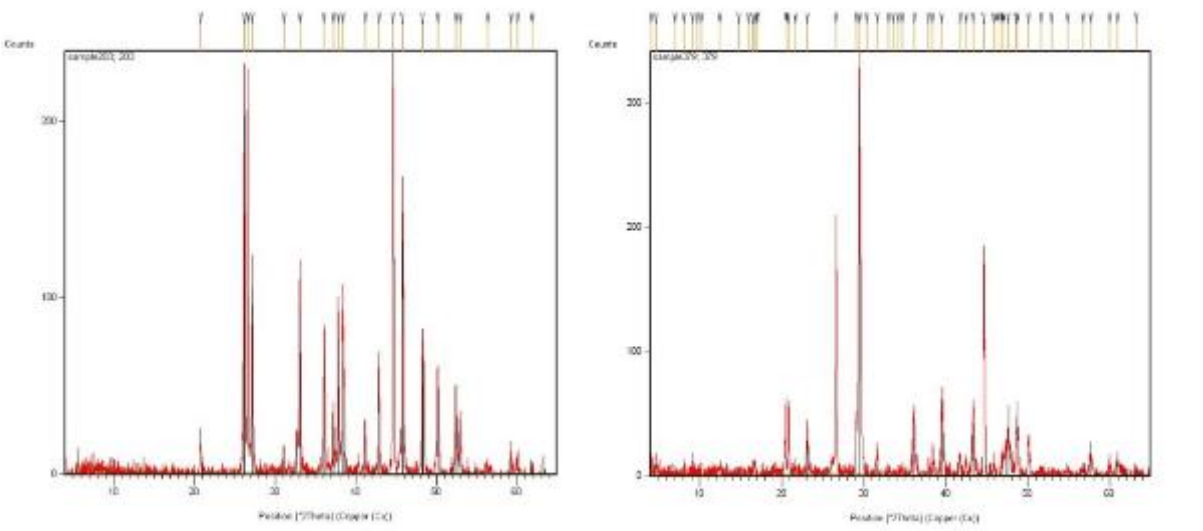
Figure 3.2: XRD trace analyses plots of aragonitic *Goniocorella dumosa* (left) and Mg calcitic *Keratoisis* spp. (right).

3.3.2. Trace elements

The trace element results from the ICP-MS confirm the XRD results. Data are presented in Appendix 1. These trace element analyses were undertaken primarily to provide more quantitative information about the exact mol% of Mg within the high Mg calcite skeletons. The aragonitic scleractinian corals were also analysed in order to determine if there is any variability in the Sr or Mg levels, and whether these are controlled by the environmental conditions in each of the regions.

Table 3.3: Average (and range) of Mg/Ca and Sr/Ca concentrations in the growing tips of deep-sea corals. Significant outliers are highlighted in yellow.

	Mg/Ca mmol/mol	Sr/Ca mmol/mol
Species or Genera (n)	Average (range)	Average (range)
Solenosmilia variabilis (14)	2.61(2.36–2.8)	10.45 (9.8–11.1)
Oculina virgosa (5)	4.14 (2.62–7.6)	10.24 (9.9–10.87)
Goniocorella dumosa (10)	2.69 (2.4–3)	10.52 (10.06–10.93)
Enallopsammia rostrata (9)	2.85 (1.99–5.3)	11.01 (10.61–11.52)
Madrepora oculata (14)	2.61 (2.3–3.13)	10.7 (6.01–11.46)
Paragorgia spp. *(8)*	97.9 (87–109)	2.97 (2.82–3.16)
Lepidisis spp. (6)	85.31 (81–91)	3.00 (2.97–3.07)
Keratoisis spp. *(13)*	88.44 (84–94)	3.06 (2.97–3.36)
Primnoa sp.(10)	9.98 (wide range 5–30)	9.00 (8.37–9.69)

It is evident that the aragonitic corals have high Sr and low Mg, while the high Mg calcite corals have low Sr and high Mg (Table 3.3; Figure 3.3. The Mg calcite corals are all considered high Mg calcite, with between 8 and 12 mol% $MgCO_3$ (Morse et al. 2006). In general, the trace elements of each genera/species cluster closely together. Interestingly, the brown organic rich nodes of the *Keratoisis* spp. (Figure 2.2.) gave similar results to the adjacent growing tips.

There is some variability in the Sr and Mg values, with some outliers (Figure 3.3), which may be due to contamination from organic matter that was not completely removed, or other small carbonate organisms attached to the coral skeleton that have different mineralogy.

Primnoa sp. show the widest range in Sr and Mg values, which warranted further investigation. Some small pieces were sent to University of Otago for mineral analysis (see Appendix 2). It was found that there were three discrete components in the *Primnoa* sp. skeleton; a central brown stem – which was very hard, this was surrounded by a shiny white layer – which was much softer, and then relatively brittle grey flakes comprising the dried outer layer of the coral colony (where the armoured scales and calyces (cups) are visible, (see Figure 2.2 of the *Primnoa* specimen). The hard brown stem was predominantly aragonite, with some samples having minor amounts of high Mg calcite (about 104 to 134 mmol/mol Mg/Ca or 10–13 mol% $MgCO_3$), while the grey flakes were medium Mg calcite (57 to 65 mmol/mol Mg/Ca or 5.7–6.5 mol% $MgCO_3$). The shiny white layer between the brown stem and the brittle grey flakes was also predominantly aragonite, with one sample exhibiting up to 43% Mg calcite (56 to 64 mmol/mol or 5.6–6.4 mol% $MgCO_3$). Thus the variability we see in the trace element data (Figure 3.3a;b) is most likely the result of different parts of the skeleton being sampled. *Oculina virgosa* may also have minor amounts of $MgCO_3$ as well, as it has slightly elevated Mg/Ca mmol/mol.
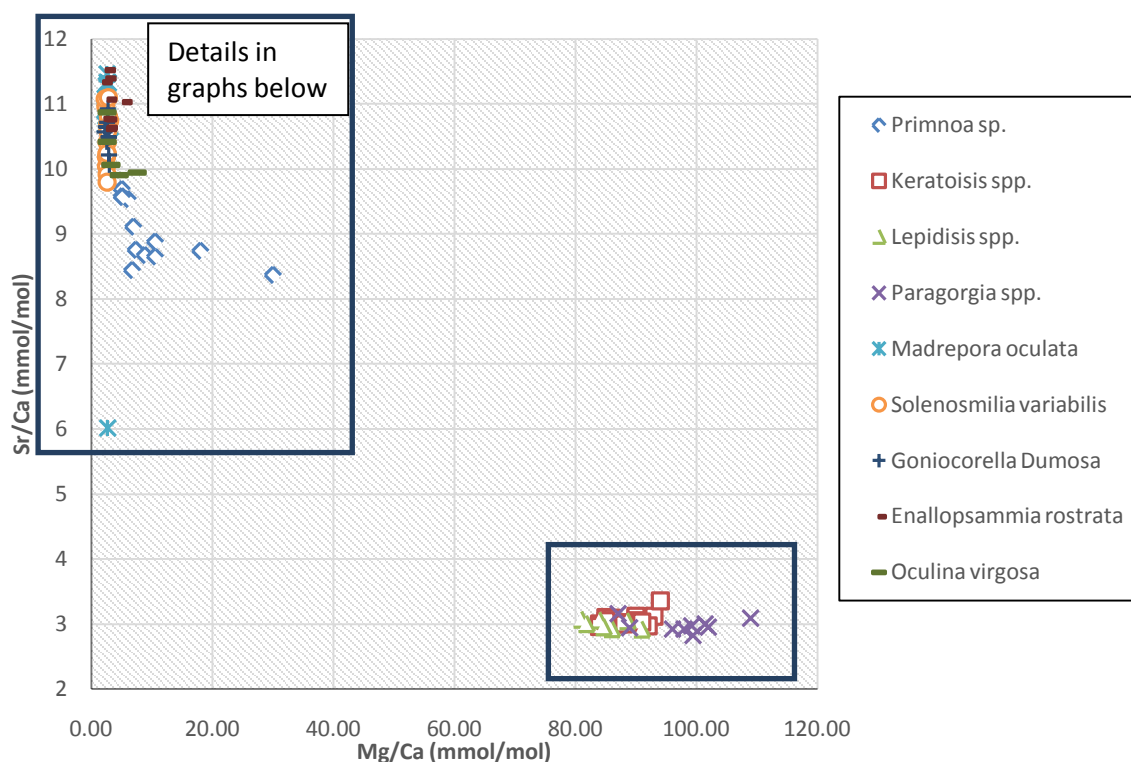
Figure 3.3a: The Mg/Ca (mmol/mol) and Sr/Ca (mmol/mol) of the growing tips of habitat forming scleractinian and gorgonian deep-sea corals. The key difference to note is the distinction between the aragonite corals with the high Sr/Ca (left cluster of data points), with the Mg calcite corals that have high Mg/Ca and low Sr/Ca (cluster of datapoints on the right. Boxes on first plot show the areas that are enlarged in the graphs below.
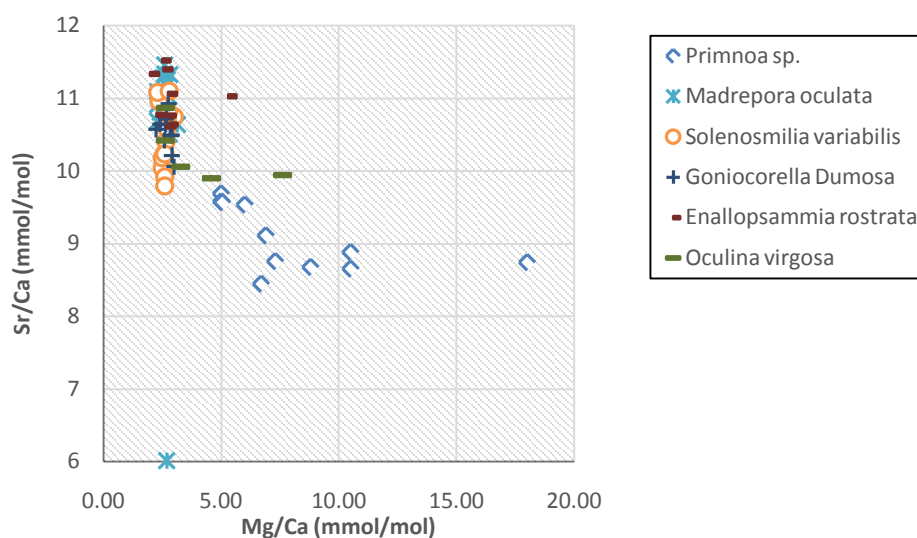
Figure 3.3b: The Mg/Ca (mmol/mol) and Sr/Ca (mmol/mol) of the growing tips of habitat forming scleractinian and *Primnoa* sp. The wide range in *Primnoa* Sr/Ca and Mg/Ca indicate that while this organism is predominantly aragonitic the skeleton also contains some Mg calcite.
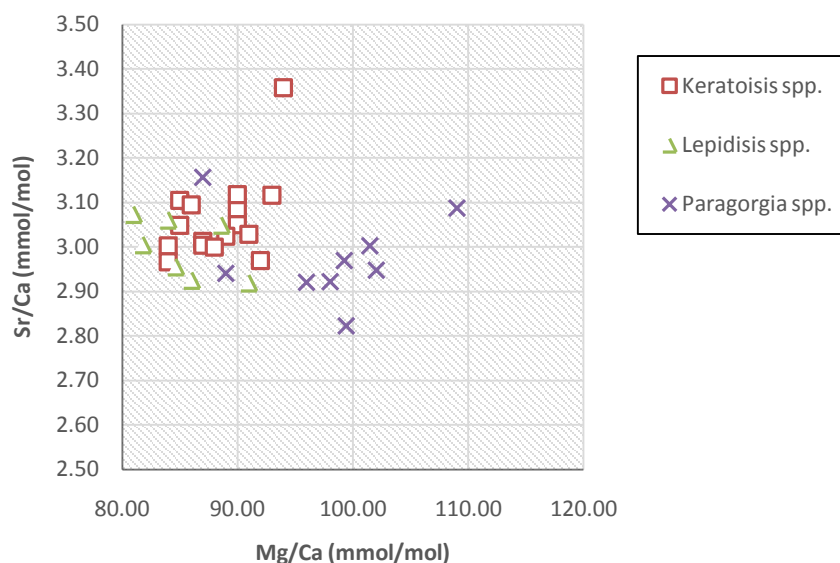
Figure 3.3c: The Mg/Ca (mmol/mol) and Sr/Ca (mmol/mol) of the growing tips of habitat forming gorgonian deep-sea corals. These corals show a broad distribution in the Mg/Ca content, with only a small variation in the Sr/Ca content.

When Mg/Ca mmol/mol is plotted against water temperature *Keratoisis* spp. and *Paragorgia* spp. show an increase in Mg/Ca with increasing temperature (r^2=0.4 and 0.3, although there is clearly a large amount of scatter; Figure 3.4). *Lepidisis* spp. does not show any trend. The scleractinian corals also show no obvious changes in Mg/Ca or Sr/Ca with temperature.
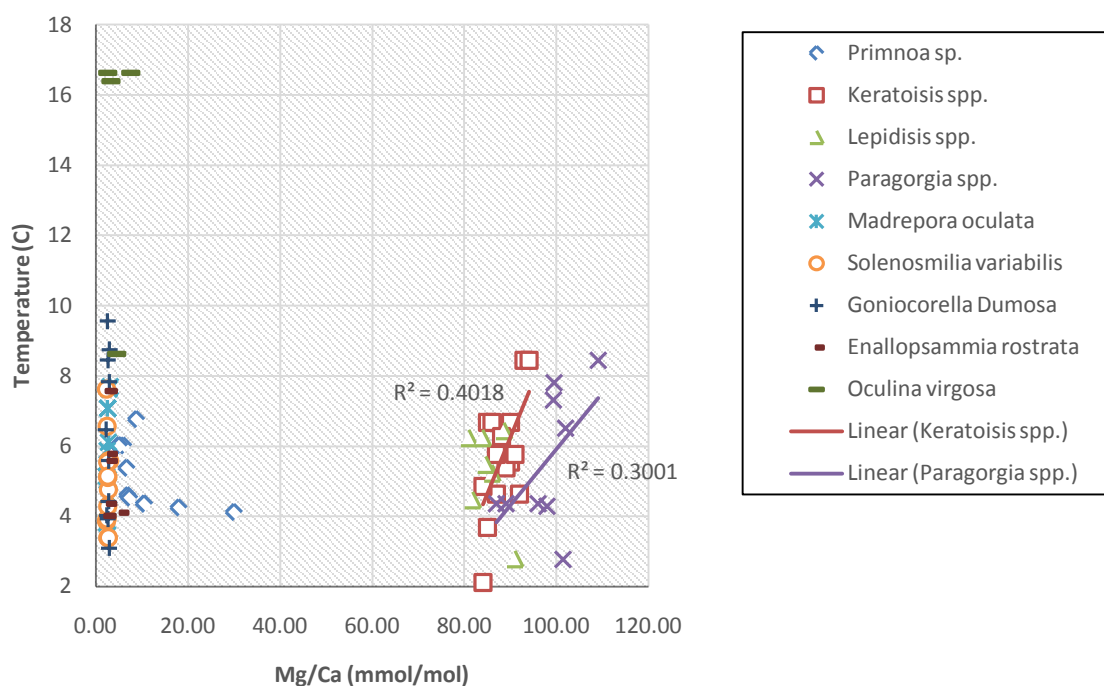
Figure 3.4a: Mg/Ca (mmol/mol) versus bottom water temperature. The high Mg calcite gorgonian corals show a large variation in Mg/Ca with temperature. *Keratoisis* spp. and *Paragorgia* show a positive correlation with temperature, suggesting that temperature may increase the amount of Mg/Ca incorporated into the calcite as their skeleton is formed.
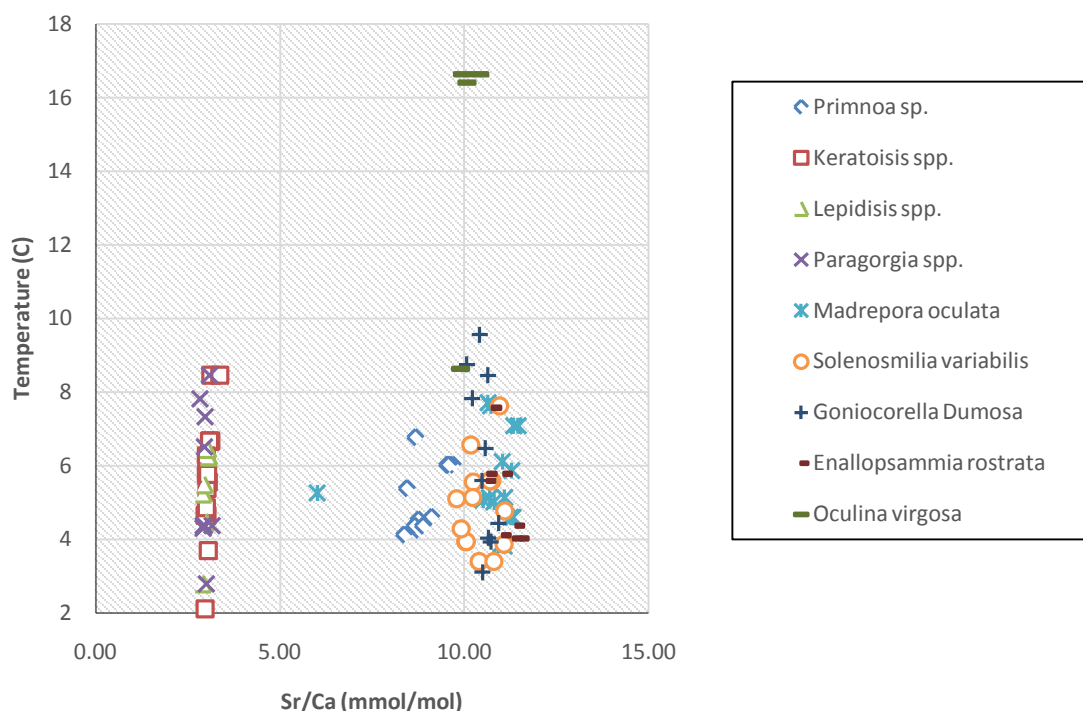
Figure 3.4b: Sr/Ca (mmol/mol) versus temperature. There is no evidence that the Sr/Ca value of these deep sea habitat forming corals varies with bottom water temperatures.

3.4. Discussion

This is the first time that such a comprehensive analysis of the mineralogy and trace elements of deep sea corals has been undertaken for the New Zealand region. Sampling covered a broad geographic area and a wide range of depths. We have confirmed that, as seen elsewhere, the scleractinian corals are aragonite, with some variation in the amount of Sr/Ca and little variation in Mg/Ca. The exception to this is a slight elevation in the Mg/Ca content of the endemic *O. virgosa*.

Our Mg/Ca and Sr/Ca results are very similar to those of Thresher et al. (2011), measured on the same species from a seamount south of Tasmania. Our *Paragorgia* spp. Mg/Ca values are slightly lower (87–109 mmol/mol versus 102–137 mmol/mol for Thresher et al. 2011). Our Sr/Ca results for the aragonitic scleractinian corals are slightly higher, while the Mg/Ca for these corals are lower than Thresher et al. (2011). These subtle differences are probably due to natural variability in these organisms and different techniques and standards used to determine the trace element concentrations. Thresher et al. (2011) used X-ray fluorescence and wavelength dispersive electron probe microanalysis (WD-EPMA), whilst we used ICP-MS.

The gorgonian corals were predominantly high Mg calcite with 81–109 mmol/mol Mg/Ca (or 8–11 weight% $MgCO_3$). The general consensus is that Mg calcite at this mol% would be as soluble, if not more susceptible to dissolution, than pure aragonite (Morse et al. 2006).

The different mineral layers within the *Primnoa* sp. carbonate skeleton were somewhat surprising and highlight the need for more detailed examination of these corals to ascertain any differences in layering, crystalline structure and mineralogy and so inform on the overall impacts of OA. Thresher et al. (2011) showed that different Primnoidae were biomineralic, with some predominantly high Mg calcite and others predominantly aragonitic. These differences in mineralogy could be caused by a regional effect, colony age, or may be a genetic effect. It is quite common for organisms such as

echinoderms and molluscs to be bimineralic, but corals are often considered more passive mineralisers and predominantly influenced by the sea water chemistry (see e.g., Stanley & Hardie 1998.

Sr/Ca has been widely used in tropical scleractinian corals as a proxy for temperature changes (Gagan et al. 1998; Correge 2006). There is no evidence for Sr/Ca concentration in the deep water scleractinian being controlled by thermodynamic differences. Mg/Ca in the high Mg calcite gorgonian corals does show a subtle, but significant, increase with increasing temperature in *Keratoisis* spp. and *Paragorgia* spp., similar to studies of other calcite and high Mg calcite organisms (Chave 1954). However, there is no evidence for this for *Lepidisis* spp. The latter observation could be due to fewer samples being analysed. More analyses are required to determine any thermodynamic influence on the Mg/Ca.

Future work should also be undertaken to determine if other environmental factors control the trace element concentrations and the mineralogy of these organisms. Many other trace elements were measured using the ICP-MS including barium, boron, aluminium, lithium, uranium and zinc. Recent work suggests that boron isotopes in deepsea scleractinian corals correlate very closely with aragonite saturation states (McCulloch et al. 2012).

Chapter 4: OCEANOGRAPHY AND CARBONATE SATURATION

Helen Bostock, Kim Currie, Sara Mikaloff-Fletcher, Mike Williams, Mark Hadfield (NIWA)

There are several common oceanographic acronyms used in this chapter, these are listed below:
STF – Subtropical Front
STW – Subtropical Surface Water
SAW – Subantarctic Surface Water
NBM or STM – Northern Biophysical Mooring site or Subtropical Mooring
SBM or SAM – Southern Biophysical Mooring site or Subantarctic Mooring
AAIW – Antarctic Intermediate Water (500–1500 m)
NPDW – North Pacific Deep Water (1500–4000 m)
CDW – Circumpolar Deep Water (1500–4000 m)
AABW – Antarctic Bottom Water (more than 4000 m)
GLODAP – Global Ocean Data Analysis Project – a global database of hydrographic and geochemical data
WOCE – World Ocean Circulation Experiment – a global series of voyages
PACIFICA – A more recent global database of hydrographic and geochemical data

The complex bathymetry around New Zealand affects the oceanography. In the surface waters, the Subtropical Front (STF), which is bathymetrically constrained to the east of New Zealand by the Chatham Rise, is the meeting of warm, low nutrient, subtropical waters (STW) from the north and the cold, high nutrient subantarctic waters (SAW) from the South (Nodder et al. 2005). The STF is not so well constrained west or south of New Zealand (Hamilton 2006; Smith et al. 2013). Below the surface waters sit the thermocline waters and the Antarctic Intermediate Water (AAIW). The AAIW is distinguished by its salinity minimum. There are two types of AAIW in the New Zealand region (Bostock et al. 2013; Figure 4.1). To the north of New Zealand there is the Tasman AAIW (AAIW-N) which is slightly saltier and warmer than the Southern Ocean AAIW (AAIW-S) which flows in from the south (Bostock et al. 2013).

The different intermediate water masses have had different histories, some are older and have mixed with other water masses (e.g., with deep waters or tropical intermediate waters), while some have formed more recently. These factors affect the water chemistry (Bostock et al. 2013). These intermediate water masses were recently formed in the Southern Ocean and have absorbed more anthropogenic CO_2, and as a result their saturation states are already reduced from pre-industrial times (Feely et al. 2012). The Southern Ocean water masses are flowing directly into the south of our region and with ocean acidification the carbonate saturation states will be reduced further, reducing the amount of calcification by corals and other carbonate benthic organisms.

Below the AAIW at around 1500 m sit the deep waters. Here we have an opposite situation with more corrosive water coming from the north and less corrosive (higher carbonate concentrations) from the south. This is because north of Chatham Rise the deep waters are primarily influenced by the North Pacific Deep Waters (NPDW), which are old and corrosive (low carbonate ion concentration). To the south the waters are the Circumpolar Deep Waters (CDW), which have come directly from the Southern Ocean and flow into the region as part of the Deep Western Boundary Current and have higher carbonate ion concentrations (Carter & McCave 1997; Bostock et al. 2011).
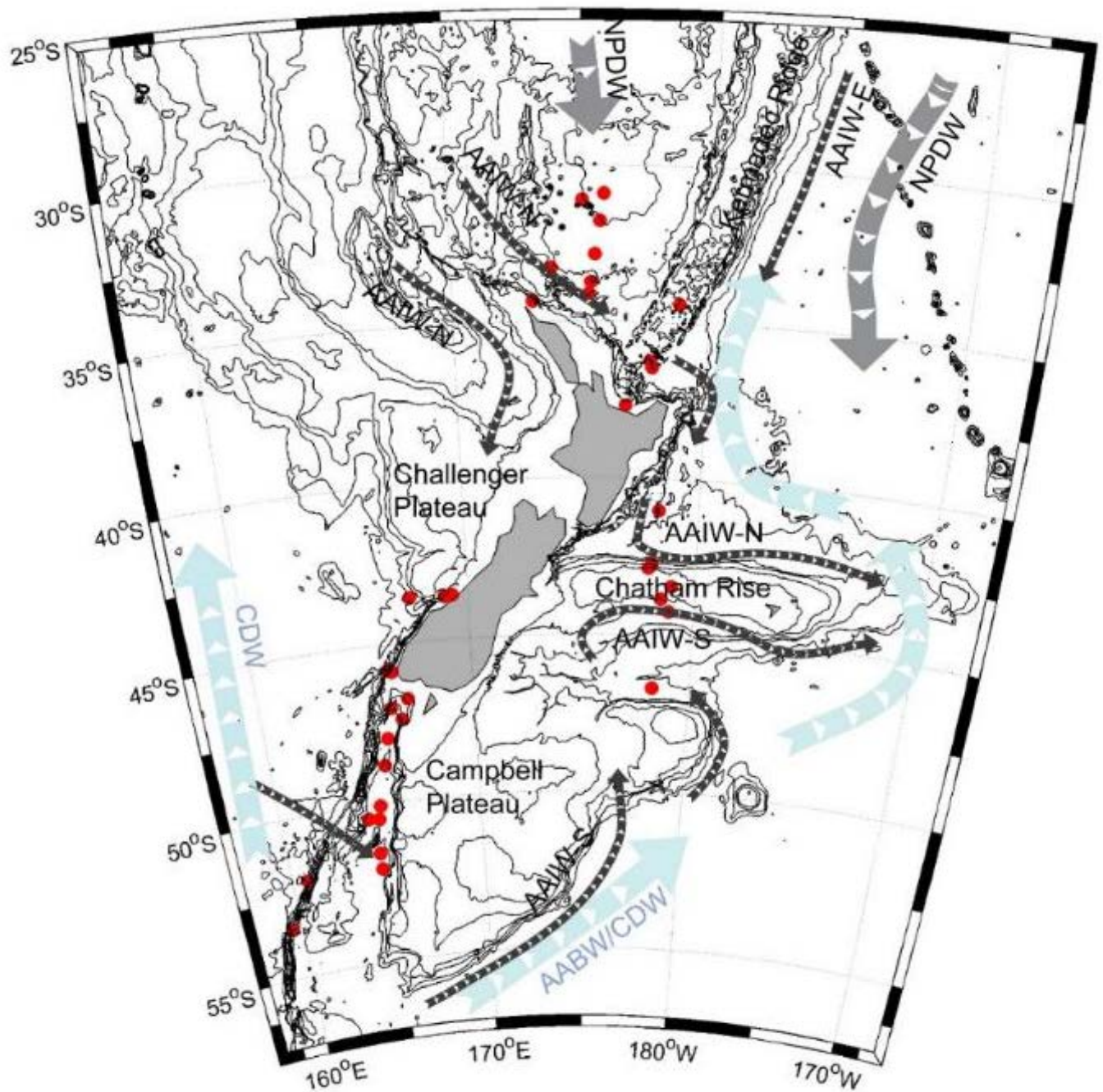
Figure 4.1: The main topographic features and currents in the New Zealand region. Thin dashed black lines with arrows highlight the main intermediate depth currents which are made up of AAIW – Antarctic Intermediate Waters (see text for details). Large blue arrows show the deep water current which is made up of AABW – Antarctic Bottom Water and CDW – Circumpolar Deep Water. Large grey arrows show the NPDW – North Pacific Deep Water. Locations of the stations sampled for alkalinity and DIC since 2008 by NIWA are shown by red dots – the voyages where alkalinity and DIC were sampled for this project are listed in Table 4.1. Recently collected West Coast of the South Island samples are yet to be analysed.

Previous maps of the aragonite and calcite saturation horizons for the New Zealand region have been based on limited samples from the global GLODAP datasets extrapolated into the New Zealand region (Figure 4.2; Feely et al. 2004). These do not take into account the complicated topography and currents in the New Zealand region.
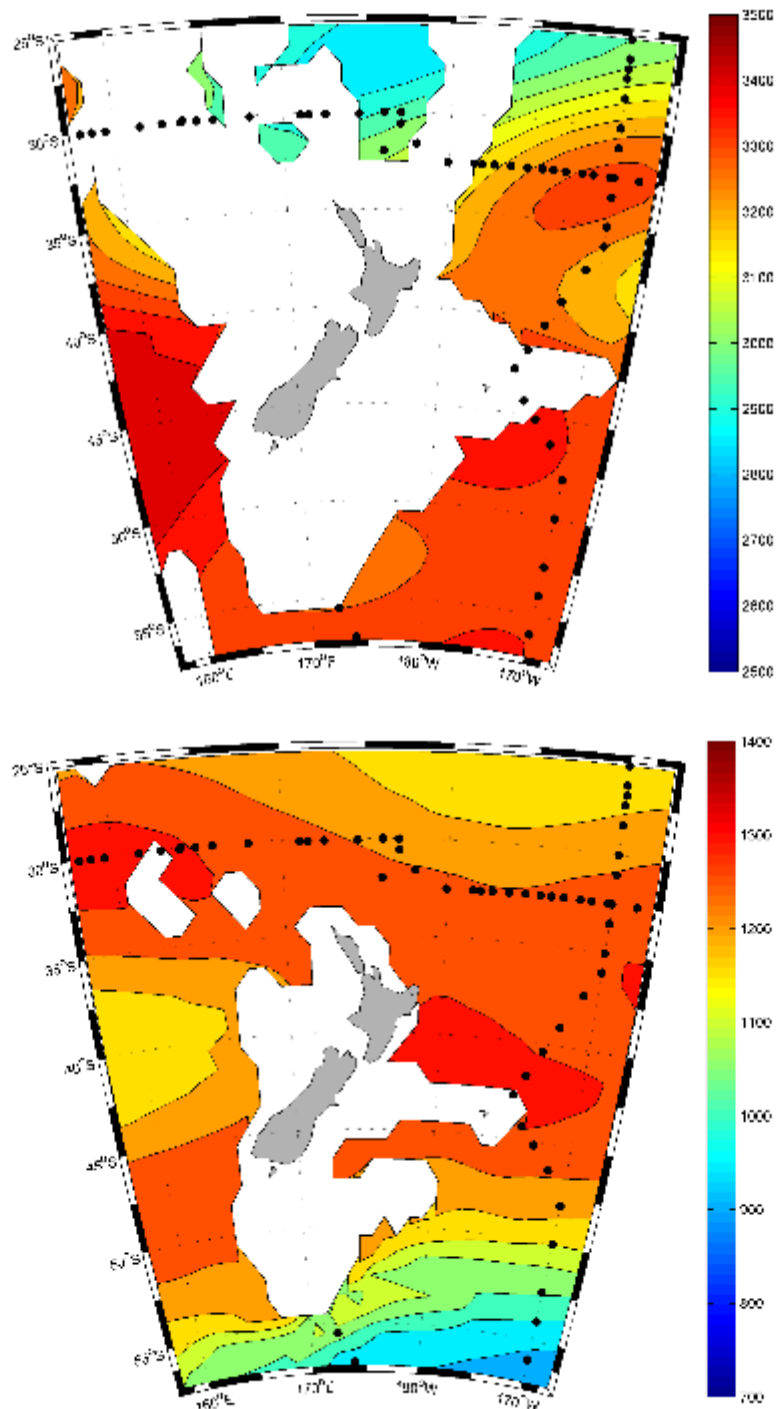
Figure 4.2: Maps of the calcite (CSH) (top) and aragonite (ASH) (bottom) saturation horizons for the New Zealand region extrapolated from the limited GLODAP database prior to this project. The locations of the GLODAP stations are shown by black dots. The line running from west to east is the World Ocean Circulation Experiment (WOCE) transect P06W and from north to south is P15S. Colour bar represents the depth of the CSH and ASH in metres. The white region represents topography shallower than the ASH and CSH.

4.1.   Water sampling and chemical analyses

Opportunistic water sampling has been undertaken on recent NIWA voyages to analyse for alkalinity and dissolved inorganic carbon (DIC) to supplement the GLODAP stations, and to provide carbonate chemistry water data from within the New Zealand EEZ (Table 4.1; Figure 4.1; Appendix 3). The opportunistic water samples have specifically been targeted on areas deemed important for both deep-sea corals and key deep-water fisheries.

Table 4.1: Samples collected for alkalinity and DIC on NIWA voyages during 2011–2013 funded by this project.

Voyage	Location	Voyage Leader
TAN1113 – Biophysical moorings	Chatham Rise	Scott Nodder
TAN1116 – Fisheries Oceanography II	Chatham Rise	Matt Pinkerton, Scott Nodder
TAN1205 – East Auckland Current	Northland	Phil Sutton
TAN1206 – Southern Kermadec Arc	BOP	Malcolm Clark

Alkalinity samples were measured using the closed cell potentiometric titration method, and DIC concentrations determined using a coulometric titration of the CO_2 evolved from an acidified sample (Dickson et al. 2007). Carbonate ion concentrations, pH and carbonate saturation indices (Ωaragonite and Ωcalcite) were calculated from the alkalinity and DIC, temperature, salinity and pressure data using the CO2SYS calculator (Lewis & Wallace 1998), and using the carbonic acid dissociation constants of Mehrbach et al. (1973), refitted by Dickson & Millero (1987).

4.2.   Results

The results are discussed by region. The data from the voyages listed above are supplemented by data from voyages between 2008 and 2011, collected prior to this project.

4.2.1. Chatham Rise (Regions 2-4 see Figure 3.1)

From the temperature and salinity profiles, the main water masses across the Chatham Rise can be readily identified, with clear differences north and south of the rise (Figure 4.3.) Some of the differences in the surface waters are due to seasonality, with summer samples showing warmer temperatures than winter samples. Below the surface, the different AAIW types can be clearly seen with the more saline Tasman AAIW found north of the rise and the fresher Southern Ocean AAIW south of the rise (Bostock et al. 2013). The north and south rise differences are also seen in the alkalinity and DIC data, which show the difference between the NPDW with high alkalinity and high DIC from the north rise, compared to the CDW from the south rise.

The calculated ASH (where Ωaragonite =1) is at 1300 m at the Northern Biophysical Mooring site (NBM – 41°S, 178.5°E; also known as the Subtropical Mooring (STM) (Nodder et al. 2005), while it is as shallow as 1000 m at the Southern Biophysical Mooring site (SBM – 46.5°S, 178.5°E; also known as the Subantarctic Mooring (SAM) (Nodder et al. 2005). This is clearly different from the GLODAP/PACIFICA data just to the east along line P15S which does not show such a clear offset between the ASH north and south of the rise. This is probably due to mixing of AAIW at the eastern end of the Chatham Rise (Chiswell & Sutton 1998) where the P15S transect has sampled. However, it highlights that the global datasets do not make sense when they are extrapolated into the New Zealand region as these data don't account for the complexity of the local current systems. The CSH is found

at the sea floor at the NBM about 3100 m (figure 19; Bostock et al. 2011). The site of the SBM is too shallow to reach the CSH at this site.
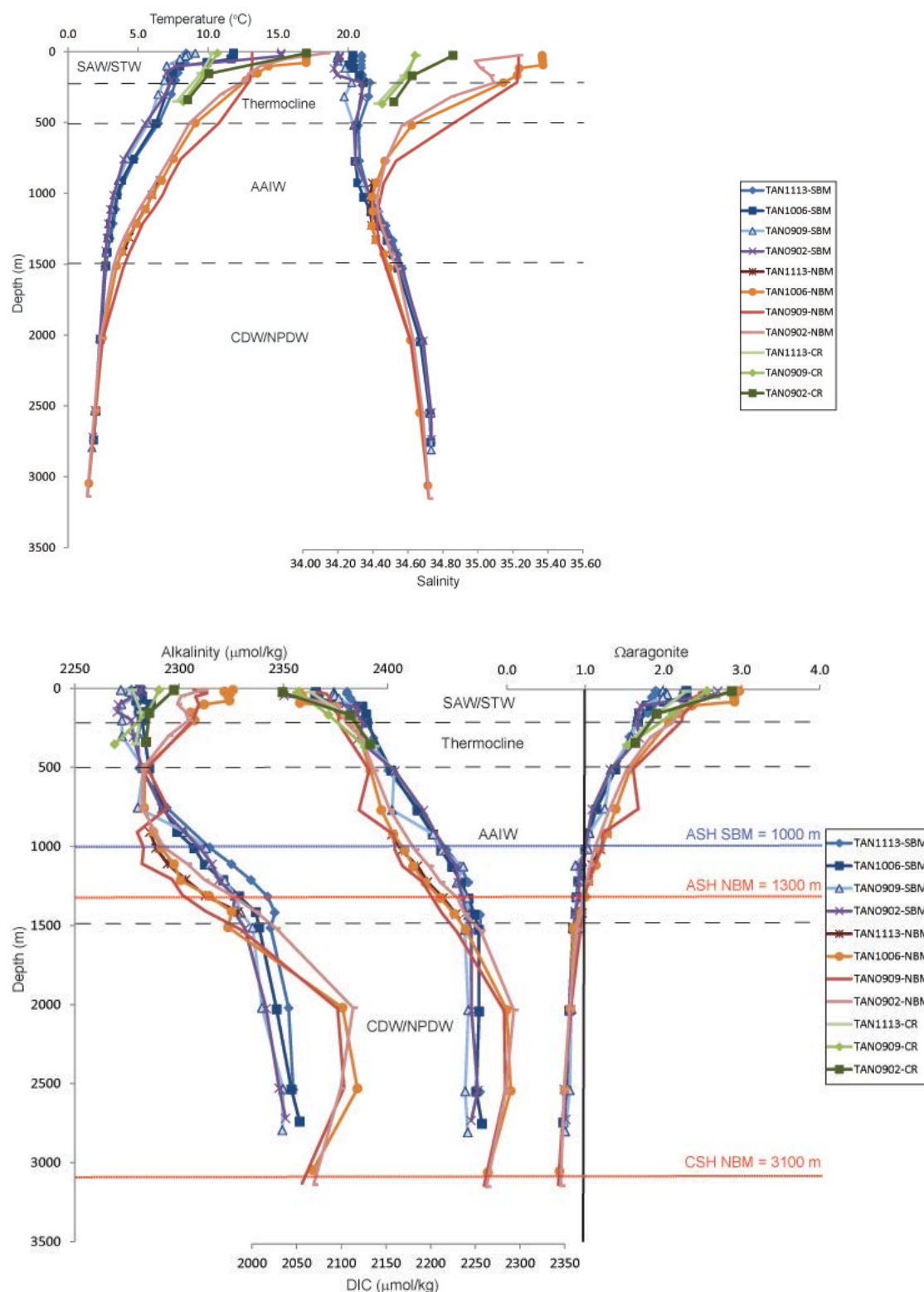
Figure 4.3: Top: Temperature and salinity profiles, Bottom: Alkalinity, DIC and aragonite saturation (Ωaragonite) from the Northern Biophysical Mooring (NBM) and the Southern Biophysical Mooring (SBM) and on top of the Chatham Rise (CR), collected during a number of RV *Tangaroa* voyages. TAN0902, January 2009, TAN0909, October 2009; TAN1006, May 2010 and TAN1113, September 2011.
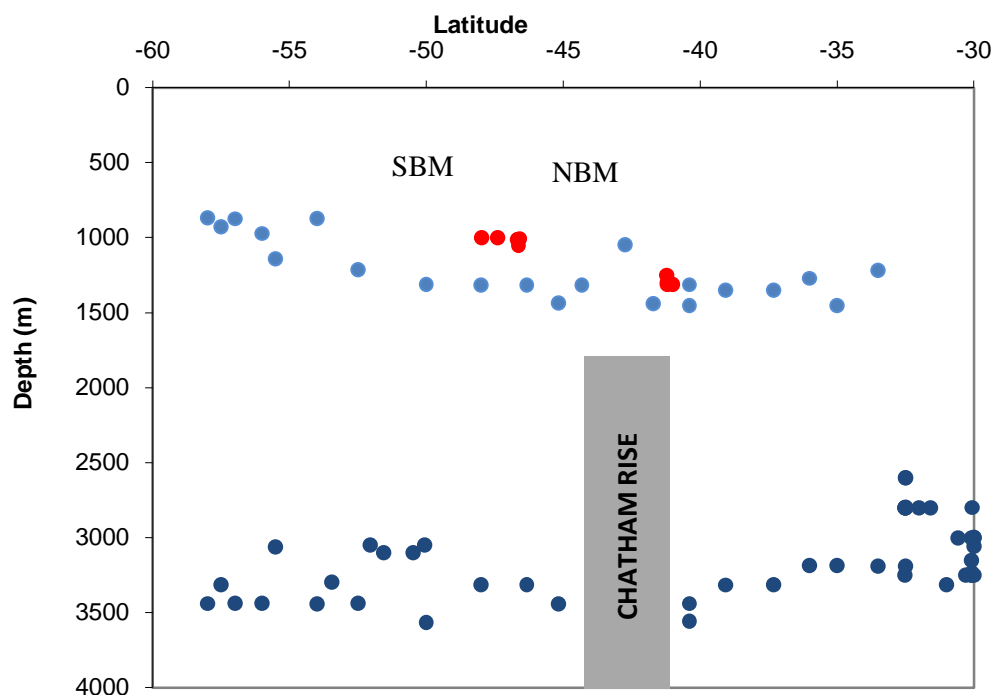
Figure 4.4: Comparison of the ASH depth at the mooring sites (NBM and SBM; red dots) from multiple trips (TAN0902, TAN0909, TAN1006, TAN1113), with the P15S GLODAP data (light blue dots) to the east of Chatham Rise. The CSH data from the GLODAP line is represented by dark blue and sits around 3100 m.

4.2.2 Macquarie Ridge (Region 5, see Figure 3.1)

The Macquarie Ridge region to the south of New Zealand shows a similar picture to the stations at higher latitudes along WOCE line P15S. The Ωaragonite and ASH decrease with increasing latitude. At 58°S the ASH is 500 m, compared to 1250 m at under 51°S (Figure 4.5). This is the result of the NPDW/CDW upwelling at the Polar Front in the Southern Ocean, bringing the deep, cold, old, corrosive waters to the surface. The CSH is also found at 3100 m in this region.
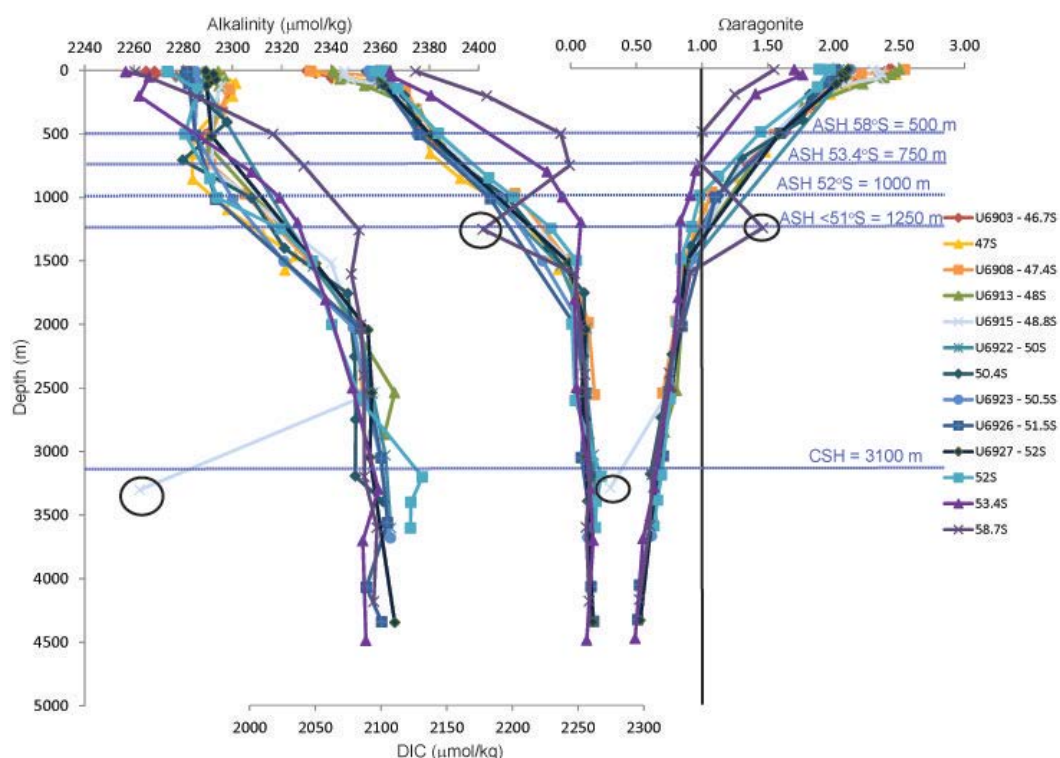
Figure 4.5: Alkalinity, DIC and Ωaragonite profiles for the Macquarie Ridge (TAN0803) and Solander Trough (TAN1106) voyages, south of New Zealand. Stations are in latitudinal order. The black circles indicate data points where the results are erroneous

4.2.3. Bay of Plenty and Northland (Regions 7 and 8, see Figure 3.1)

The surface waters of this region are fed by the Tasman Front and the East Auckland Current, which are sourced from warm, salty waters of the East Australian Current. At intermediate depths, the waters are the low salinity Antarctic Intermediate Waters (AAIW), but they come from the north and east, the so-called Tasman AAIW. Due to the Lord Howe Rise and the Kermadec Ridge, the bottom waters are sourced from the north as well, through the South Fiji Basin, and these are the old, low oxygen, highly corrosive North Pacific Deep Waters (NPDW). These have very high DIC and alkalinity. The ASH sits somewhere between 1000 m and 2000 m, while the CSH sits around 3000 m (Figure 4.6).

The P06W (GLODAP line) lies just to the north of this region and shows a very consistent ASH around 1200 m, while the CSH shoals from west to east, deeper in the Tasman Sea, around 3250 m, slightly shallower in the South Fiji Basin and then only 2800 m in the South Pacific Basin (Figure 4.7; Bostock et al. 2011).
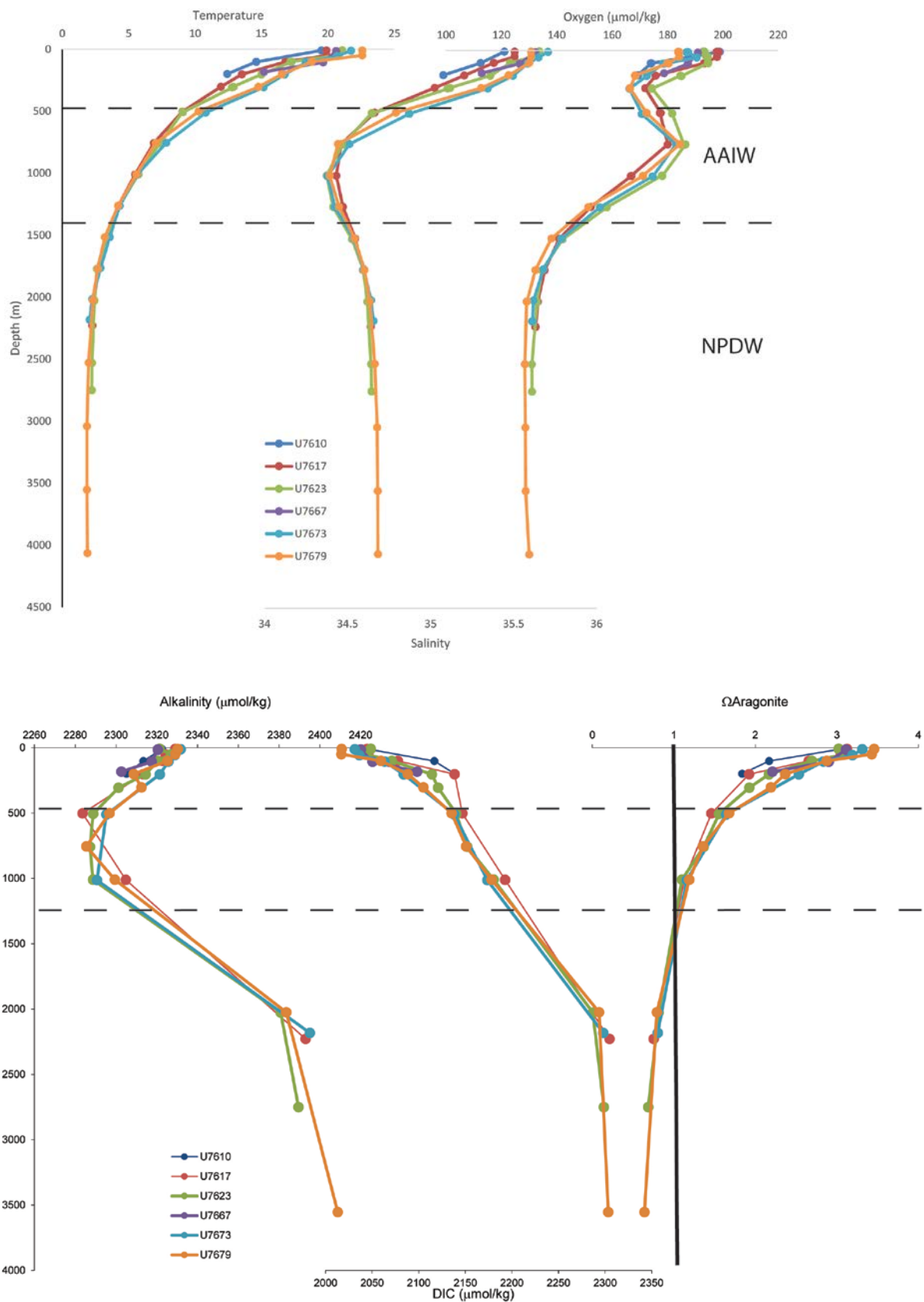
Figure 4.6: Hydrographic data from TAN1205, highlighting the main water masses in the northeast Northland region, AAIW – Antarctic Intermediate Water, NPDW – North Pacific Deep Water. Below is the measured alkalinity and DIC from TAN1205, and calculated aragonite saturation state (ΩAragonite).
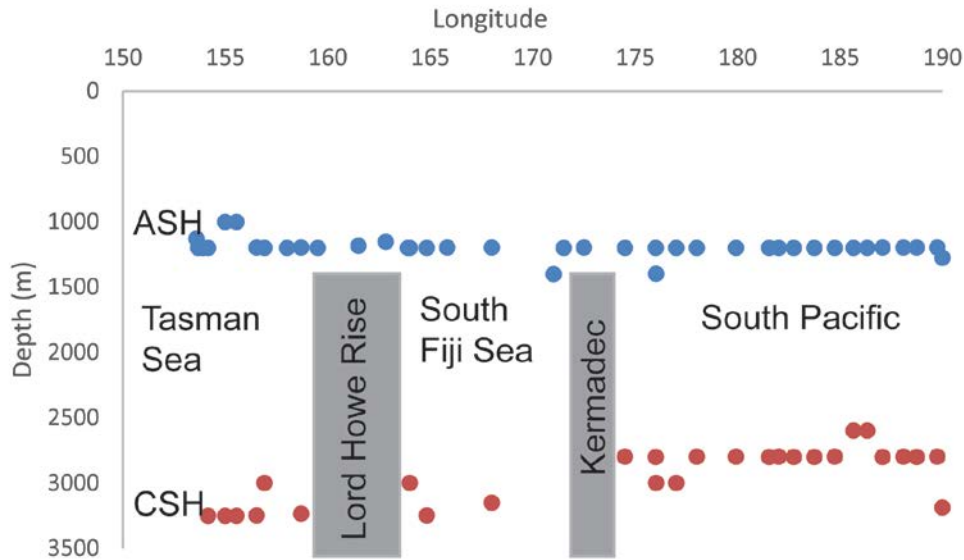
Figure 4.7: P06W2003 line along 30-32°S, to the north of New Zealand. ASH – Aragonite saturation horizon at 1200 m, CSH – Calcite saturation horizon at 3250 m in the Tasman Sea, and 2800 m in the South Pacific basin.

4.3. Summary

From this expanding dataset of alkalinity and DIC for the waters around New Zealand, it is evident that there are large variations in the carbonate saturation states in the region. These variations are the result of the different intermediate and deep-water water masses and currents that affect the region due to the complex topography. While we have significantly increased the number of water sampling sites within the New Zealand EEZ during this project, the coverage is still sparse.

We recommend that continued opportunistic water sampling is undertaken for alkalinity and DIC to improve the coverage of the New Zealand region and to monitor changes in the carbonate saturation states with future climate change as well as to ground-truth the alkalinity and DIC estimates from the hydrographic data (see Section 4.4. below).

4.4. Carbonate chemistry estimates from algorithms
 (For full details see Bostock et al. 2013, Biogeosciences)

The coverage provided by the water samples in the WOCE and the NIWA voyages since 2008 is insufficient to produce a detailed map of the aragonite and calcite saturation horizons given the complex topography and oceanography of the New Zealand region.

We have developed a way to estimate the carbonate parameters from the more detailed hydrographic data for the region. We used multiple linear regressions (MLR) to determine the relationship between carbonate species and hydrographic data for stations where there are existing carbonate data. These relationships are then used with high resolution hydrographic data to obtain improved spatial resolution of the carbonate parameters. This MLR approach was first used to predict carbonate species by Wallace (1995), based on observations that carbon exhibited strong correlations with other oceanographic parameters (Brewer et al. 1995). Over the last couple of decades, several publications have used MLR techniques to estimate the carbonate parameters (or carbonate saturation), and changes in anthropogenic carbon uptake from hydrographic measurements (e.g., Archer 1996; Brewer et al. 1997).

4.5 Regression method

In this approach, we treat the observed DIC and alkalinity (Alk), from the WOCE/CLIVAR cruises as a linear combination of temperature, (T), salinity, (S), with a background salinity of 35 removed, dissolved oxygen, (O_2), and a constant offset, (C),

$$DIC = \alpha T + \beta (S - 35) + \gamma\, O_2 + C$$

$$Alk = \alpha T + \beta (S - 35) + \gamma\, O_2 + C,$$

where T has units of °C and DIC, Alk, and O_2 have units of µmol/kg. Then, a Singular Value Decomposition (SVD) is used to determine the best values of the parameters α, β, γ, and C to fit the observations.

Table 4.2: Coefficients and constants, Residual Standard Error (RSE) and R^2 for the MLR algorithms.

Depth	Parameter	Coefficients for T, S-35, dissolved O respectively				RSE	R^2
		α	β	γ	Constant		
Intermediate	Alk	-7.418	96.957	-0.079	2412.5	9.8	0.91
(200 m to <27.5±0.05 σ_θ)	DIC	-14.866	53.682	-0.569	2410.5	7.3	0.98
Deep (>27.5±0.05 σ_θ)	Alk	-17.027	100.25	-0.663	2543.4	9.8	0.91
	DIC	-23.154	13.524	-1.017	2493.6	7.3	0.98

We have excluded the surface waters (0–200 m) as these are highly variable and have very large errors and will require regional algorithms. For this project, we focussed on the intermediate and deep waters as our aim was to provide better estimates of the aragonite and calcite saturation horizons (ASH, CSH) for the Southern Hemisphere Oceans, including the SW Pacific, in relation to deep-water corals and fisheries. The cut off between intermediate and deep waters was undertaken on a density surface rather than a depth. This allows the shoaling of intermediate and deep waters in the Southern Ocean to be more easily accounted for. For more information on the data handling and method see Bostock et al. (2013; Biogeosciences Discussions).

The independent NIWA water data analysed for alkalinity and DIC (Section 4.1) were then used to ground-truth these algorithms, and, together with the CSIRO Atlas of Regional Seas (CARS) climatology, used to produce detailed maps of the ASH and CSH for the New Zealand region.

4.6. Results

There is a very good correlation between measured and estimated DIC, and a slightly lower correlation for alkalinity (Table 4.2). The largest residuals in these estimates are present in the thermocline waters and the NPDW (Bostock et al. 2013). However, calculation of the aragonite and calcite saturation states for the Southern Hemisphere oceans using CO2Sys program showed a good correlation between the values determined from the measured versus estimated alkalinity and DIC. Carbonate ion concentrations have an $R^2 = 0.96$, Residual Standard Error (RSE) = ±4 µmol/kg, while Ωaragonite and Ωcalcite have a $R^2 = 0.99$, RSE = ±0.05 and ±0.08, respectively (Figure 4.8). This is just greater than the overall uncertainties of the aragonite and calcite saturation state calculations of ±0.03 and ±0.05, respectively (Mucci 1983; Millero 1995; Feely et al. 2012).
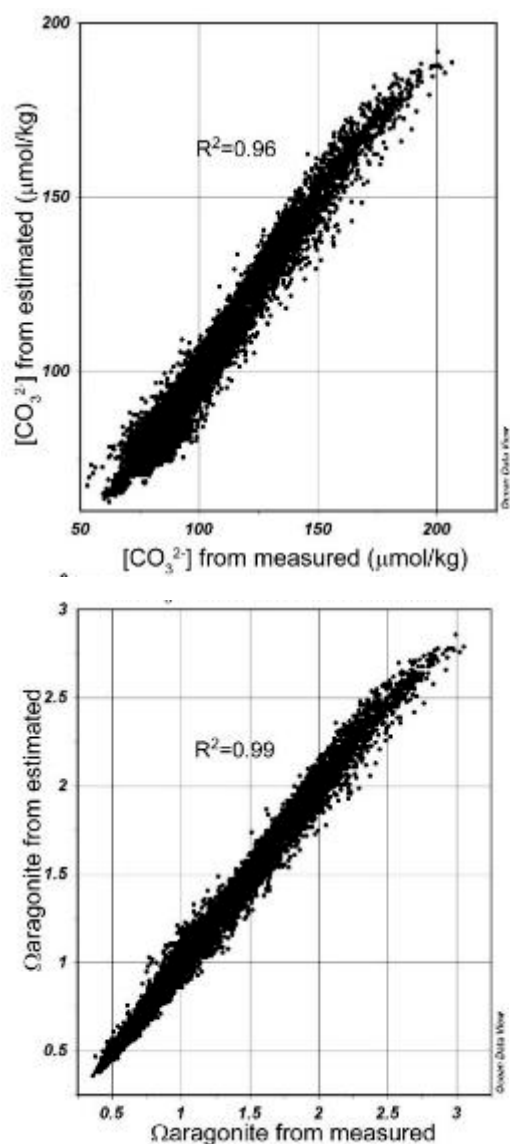
Figure 4.8: Comparison between the carbonate ion [CO32-], aragonite and calcite saturation calculated using measured alkalinity and DIC and estimated alkalinity and DIC using this algorithm.

As an independent test of these algorithms, we compared the measured alkalinity and DIC collected in Section 4.2 with alkalinity and DIC estimated from the hydrographic data at the same stations and depths using the algorithms. The correlation is very similar to the R^2 values for the original GLODAP data used to develop the algorithms (Figure 4.9). Thus, we are confident that the algorithm will work in the New Zealand region. However, with increasing CO_2 uptake by the ocean the algorithms will change over time and we will need to continue to collect and measure alkalinity and DIC samples around New Zealand to monitor these changes.
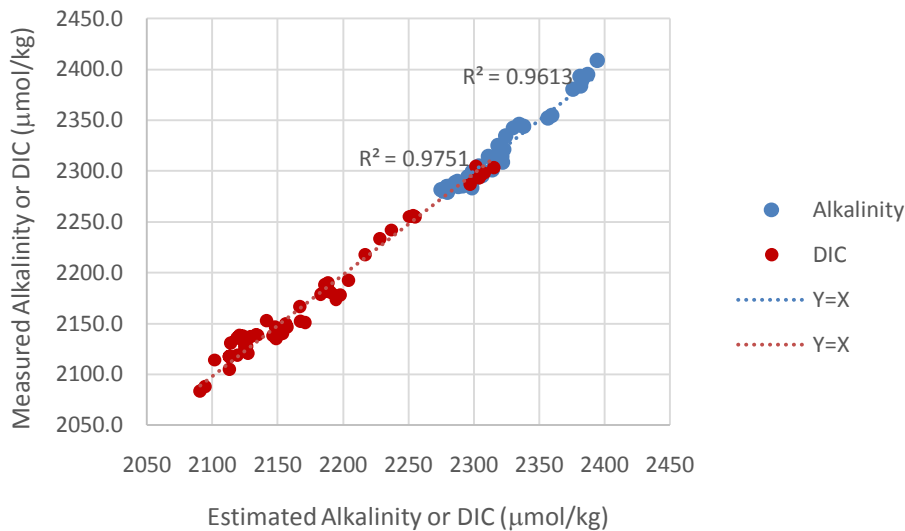
Figure 4.9: Measured alkalinity and DIC for >200 m from the NIWA voyages versus estimated using the hydrographic data and the algorithms from these same stations. The correlation between the measured and estimated is very similar to the original GLODAP data used to develop the algorithm.

The detailed ASH and CSH maps produced using CARS (Figure 4.10), show a significant improvement to the original GLODAP extrapolation across the SW Pacific (Figure 4.2). The new maps agree with the hydrography of the region and take into account the complex topography. The largest differences in the ASH are seen to the southeast of New Zealand, over the Campbell Plateau, where there is a significant shoaling of the ASH, not evident in the GLODAP map (Figure 4.2). For the CSH, the topography plays a significant role. The south Tasman Sea and southern New Zealand have fresh CDW and AABW coming in directly from the Southern Ocean. These younger, fresher water masses have lower DIC and alkalinity and therefore the CSH is deeper. To the north, the CSH is shallower due to the influence of the old, high DIC, high alkalinity NPDW.

We recommend that these maps are used to target future water sampling in the region, both to determine where to carry out the sampling and at what depths. These algorithms are only suitable for the intermediate and deep waters around New Zealand.
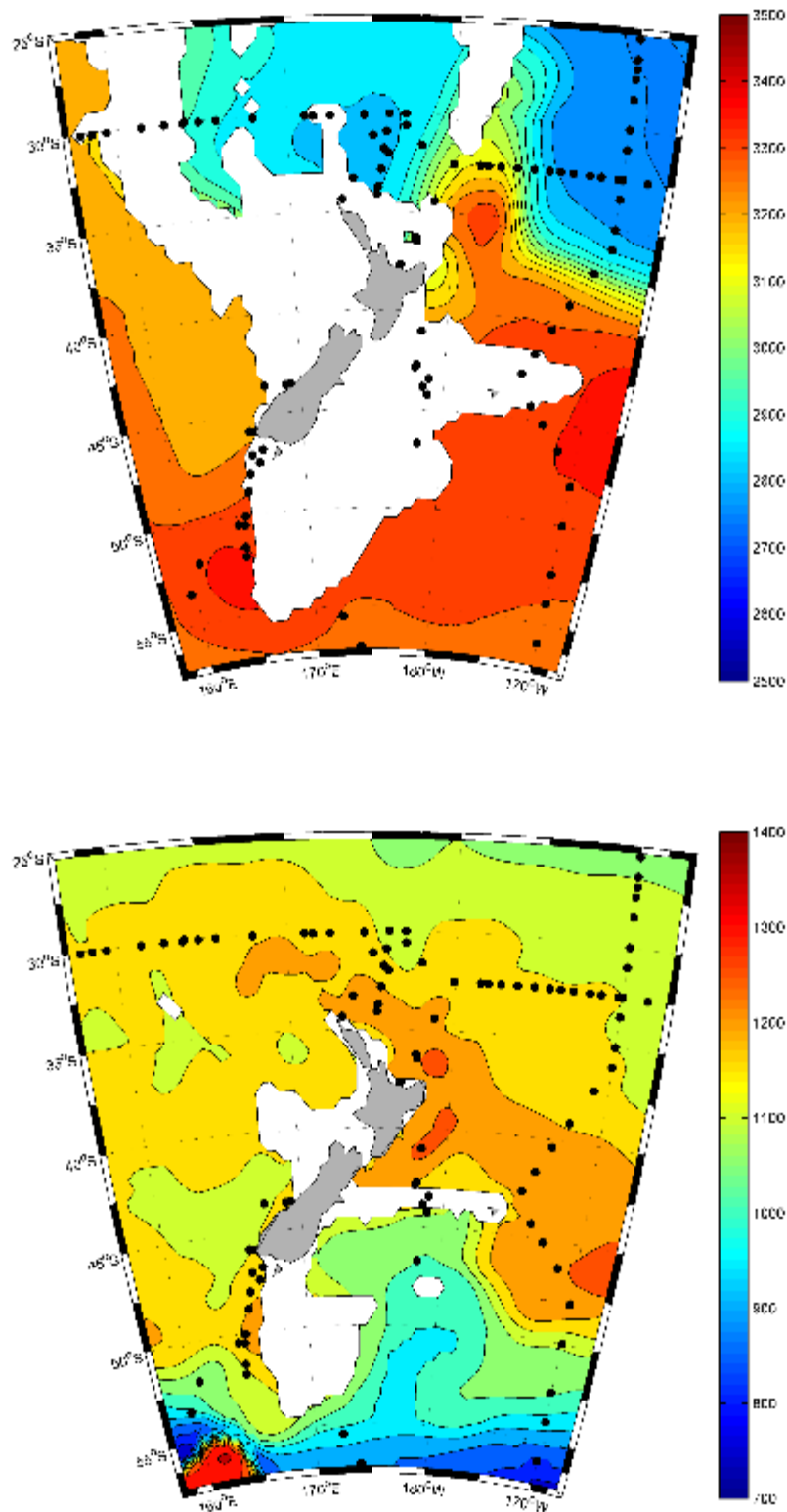
Figure 4.10: Detailed maps of the calcite (CSH) (top) and aragonite (ASH) (bottom) saturation horizons using the NIWA algorithms and the CARS climatology for the New Zealand region. The location of the World Ocean Circulation Experiment (WOCE) and NIWA stations where alkalinity and DIC were sampled on recent *Tangaroa* voyages is shown by black dots. These data were used to validate the model results. The white region represents topography (habitat for corals) shallower than the ASH and CSH.

We have overlain the current ASH and CSH data lines (present day and predicted) in Chapter 5 and discuss the overlap with fishery areas.

4.7. Modelling studies to identify the risk of additional ocean acidification due to upwelling

Most ocean acidification research to date has focused on ocean acidification that results from CO_2 being absorbed from the atmosphere and decreasing the pH of the oceans (e.g. Orr et al. 2005). However, several recent studies have demonstrated that changes in ocean physics, in response to climate change, can play a critical role in accelerating ocean acidification in some regions, such as the coastal region (e.g. Feely et al. 2008.) In regions with strong upwelling, DIC-rich deep waters are brought to the surface, leading to more acidic surface waters. This occurs naturally as a result of ocean dynamics, but recent changes in climate linked to anthropogenic climate change have led to more vigorous upwelling in many of these regions, enhancing this upwelling-driven ocean acidification. Furthermore, future changes in climate are expected to further enhance upwelling-driven acidification (e.g. Gruber et al. 2012; Lakhar & Gruber 2013.)

One aim of this study is to use high-resolution regional modelling to characterise the upwelling in New Zealand's EEZ at depths that are critical to New Zealand fisheries and undertake a preliminary assessment of the risk of upwelling-driven ocean acidification. To this end, we have used the Regional Ocean Model (ROMS) to investigate upwelling in the present-day climate and identify potential risk areas. This model has been used in other published studies investigating the role of upwelling on ocean acidification (e.g. Gruber et al. 2012; Lakhar & Gruber 2013). We have chosen four depths as the focus for our study: 200 m; 500 m; 750 m and 1250 m. A reasonable amount of vertical continuity would be expected in the ocean, so these depths should be considered fairly representative. The range also covers inhabited depths of middle-depth (hoki and scampi), and deepwater (orange roughy, black cardinalfish, and oreo) species.

4.7.1 Model description

ROMS is an ocean model that has been applied to a variety of problems on ocean basin- to coastal- and estuarine-scales (Haidvogel et al. 2000; Marchesiello et al. 2003; Wilkin et al. 2005; Hadfield et al. 2007). The ROMS hydrodynamic core solves the free-surface, hydrostatic, primitive equations on a grid with a stretched, terrain-following vertical coordinate and curvilinear, orthogonal horizontal coordinates (Song & Haidvogel 1994, Shchepetkin & McWilliams 1998; 2003; 2005). We employed the Rutgers University version of ROMS, which was updated in March 2013.

The grid covered the ocean around New Zealand region (Figure 4.11) at a horizontal resolution of 10 km. With the exception of the surface stress, we used climatological forcing, following the work of Rickard et al. (2005), but with a different model and different forcing datasets. Lateral boundary conditions were based on a monthly climatology calculated from 10 years' output of the Simple Ocean Data Assimilation (SODA) global ocean reanalysis, version 1.4.2 (Carton & Giese 2008). Surface fluxes (other than stress) were from the NCEP Reanalysis monthly climatology (Kalnay et al. 1996), with nudging of sea-surface temperature (SST) towards a monthly climatology from the NOAA optimum interpolation SST analysis (Reynolds et al. 2002). The surface stresses comprised twelve-hourly data from NOGAPS (http://www.usno.navy.mil/FNMOC) beginning on 1 January 2005, with stresses scaled up by a factor of 1.4 to improve agreement with velocity data on the continental shelf.

In order to investigate carbonate species and other ocean biogeochemical tracers, the ROMS ocean model has been coupled with the Pelagic Interaction Scheme for Carbon and Ecosystem Studies (PISCES) ocean biogeochemistry model (Echevin et al. 2008). The biogeochemical boundary conditions were taken from a global model simulation using the same biogeochemical model (Aumont

2003; Aumont & Bopp 2006.) The model was run for 1800 days and statistics calculated from the last two years based on 4-day average output.

4.7.2 Identifying upwelling regions from model simulations

Contemporary upwelling regions can be identified by analysing gradients in DIC observations. Local high values of DIC can reflect upwelling from deep carbon-rich waters that might potentially lead to additional ocean acidification. Figure 4.11 shows the mean DIC (left column) as a reference point; the amplitude of the seasonal cycle based on a seasonal harmonic fit to the data (centre column) as a metric for the strength of seasonal upwelling; and the standard deviation of the residuals between the modelled value and the harmonic fit (left column) to investigate sub-seasonal variability in upwelling.

This figure suggests that upwelling is not likely to be a substantial contributor to ocean acidification in the New Zealand EEZ. Upwelling is currently leading to increases in DIC of less than 30 μmol/kg, and usually less than 15 μmol/kg, throughout most of New Zealand's EEZ, which is small relative to increases that are expected due to the uptake of CO_2 from the atmosphere over the next century.

The strongest upwelling effects occur at the 200 m depth range. At this depth, seasonal and intra-seasonal upwelling is the strongest in the Tasman Sea, most likely due to eddies from the East Australia current. Elevated DIC values also suggest that upwelling may be occurring over the Hikurangi Plateau and Southwest Pacific Basin, which is probably due to movements of frontal systems. Below this depth range, seasonal and intra-seasonal perturbations to DIC are generally less than 10 μmol/kg, with the strongest perturbations occurring over the Southwest Pacific Basin and in the southwest corner of New Zealand's EEZ, most likely due to seasonal variations in upwelling along the oceanographic fronts associated with the Antarctic Circumpolar Current in the Southern Ocean.
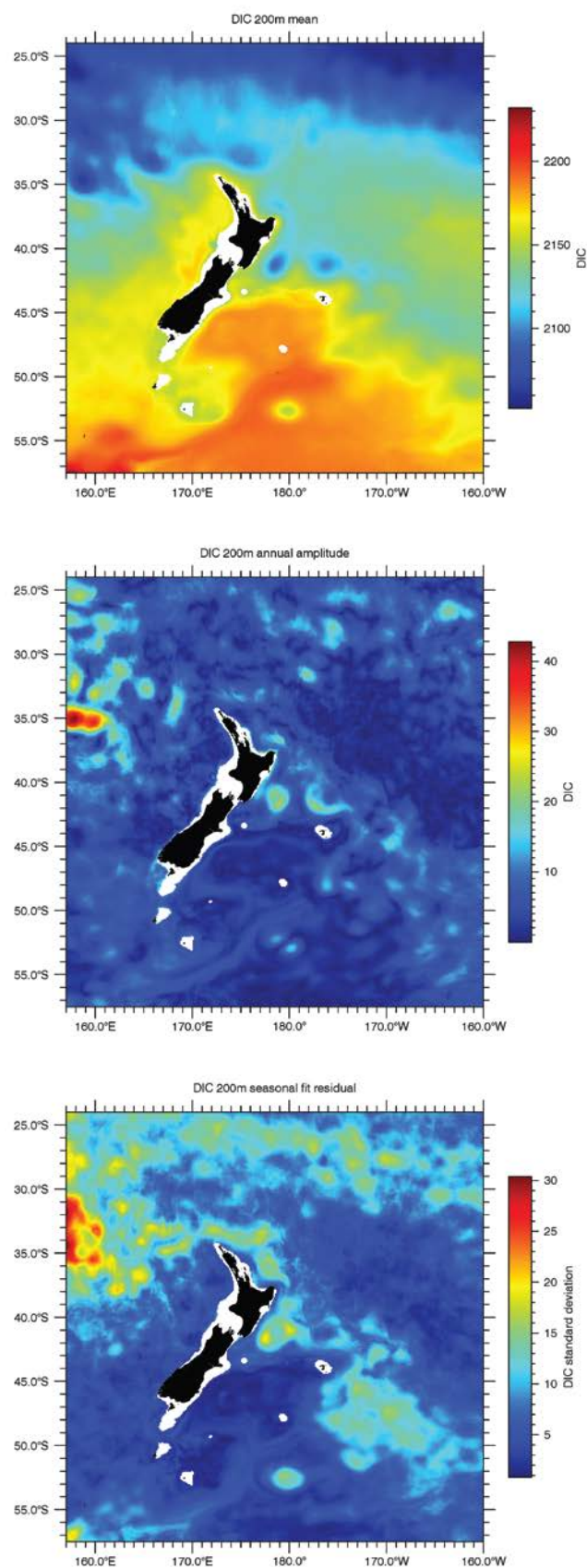
Figure 4.11a: Dissolved inorganic carbon (DIC) in units of μmol/kg modelled using the ROMS model coupled to the PISCES biogeochemistry model at 200 m water depth. Top: mean DIC, middle: seasonal amplitude and bottom: standard deviations from the seasonal amplitude.
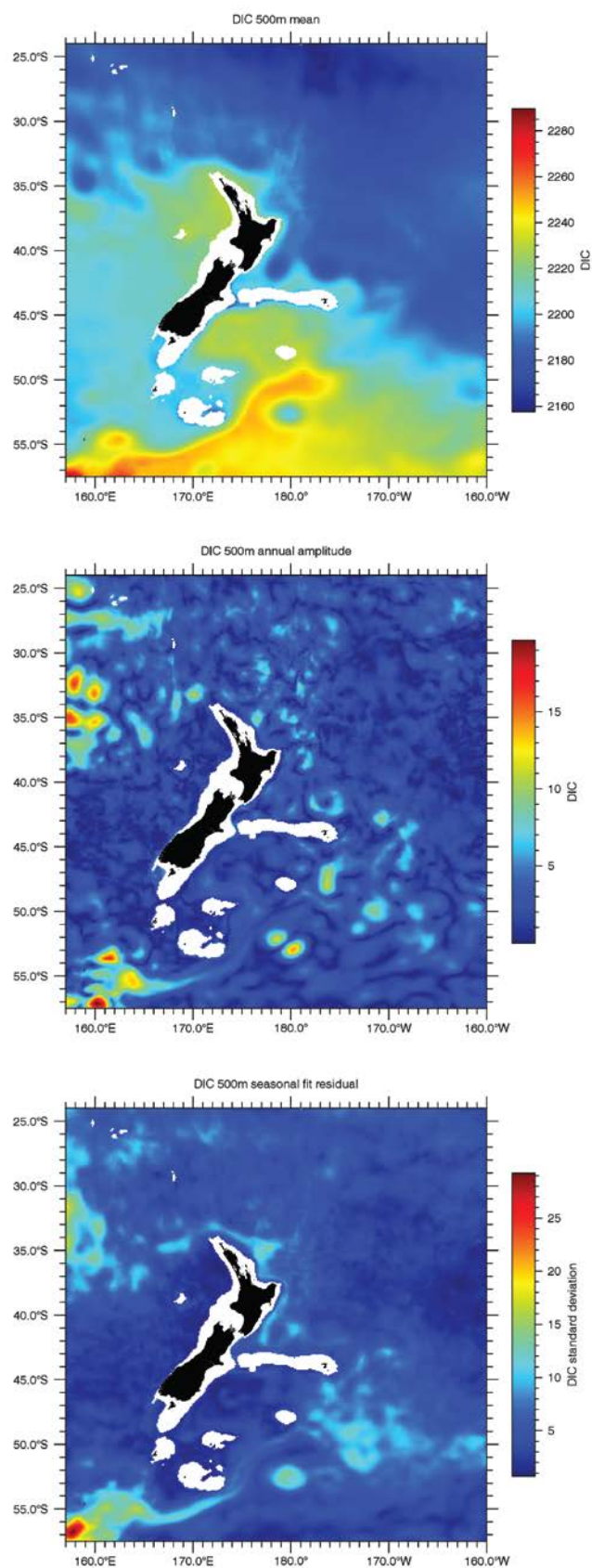
Figure 4.11b: **Dissolved inorganic carbon (DIC) in units of μmol/kg modelled using the ROMS model coupled to the PISCES biogeochemistry model at 500 m water depth. Top: mean DIC, middle: seasonal amplitude and bottom: standard deviations from the seasonal amplitude.**
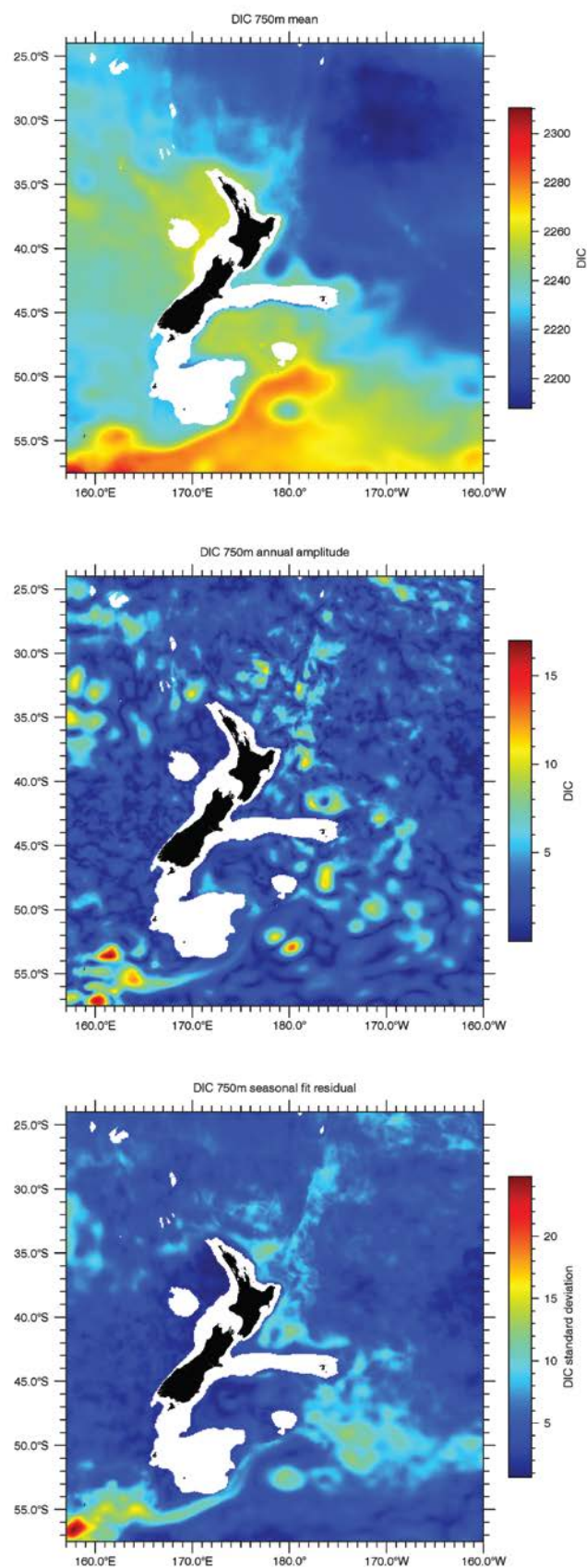
Figure 4.11c: Dissolved inorganic carbon (DIC) in units of µmol/kg modelled using the ROMS model coupled to the PISCES biogeochemistry model at 750 m water depth. Top: mean DIC, middle: seasonal amplitude and bottom: standard deviations from the seasonal amplitude.
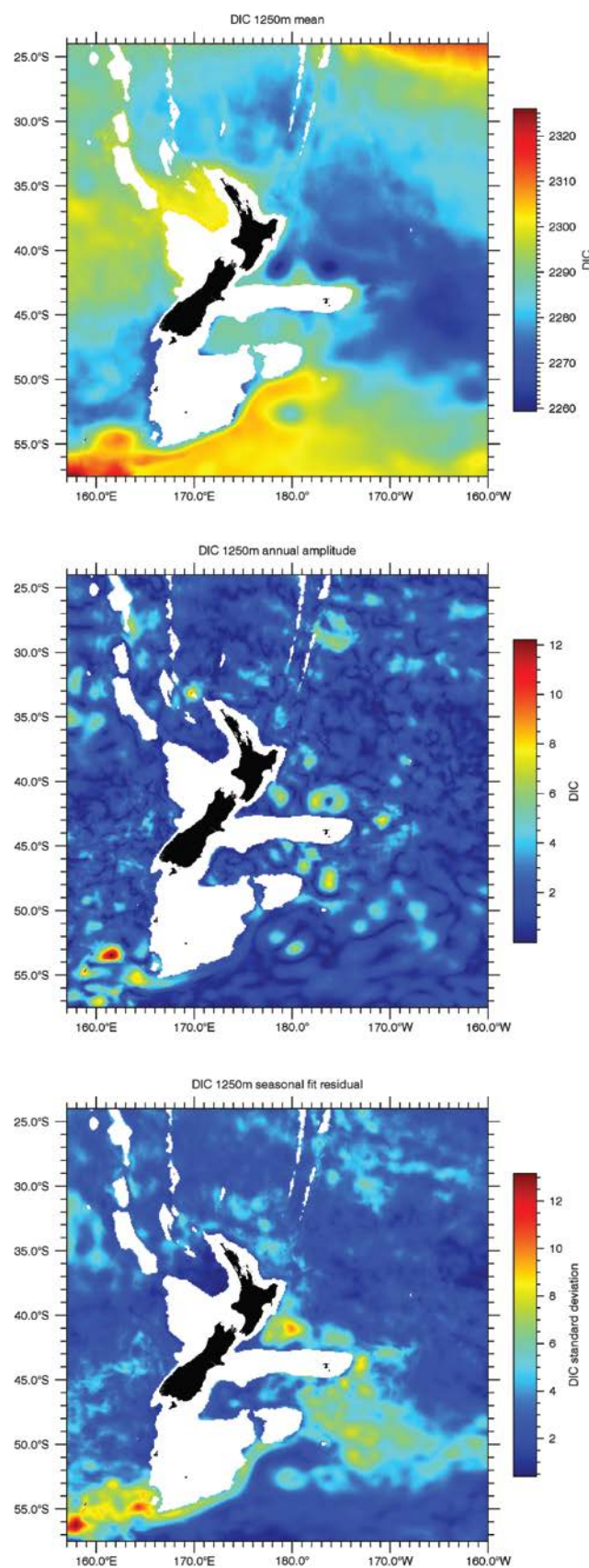
Figure 4.11d: Dissolved inorganic carbon (DIC) in units of μmol/kg modelled using the ROMS model coupled to the PISCES biogeochemistry model at 1250 m water depth. Top: mean DIC, middle: seasonal amplitude and bottom: standard deviations from the seasonal amplitude.

4.7.3 Determining the risk of increased upwelling in response to wind or storminess events

The simulations described above were conducted using climatological forcing fields and boundary conditions. As a result, they capture seasonal variations and provide an estimate of the mean magnitude of intra-seasonal variability; however, they do not capture synoptic scale events such as storms, which may intensify under future climate change. In order to evaluate the potential effect of synoptic scale events, we introduced an artificial depth tracer into the model. This depth tracer was initially set equal to the depth at each grid point and was continuously nudged toward the local depth with an exponential time scale of 60 days. Deviations from the local depth are therefore evidence of vertical motion and/or vertical mixing in the last 60 days or so.

Simulations using this depth tracer (Figure 4.12) show that on these time scales vertical motion is generally quite modest over the New Zealand EEZ. However, there is some substantial ventilation of deeper waters occurring at the 500 m depth range south and especially southwest of New Zealand.

Based on these model simulations, we find little risk of substantial upwelling-driven acidification in the New Zealand EEZ. Model simulations for the current period suggest that upwelling-driven perturbations to DIC are generally less than 30 μmol/kg. Under future climate change, some of these upwelling features may strengthen. In order to fully quantify this effect, a future projection using a high resolution regional model such as ROMS forced with boundary conditions from an earth system model (e.g. Gruber et al. 2012; Lakhar & Gruber 2013) would be needed. Capability is available to undertake such simulations at NIWA; however, this preliminary analysis suggests that local upwelling effects are likely to be a second-order contributor, after anthropogenic CO_2 uptake, to ocean acidification in the New Zealand EEZ.
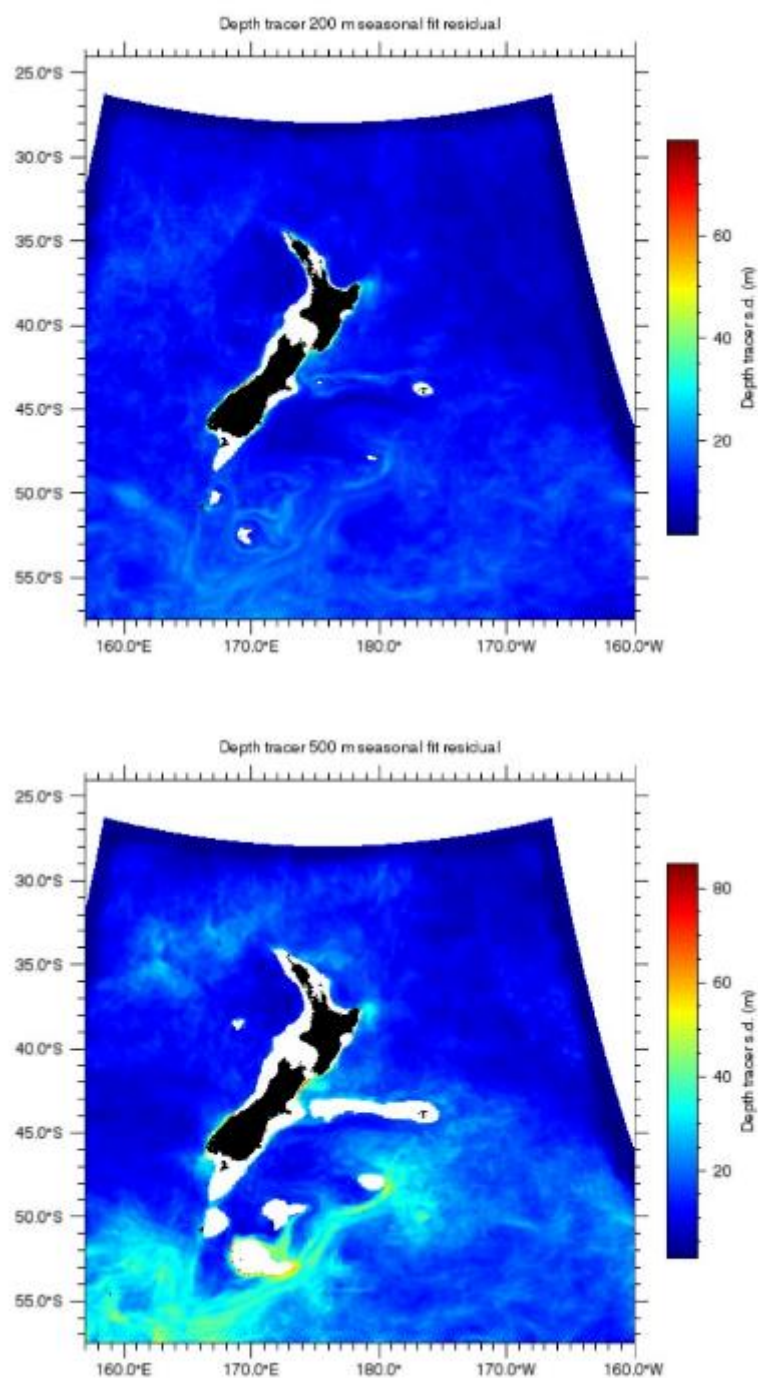
Figure 4.12: Simulations of a depth tracer in the ROMS ocean model at 200 m (top) and 500 m (bottom). This depth tracer is initially set to the depth at each model grid point. Non-zero values indicate vertical motion.

Chapter 5. COMPARISON OF THE DEEPSEA CORAL DISTRIBUTION WITH CARBONATE SATURATION STATES AND FISHERIES AREAS

Helen Bostock and Di Tracey (NIWA)

It has been suggested that the depth and spatial distribution of aragonitic habitat-forming scleractinian corals is controlled by the ASH (Guinotte et al. 2006; Davies & Guinotte 2011; Tittensor et al. 2010). Similarly, benthic habitat models for gorgonian corals also indicate that calcite saturation state is an important factor (Yesson et al. 2012).

This section compares the coral depth distribution from Section 2, and the knowledge of the mineralogy in Section 3, with the new detailed ASH maps for the New Zealand region discussed in Section 4.2 (Figure 4.10). We have compared both the aragonitic scleractinian and the high Mg calcite gorgonians to the ASH, because 8–12 mol% $MgCO_3$ has similar solubility to aragonite (Walter et al. 1984; Figure 5.1 and 5.2). *Primnoa* sp. are included with the other gorgonian genera. FMA boundaries are shown to enable the consideration of the potential impact of ocean acidification on deep-sea corals and fisheries habitat.

Approximately 11% of scleractinian corals live below the current ASH, with 89% shallower. The fact that 9% live just below the ASH (less than 200 m) may be historical as we know that these deepsea corals are slow growing, and may have started growing above the ASH, which has since shoaled (Feely et al. 2012). Or alternatively they can tolerate some undersaturation. The species with the highest number of individuals found living below the ASH is *S. variabilis*. It is possible that different species have different tolerances to undersaturation. *Goniocorella dumosa* on the top of the Chatham Rise, *Oculina virgosa* in the shallow northern waters for example.

The gorgonians show a similar undersaturation tolerance; 17% live below the current ASH, and 83% are found above (Figure 5.1). This may be due to the fact that they may have some control over their Mg content, and that the ASH is not a perfect analogy for the high Mg calcite saturation horizons (which will vary according to their Mg content). Some of these corals may be able to tolerate minor undersaturation, with *Keratoisis* spp. being the most tolerant and *Paragorgia* spp. the least tolerant of undersaturation.
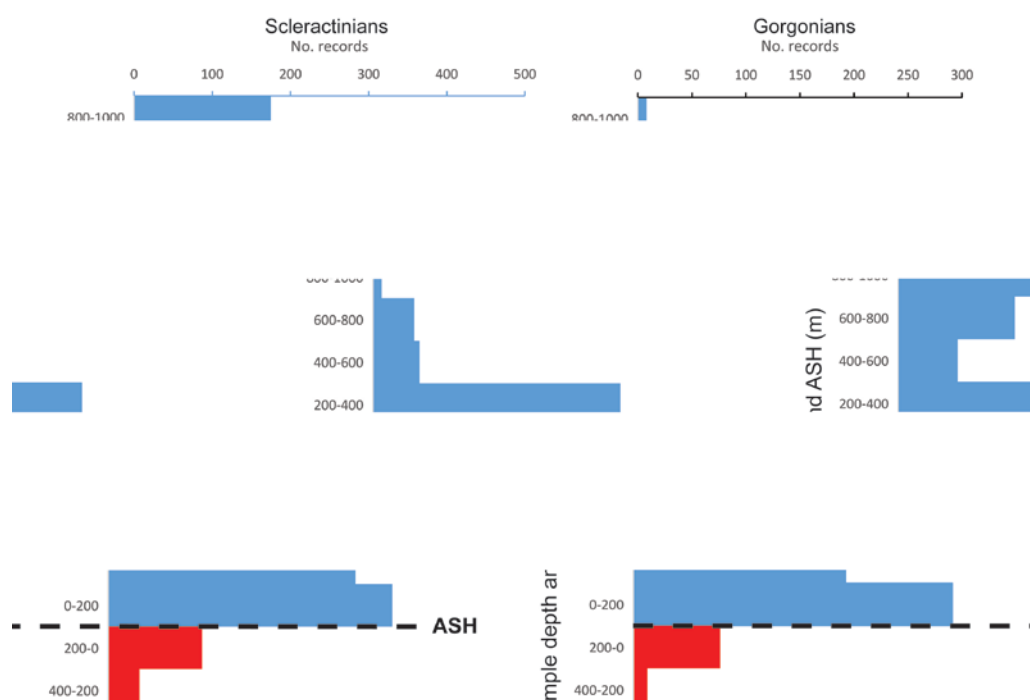
Figure 5.1: Difference between the average depth of the coral sample and the ASH at the same location (Figure 4.10).

Thus it would appear that the carbonate saturation state may have a strong control on the distribution of these organisms. However, this will be in combination with other environmental variables such as depth, location relative to a seamount, tidal current speed, particulate organic carbon flux, and level of primary production (Tracey et al. 2011a; Baird et al. 2013, and temperature, oxygen, salinity, food supply, or substrate (Tittensor et al. 2009; Davies & Guinotte 2011; Yesson et al. 2012). Sampling bias cannot be ruled out as the majority of deep samples in the New Zealand region have been collected from less than 1500 m, with significantly less recovered from more than 1500 m (Tracey et al. 2011a).

Global ocean carbon cycle models suggest that under a stabilisation scenario (IPCC-S650, atmospheric CO_2 = 563 ppm in the year 2100), the ASH will shoal to 600 m in the New Zealand region (Orr et al. 2005). Assuming this climate change scenario, that scleractinian corals are controlled by aragonite saturation state, and that there is no change in the ocean circulation, stratification or upwelling, then only 28% of the current known scleractinian corals in the New Zealand region would sit above the predicted 2100 ASH. In stark contrast, only 7% of the gorgonian corals would sit above the predicted 2100 ASH (Figure 5.1).

Under this scenario, the main remaining habitat for these coral groups in the New Zealand region would be the continental shelf, top of Chatham Rise, and small pockets on the Campbell Plateau including Pukaki Rise, Campbell Rise, Bounty Plateau and around the Auckland Islands, small patches along the Macquarie Ridge and the tops of Kermadec seamounts that rise above 600 m water depth (Figure 5.2). This does not take into account other factors that may impact where the habitat-forming deep-sea corals live, such as temperature.
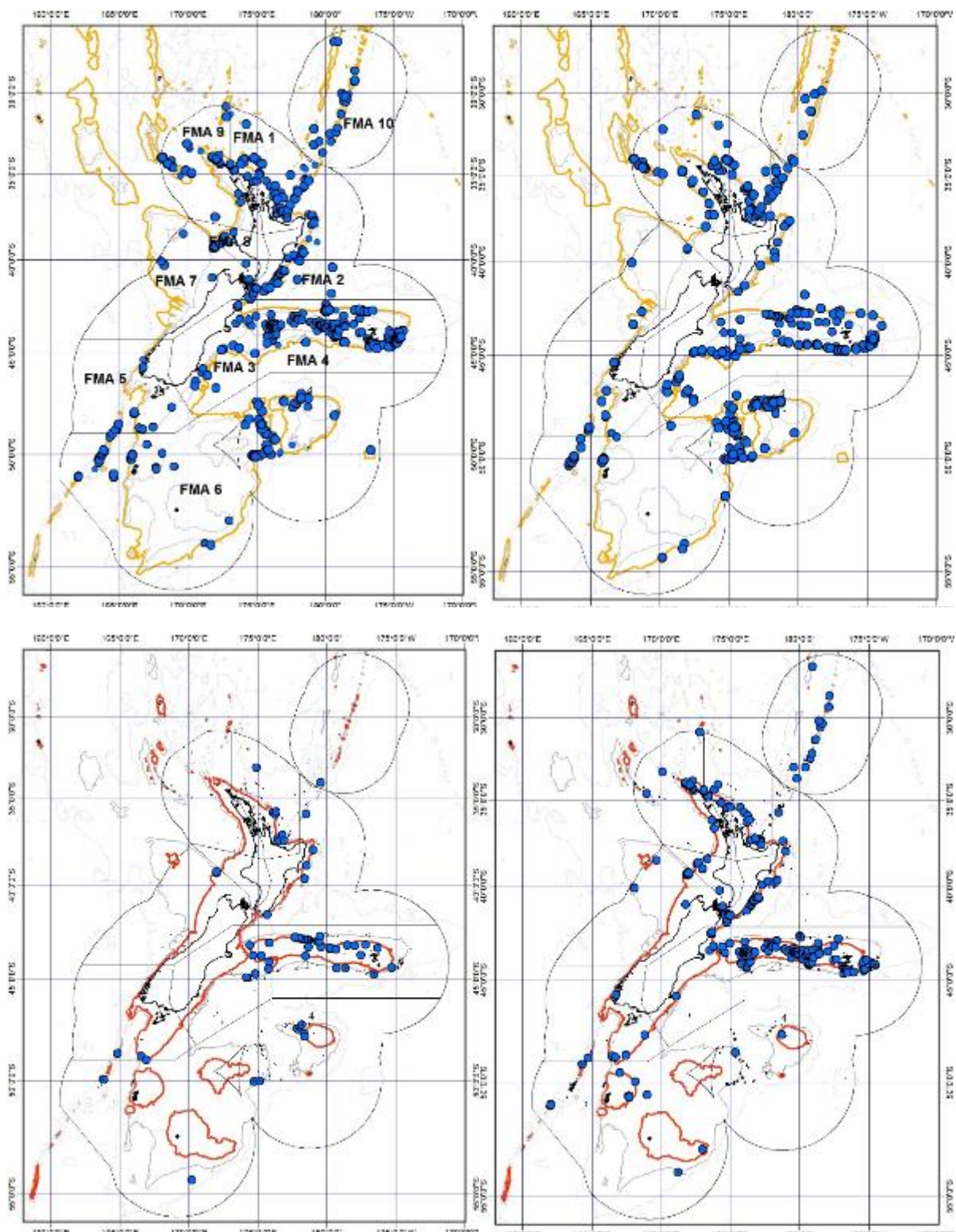
Figure 5.2: Top maps – Left: the distribution of scleractinian corals with the current ASH as an orange line (horizon depth varies from 1000–1250 m, equivalent to the white area in Figure 4.10). Fishery Management Area (FMA) boundaries are shown by the black lines. Right: the distribution of gorgonian corals with the current ASH. Bottom maps - Predicted ASH of 600 m for 2100 under scenario S650 – shown as a red line. Left: blue dots show the distribution of scleractinians that will sit above the predicted 2100 ASH, right: blue dots show the distribution of gorgonians that will sit above the predicted 2100 ASH.

As shown by overlaying the FMA boundary layers with the ASH and CSH line and coral distributions, several deepsea fisheries overlap with the areas including those for orange roughy and

oreos. Tracey et al. (2011b) and Baird et al. (2013) provide more detail of the overlap for these and other fish species. Under a business as usual scenario (IPCC-IS92a, atmospheric CO_2 = 788 ppm in the year 2100) the ASH is predicted to shoal to 100 m (Orr et al. 2005). This would leave only the small number of *O. virgosa* sitting above the predicted ASH. Clearly, the saturation horizon will be above the depth the corals currently prefer and as such the habitat they provide for other invertebrates, and are assumed to provide for the benefit of fishery populations, will disappear. A significant proportion of the records *Goniocorella dumosa* are from the top of plateaus and rises – particularly from the Chatham Rise, this species may have an important future role as providing refuge.

5.1   Future work

We suggest that future work using benthic habitat models should include carbonate saturation states, along with other more typical environmental variables. We recommend that the high Mg calcite corals are compared to high Mg calcite saturation states, rather than the ASH. This was beyond the scope of this study as there are currently no standard formulae to calculate the Mg calcite saturation states.

While we have compared the coral distribution with the models of predicted ocean acidification by 2100 (Orr et al. 2005), there are some new improved models available. We recommend a future project to look at the latest global climate models outputs (from the CMIP5 project) coupled with a high resolution ROMS model to determine how the oceans around New Zealand might be affected by chemical and physical climate change and the implications for suitable spatial and depth habitat for these habitat forming deep-sea corals in 2100. Recent modelling for the southern Australian region suggests that the area of suitable habitat may be further reduced by increases in temperature at intermediate depths (Thresher CSIRO, pers comm.).

Currently our Australian and U.S. collaborators are continuing their work on effects of climate change on Australia's deep marine reserves (Thresher et al. 2012) by developing a predictive model as to the "likely impacts of climate change, in general, and ocean acidification in particular, on the long-term viability of the deep *Solenosmilia* reefs in Australian waters". The Australian research parallels some of the work described in this project. To help manage the impacts of OA various options are being investigated by Ron Thresher and John Guinotte (Marine Conservation Institute, U.S.A.) to help reduce the exposure and sensitivity of scleractinian corals. Proposals as part of a cost benefit analysis of their research includes mitigation and adaptation options, for example:
- moving corals to shallower regions,
- artificially enhancing recruitment, and
- restricting benthic habitat impact from commercial fishing and other human activities in specific locations.

Chapter 6.   DEEP-SEA CORAL AGE AND GROWTH, METHODS TO ASSESS OCEAN ACIDIFICATION

Helen Neil, Claire Guy (NIWA)

In this Chapter, we summarise current knowledge of: (1) tools to age deep-sea, habitat-forming corals; and (2) potential impacts of ocean acidification on deep sea habitat forming corals; From the review, recommendations on the best approach for future assessments of the direct effects of changes in ocean pH on these key fauna are then made.

6.1   Cold Water Coral Age and Growth

Deep-water organisms are often considered to be slow growing and long lived, with growth and longevity difficult to measure – the deep-sea or cold-water corals are no exception. Azooxanthellate corals are considered to have low growth (and calcification) rates due to the absence of symbiotic algae and the associated photosynthetic activity enhancing calcification (e.g. Goreau 1959; Pearse & Muscatine 1971). Cold-water coral biology and the ecological aspects of cold-water corals are often unknown or have only been examined in the past decade, with recent studies summarised by Freiwald et al. (2004) and Roberts et al. (2009). Important factors that can exert control on the age and growth (and distribution) of cold-water corals are hydrographic and environmental parameters such as temperature, salinity, ocean chemistry and nutrient supply and the geomorphology of the seabed, as well as reproduction and predation.

The strong dependency of coral distribution on the saturation state of aragonite and calcite is noteworthy. A reduction in the availability of carbonate ions through acidification of the oceans will potentially limit the ability of stony and gorgonian corals to form their hard skeletons and, therefore, affect the amount of suitable biogenic habitat they provide for invertebrate taxa including other corals, and fish. Our ability to assess the potential recovery rate of these habitats and their associated communities is at present limited by our lack of knowledge on the age and growth of the main New Zealand coral species.

The deep-sea coral groups, which are the focus of this project, are the branching stony (scleractinia) and selected gorgonian corals (gorgonacea). Both have skeletons comprised of calcium carbonate, are vulnerable to OA-associated dissolution, and are the only two groups within New Zealand to have been subject to initial age and growth studies.

6.1.2   Growth Rates

Some research on the age and growth of deep sea corals has been conducted, although the number of estimates available globally for the key branching stony coral species are small in number. It is difficult to assess growth and calcification rates in cold water corals due to their inaccessibility (depth of habit), lack of annual banding (in many cases), and slow rates of growth.

Despite this, there have been various studies estimating growth and longevity of cold water corals, many of which are summarised in Table 6.1, which is modified and updated from Roberts et al. (2009) and references therein. Studies focussing on scleractinians and gorgonians typically determine and report growth as linear extension rates or radial thickening rates, respectively. This is primarily due to the nature of skeletal and colony formation within these two groups of deeepsea corals, such that the height (linear extension) a 3-D matrix forming scleractinian colony may develop to above the seafloor can be more readily derived than branch thickness (radial growth). In contrast, branch thickness is defined for gorgonians, driven by both their long life spans (and therefore significant height above seafloor such that complete colonies are often unable to be collected) and the desire by researchers / paleoclimate researchers to use the full lifespan of these cold water corals as environmental archives.

A range of ageing techniques including direct observation, linear measurement, visual growth band patterns and indirect geochemical analyses have been used. There are a number of potential advantages and disadvantages inherent within each technique, which are elucidated within publications referenced in Table 6.1. Cold water corals have been demonstrated to be slow growing (0.5 to 25 mm per year), an order of magnitude lower than those of branching tropical symbiotic corals, which grow at a rate of 100 to 200 mm per year (e.g., Buddemeier & Kinzie 1976), but about the same as most massive tropical corals (e.g., Freiwald et al. 2004). However cold water corals exhibit high variability in morphology and growth rates both between and within the cold water coral species, probably reflecting differing environmental, ecological and competitive conditions, and adaptive abilities (e.g., Freiwald et al. 2004; Roberts et al. 2009; Orejas et al. 2011a; (Orejas et al. 2013). Cold water corals also display allometric growth and linear extension rates that are considered to decrease significantly with increasing age. Studies of *Lophelia pertusa* indicate that the highest growth is associated with the early stages of polyp growth and that rapid growth can be followed by periods of slow growth (i.e. episodic growth events; Mortensen 2001; Brooke & Young 2009; Gass & Roberts 2006).

Although data on cold water coral growth rates are sparse, some trends relating to the controls on growth are evident e.g., cold water corals removed from surface production, typically deep corals, grow slower than those in shallower waters (Roberts et al. 2009), when considering both linear extension and radial thickening rates. Although little work has been done to date on environmental controls, both temperature and food supply differences would be expected.

6.1.3   New Zealand Deepsea Coral Growth Rates

While there is little information on cold-water coral growth around New Zealand, two studies have looked at the age of: (a) the most abundant matrix-forming scleratinian, *S. variabilis*, and (b) the gorgonian family of bamboo corals. These studies are summarised below. In addition, a single age has been derived via $\Delta^{14}C$ from the gorgonian *P. arborea*, bubblegum coral, from south of New Zealand, indicating an age of 300–500 years for a single colony (Tracey et al. 2003) or an estimated linear growth rate of 15–25 mm per year.

6.1.4   Growth rates –stony branching coral Solenosmilia variabilis

One of the most widespread species in the South Pacific is *S. variabilis*. In a preliminary study, a first assessment of the age of this species was made using linear measurement and radiocarbon content ($\Delta^{14}C$). Linear growth rates ranged from 0.4 to 1.6 mm year^{-1}, while colony growth rates, estimated as a straight line from base to growing tip, were reported to range from 0.3 to 1.3 mm year^{-1} (Neil et al. in review). These rates are consistent with those reported for other cold water corals (See Table 6.1), in particular *L. pertusa*, with estimated linear growth rates of 5 and 34 mm year^{-1} (e.g., Mortensen & Rapp 1998; Roberts et al. 2009) and a *Lophelia* reef, with an overall growth rate of about 1.3 mm year^{-1} (Mortensen 2000).

6.1.5   Growth rates –bamboo coral Isididae

An assessment of the age and growth of bamboo corals from the New Zealand region applied lead-210 (^{210}Pb) dating in combination with growth zone counts. Average radial growth rates of 0.15–0.32 mm year^{-1} and 0.22 mm year^{-1} were reported for *Lepidisis* spp. and *Keratoisis* sp., respectively (Tracey et al. 2007), similar to radial growth rates in studies of *Keratoisis* sp. from other regions (Table 6.1). A linear extension rate of 21–57mm year^{-1} was also reported for *Lepidisis* spp by Tracey et al. (2007).

6.1.6 Longevity

Cold-water coral structures formed by scleractinian coral species are considered to be one of the longest lasting marine structural habitats. Some of these banks and reefs have existed for hundreds of thousands of years. They may vary tremendously in size from small patches of reef a few metres in diameter to vast reef complexes measuring several tens of kilometres across (reviewed in Friewald et al. 2004; Roberts et al. 2009). Cold-water coral reefs and mounds are the result of both biological and geological processes. As these coral colonies grow, they form intermingling complex matrices and with increasing size and density, can form significant biogenic habitats, that range from thickets, coppices, reefs, and mounds, with a marked differentiation between the living and dead framework (e.g., the Squires (1965) coral coppice found within the New Zealand subantarctic region).

Lophelia reefs have a large dead coral framework that supports a thin and young, live zone (Freiwald et al. 2004). Similarly, the living zone of *S. variabilis* is very small compared to the underlying dead coral framework, which supports this cap of living corals. Seafloor images of *S. variabilis* from the New Zealand region show a live matrix height of about 20 cm. Growth rates indicate about 150–660 years of continuous unidirectional growth would be required for a colony to reach this height, and assuming a centrally located, multi-branch colony, it is estimated that it would take about 380–1700 years to build a reef-like habitat with a diameter of 1 m (Neil et al. in review). Reef development,while dependent on the growth of live coral, can thus be influenced by processes that impact both the living cap and the dead substrate, with future undersaturation of seawater carbonate concentrations having significant implications for the global distribution of coldwater corals and coral reefs (See Section 3).

Some cold-water coral individuals are long-lived and can be valuable as archives of environmental conditions. Individuals have been recorded to have life spans ranging from 70 years (*Corallium secundum*, Roark et al. 2006) to 800–1800 years (Pacific and Atlantic *Gerardia* sp., respectively, Druffel et al. 1995, Roark et al. 2006) to greater than 4000 years (*Leiopathes* sp., Roark et al. 2009). Bamboo coral colonies (*Keratoisis* sp.) from Tasmania have been aged at 400 years (Thresher et al. 2004, 2007). Coral specimens in the same family (Isididae), collected from the Gulf of Alaska, indicate colony age ranges from 75 years to over 200 years (Roark et al. 2005). New Zealand bamboo corals have been recovered with basal diameters of up to 10 cm, and using the growth rates derived by Tracey et al. (2007), implies they may also have longevities of several centuries. The estimates of age and growth for the bamboo corals provide some insight into the regeneration potential of these long-lived and slow growing organisms.

Defining the age, growth, longevity and therefore restoration timeframes of deep-sea coral matrices (and individuals) in the New Zealand region has implications for resilience of deep-sea corals to environmental stressors and the management of deep-sea habitats around New Zealand.

Table 6.1: Growth rates of cold water corals - Scleractinia and Gorgonacea (after Roberts et al. 2009).

Order	Species and depth	Growth rate (mm yr^{-1})	Growth parameter and method	Reference
Scleractinia	*Desmophyllum cristagalli (= D. dianthus)*	0.5–2.0	Linear extension from ^{226}Ra/^{210}Pb radionuclide decay technique	Adkins et al. (2004)
	Desmophyllum cristagalli (= D. dianthus)	0.5–1.0	Linear extension from coupled U/Th and ^{14}C dating	Risk et al. (2002)
	Desmophyllum cristagalli (= D. dianthus) (421–2180 m)	0.1–3.1	Linear septal extension from U/Th dating	Cheng et al. (2000)
	Desmophyllum cristagalli (= D. dianthus)	3–4		Försterra and Häussermann (2008)
	Enallopsammia rostrata (1410 m)	5	Linear extension from 226Ra/210Pb radionuclide decay technique	Adkins et al. (2004)
	Enallopsammia rostrata (1410 m)	0.07	Radial growth from 226Ra/210Pb radionuclide decay technique	Adkins et al. (2004)
	Lophelia pertusa (955–1006 m)	7	Linear extension from sample from man-made structure of known age	Duncan (1877)
	Lophelia pertusa (800 m)	6	Linear extension from sample from man-made structure of known age	Wilson (1979)
	Lophelia pertusa (300 m)	25	Linear extension from apparently annual cycles of C&O stable isotopes	Mikkelsen et al. (1982)
	Lophelia pertusa (250 m)	19	Linear extension from apparently annual cycles of C&O stable isotopes	Freiwald et al. (1997)
	Lophelia pertusa (200–350 m)	5.5	Linear extension of corallites from apparently annual cycles of C&O stable isotopes	Mortensen & Rapp (1998)
	Lophelia pertusa (60–109 m)	26	Linear extension from sample from man-made structure of known age	Bell & Smith (1999)
	Lophelia pertusa (100 m)	5	Linear extension from sample from man-made structure of known age	Roberts (2002)
	Lophelia pertusa (94–115 m)	19.0–34.0	Linear extension from sample from man-made structure of known age	Gass & Roberts (2006)
	Lophelia pertusa	9.4	Linear extension from live coral grown in aquaria	Mortensen (2001)
	Lophelia pertusa (214–218 m)	15.0–17.0	Linear extension from live coral grown in aquaria	Orejas et al. (2008)
	Lophelia pertusa	0–7	Linear extension from live coral in situ video	Lundälv et al. (2012)
	Lophelia pertusa	1.3	Reef structure growth rate	Mortensen (2000)
	Lophelia pertusa (460 m)	2.44–3.77	Linear extension from in situ measurements of transplanted live coral	Brooke & Young (2009)
	Lophelia pertusa	8.76	Linear extension from live coral grown in aquaria	Orejas et al. (2011ba)

Scleractinia	*Madrepora oculata* (214–218 m)	3.0–18.0	Linear extension from live coral grown in aquaria	Orejas et al. (2008)
	Madrepora oculata	5.11	Linear extension from live coral grown in aquaria	Orejas et al. (2011aa)
Gorgonacea	*Primnoa pacifica* (revised from *P. resedaeformis*) (<200 m)	17	Linear extension from ^{210}Pb decay and visual growth rings	Andrews et al. (2002)
	Primnoa pacifica (revised from *P. resedaeformis*) (<200 m)	0.18	Radial growth from ^{210}Pb decay and visual growth rings	Andrews et al. (2002)
	Primnoa pacifica (350–505 m)	0.12	Radial growth from assumed annual growth rings	Matsumoto (2007)
	Primnoa resedaeformis (450 m)	1.5–2.5	Linear extension from ^{14}C dating and comparison with live specimens	Risk et al. (2002)
	Primnoa resedaeformis (450 m)	0.044	Radial growth from ^{14}C dating	Risk et al. (2002)
	Primnoa resedaeformis (262–542 m)	17	Linear extension from colony height and assumed annual growth rings	Mortensen & Buhl-Mortensen (2005)
	Primnoa resedaeformis (262–542 m)	<0.5	Radial growth from assumed annual growth rings	Mortensen & Buhl-Mortensen (2005)
	Corallium niobe (640 m)	0.13	Radial growth from ^{14}C dating	Griffin & Druffel (1989)
	Corallium niobe (600 m)	0.11	Radial growth from ^{210}Pb decay and ^{14}C dating	Druffel et al. (1990)
	Corallium rubrum (15–62 m)	0.18	Radial growth from growth rings in calcein-stained organic matrix	Marschal et al. (2004)
	Corallium secundum (450 m)	0.17	Radial growth from ^{14}C dating	Roark et al. (2006)
	Corallium sp. possibly *C. regale* (1482 m)	0.043	Radial growth from ^{210}Pb decay	Andrews et al. (2005)
	Unidentified Isididae (700 m)	0.05–0.16	Radial growth from ^{14}C dating and visual growth rings	Roark et al. (2005)
	Keratoisis sp. (1000 m)	0.11	Radial growth from ^{210}Pb decay and $^{U/Th}$ dating	Thresher et al. (2007)
	Keratoisis sp. (680 m) Mid Holocene fossil	0.2	Radial growth from ^{14}C dating and visual growth rings	Noé et al. (2008)
	Keratoisis sp. (935 m)	??	Linear extension from ^{210}Pb decay, colony height and visual growth rings	Tracey et al. (2007)
	Keratoisis sp. (935 m)	0.22	Radial growth from ^{210}Pb decay and visual growth rings	Tracey et al. (2007)
	Lepidisis spp. (690–1030 m)	21-57	Linear extension from ^{210}Pb decay, colony height and visual growth rings	Tracey et al. (2007)
	Lepidisis spp. (690–1030 m)	0.15–0.32	Radial growth from ^{210}Pb decay and visual growth rings	Tracey et al. (2007)
	Paramuricea placomus	4–5	Linear extension from live coral in situ video	Lundälv et al. (2012)

6.1.7 Calcification rates

Most investigations into cold-water coral growth have focused on radial and linear extension as assessments of factors such as temperature, pH, coral age and nutritional state are not readily made from archived or collected coral colonies. In addition, there is minimal information on how growth may be modified by ocean acidification. While linear growth is only one way in which impacts of

ocean acidification on corals may become apparent, it is important to also evaluate the state of knowledge of other key parameters such as calcification. The advent of cold-water coral in-aquaria experiments has resulted in data on rates of calcification ($CaCO_3$ precipitation) becoming available in recent years (within the last five years). Success in sustaining cold-water corals alive within incubation or aquaria experiments has primarily been with *Lophelia pertusa*, (see Table 6.2 and references therein).

Maier et al. (2009) published the first study to provide measurements of calcification rates in cold-water corals, namely *L. pertusa*. These short term (24 hour) perturbation experiments showed an average rate of calcification of 0.067 % d^{-1}, but calcification rates spanned two orders of magnitude between 0.0027 and 0.1923 % d^{-1}, attributed to more rapid calcification in the youngest polyps. Overall, reduced calcification rates were recorded at increased pCO_2, with calcification reduced more in the faster growing, young polyps than in older polyps. Maier et al. (2011) have since demonstrated that calcification in *L. pertusa* is four orders of magnitude lower in older than in younger polyps.

Several aquaria-based studies have since followed including a study of the growth rates of four Mediterranean scleractinian cold water coral species that have been maintained under the same controlled conditions (Orejas et al. 2011a) (Table 6.2). Results showed a high variability in growth rates both between and within species, with differences in growth rates within this experiment attributed to physiological differences as opposed to environmental factors.

During a short-term (one week), high pCO_2 (981 ppm) exposure of *L. pertusa*, Form & Riebesell (2012) report a decline in calcification, while a long-term (6 month) exposure experiment indicated acclimation to high pCO_2 (982 ppm) exposure (and slightly enhanced rates of calcification). Similarly, a short-term, repeated incubation of *M. oculata* revealed that calcification rates have already dropped by 50% since pre-industrial times (pCO_2 about 280 ppm), while an increase from ambient to higher pCO_2 (1000 ppm) had no further effect on calcification rates (Maier et al. 2012). Further long-term experiments (9 months) on three Mediterranean cold-water coral species (*M. oculata, L. pertusa and Desmophyllum* sp.), subjected to a pCO_2 range between 400 and 1000 ppm, revealed that no acclimation to ocean acidification takes place when corals are subjected to higher pCO_2 over the longer-term (Maier 2012). *M. oculata* from this same study was then subjected to further increased pCO_2 and a significant decline in calcification could be observed for these elevated pCO_2 levels (1600 and 2000 ppm), (Maier 2012). In summary, the response of deepsea corals to elevated pCO_2 varies between and within species, with acclimation and adaptation times influencing the response.

While experiments assessing cold-water coral calcification within aquaria and the response of calcification to ocean acidification are in their infancy, results from various experiments indicate that the calcification response to ocean acidification may be non-linear and affected by several interacting environmental and growth factors. Cold-water corals appear to maintain relatively constant calcification rates within a certain range of CO_2 concentrations, with some studies of temperate corals indicating that calcification rates can remain unaffected by pCO_2 levels as high as that projected for the end of the century, although this response is again non-linear (Ries et al. 2010, Rodolfo-Metalpa et al. 2010). Hence, significant negative and positive calcification (and therefore growth) responses above and below pCO_2 thresholds, or critical tipping points, could occur. To date the three most common methods to determine calcification rates of cold water corals are [45]Ca-labelling, buoyant weight determination and the alkalinity anomaly technique, all of which are discussed below in Section 6.2.

Table 6.2: Calcification rates of cold water corals – Scleractinia.

Order	Species (and $p\text{CO}_2$)	Calcification rate (% day^{-1})	Experimental length and method	Reference
Scleractinia	*Lophelia pertusa* (509– ambient)	0.0068	Calcification rates from live coral grown in aquaria (1 week), alkalinity anomaly	Form & Riebesell (2012)
	Lophelia pertusa (605)	0.00178	Calcification rates from live coral grown in aquaria (1 week), alkalinity anomaly	Form & Riebesell (2012)
	Lophelia pertusa (856)	0.00073	Calcification rates from live coral grown in aquaria (1 week), alkalinity anomaly	Form & Riebesell (2012)
	Lophelia pertusa (981)	0.00127	Calcification rates from live coral grown in aquaria (1 week), alkalinity anomaly	Form & Riebesell (2012)
	Lophelia pertusa (604)	0.0087	Calcification rates from live coral grown in aquaria (6 month), alkalinity anomaly	Form & Riebesell (2012)
	Lophelia pertusa (778)	0.014	Calcification rates from live coral grown in aquaria (6 month), alkalinity anomaly	Form & Riebesell (2012)
	Lophelia pertusa (982)	0.0188	Calcification rates from live coral grown in aquaria (6 month), alkalinity anomaly	Form & Riebesell (2012)
	Lophelia pertusa (1097 – ambient)	0.067	Calcification rates (average) from live coral grown in aquaria (24 hour), alkalinity anomaly	Maier et al. (2009)
	Lophelia pertusa (518 – ambient)	0.046	Calcification rates (average) from live coral grown in aquaria (24 hour), alkalinity anomaly	Maier et al. (2009)
	Lophelia pertusa (1054)	0.033	Calcification rates (average) from live coral grown in aquaria (24 hour), alkalinity anomaly	Maier et al. (2009)
	Lophelia pertusa (1389)	0.02	Calcification rates (average) from live coral grown in aquaria (24 hour), alkalinity anomaly	Maier et al. (2009)
	Lophelia pertusa (518 – ambient)	0.021	Calcification rates (average) from live coral grown in aquaria (24 hour), alkalinity anomaly	Maier et al. (2009)
	Lophelia pertusa (1054)	0.015	Calcification rates (average) from live coral grown in aquaria (24 hour), alkalinity anomaly	Maier et al. (2009)
	Lophelia pertusa (1389)	0.01	Calcification rates (average) from live coral grown in aquaria (24 hour), alkalinity anomaly	Maier et al. (2009)
	Lophelia pertusa (ambient)	0.02	Calcification rates (average) from live coral grown in aquaria (8 month), buoyant weight	Orejas et al. (2011a)
	Madrepora oculata (ambient)	0.11	Calcification rates (average) from live coral grown in aquaria (8 month), buoyant weight	Orejas et al. (2011a)

Scleractinia	*Madrepora oculata* (ambient)	0.2	Calcification rates (average) from live coral grown in aquaria (3 month), buoyant weight	Orejas et al. (2011b)
	Desmophyllum dianthus (ambient)	0.06	Calcification rates (average) from live coral grown in aquaria (8 month), buoyant weight	Orejas et al. (2011a)
	Dendrophyllia cornigera (ambient)	0.04	Calcification rates (average) from live coral grown in aquaria (8 month), buoyant weight	Orejas et al. (2011a)
	Lophelia pertusa (ambient)	0.05	Calcification rates (average) from live coral grown in aquaria (24 hour), alkalinity anomaly	Maier et al. (2012)
	Madrepora oculata (ambient)	0.05	Calcification rates (average) from live coral grown in aquaria (24 hour), alkalinity anomaly	Maier et al. (2012)
	Madrepora oculata (331)	0.12	Calcification rates (average) from live coral grown in aquaria (24 hour), alkalinity anomaly	Maier et al. (2012)
	Madrepora oculata (629)	0.06	Calcification rates (average) from live coral grown in aquaria (24 hour), alkalinity anomaly	Maier et al. (2012)
	Madrepora oculata (1186)	0.06	Calcification rates (average) from live coral grown in aquaria (24 hour), alkalinity anomaly	Maier et al. (2012)
	Desmophyllum dianthus (ambient)	0.01	Calcification rates (average) from live coral grown in aquaria (24 hour), alkalinity anomaly	Maier et al. (2012)
	Desmophyllum dianthus (year 2100- ambient)	0.29	Calcification rates (average) from live coral in situ (2 weeks), buoyant weight	Jantzen et al. (2012)
	Desmophyllum dianthus *(pH 7.8)	0.003–0.007	Calcification rates (average) from live coral grown in aquaria (8 month), buoyant weight	Carreiro-Silva & Purser (2012)
	Desmophyllum dianthus *(pH 8.1)	0.003–0.005	Calcification rates (average) from live coral grown in aquaria (8 month), buoyant weight	Carreiro-Silva & Purser (2012)
	Desmophyllum dianthus *(pH 7.8)	0.002	Calcification rates (average) from live coral grown in aquaria (8 month), alkalinity anomaly	Carreiro-Silva & Purser (2012)
	Desmophyllum dianthus *(pH 8.1)	0.002	Calcification rates (average) from live coral grown in aquaria (8 month), alkalinity anomaly	Carreiro-Silva & Purser (2012)
	Lophelia pertusa *(pH 7.9)	0.009	Calcification rates (average) from live coral grown in aquaria (short term), method not stated	Lunden et al. (2012)

| Scleractinia | *Lophelia pertusa* *(pH 7.6) | -0.003 | Calcification rates (average) from live coral grown in aquaria (short term), method not stated | Lunden et al. (2012) |

* pCO_2 not reported

6.1.8 Summary

Growth and longevity is difficult to assess within cold-water corals due to their inaccessibility, lack of banding and slow growth rates. Cold-water corals are widely distributed throughout the New Zealand region; however, only two groups have been subject to initial growth and longevity estimates. A single study of *S. variabilis* has reported growth rates of 0.3–1.3 mm year^{-1} and an estimated longevity of 150–660 years required to attain a living matrix of 20 cm in height. These estimates are in keeping with growth rates reported within a number of studies of the habitat-forming *L. pertusa*. The thin living zone of matrix-forming corals is usually supported by an underlying dead coral framework, with cold-water coral structures formed by scleractinian species considered to be one of the longest lasting marine structural habitats. An assessment of the age and growth of bamboo corals from the New Zealand region reported average radial growth rates of 0.15–0.32 mm year^{-1}, a single linear extension rate of 21–57 mm year^{-1}, and an estimated longevity for a single colony of several centuries.

Recent successes in sustaining cold-water corals alive within incubation or aquaria experiments have provided preliminary data on calcification rates, primarily of *L. pertusa*. These initial studies highlight the high variability in calcification both within and between species, as well as the potentially non-linear response to ocean acidification, due to both physiological and environmental factors. No calcification rate data is available for corals collected within the New Zealand region.

Information on the growth and longevity of cold-water corals in the New Zealand region, primarily from extension rate estimates, has been collected with some knowledge of the oceanography and geomorphology. However, these estimates are sparse (two studies) and should be coupled with assessments of in situ environmental parameters such as temperature, salinity, ocean chemistry and nutrient supply. In-aquaria (or incubation) studies are required to define calcification rates, and, while in their infancy, indicate that the calcification response may be non-linear and affected by several environmental and physiological factors. Hence, studies within the New Zealand region will need to use the information in this report to help consider natural environmental conditions, multiple environmental stressors, and variability in growth and calcification rates both between and within species. In addition, this information should be coupled with growth and longevity estimates since corals display allometric growth and linear extension rates that are considered to decrease significantly with increasing age. Calcification rates are also indicated to decrease with increasing age, with longer term calcification rate studies suggesting that cold-water corals are able to maintain constant calcification rates until a threshold, or critical tipping point, is reached.

Defining the age, growth, longevity, calcification rates and response to stressors of cold-water corals is required in order to provide insight into the resilience of these species, regeneration or restoration timeframes for both the corals and the habitat they provide, and for the conservation of cold-water corals within the New Zealand region, especially in relation to fisheries.

6.2 Methods of assessing the impact of OA

Ocean acidification (OA) will pose a multifactorial problem with regards to deep-water coral species. It is expected under OA conditions that:
1. Exposed calcium carbonate ($CaCO_3$) structures will start to dissolve (Rodolfo-Metalpa et al. 2011).

2. Individuals will have to increase metabolic rates and divert energetic allocation to precipitate and maintain their $CaCO_3$ structures due to reduced carbonate concentrations in sea water (Cummings et al. 2011), thereby reducing the amount of energy available for growth and reproduction.

3. Physiological processes will be disrupted by changes in the acid-base balance (Langenbuch & Pörtner 2003; Munday et al. 2009), and by temperature (Naumann et al. 2013)

The combination of reported issues related to OA will result in a reduction of fitness for many species and may have repercussions on ecosystem functioning. Efforts must be focused on investigating how CO_2 related physiochemistry and ocean warming work synergistically, beyond empirical observations, resulting in the elucidation of cause and effect relationships (Pörtner 2008) in order to understand how these deep water communities might respond to OA. A recent study by Naumann et al. (2013) revealed species-specific physiological responses of the cold-water corals *L. pertusa* and *M. oculata* within their natural temperature range. The authors concluded that species-specific thermal acclimation may significantly affect the occurrence and local abundance of these two species.

At present most of our understanding regarding the implications of OA are based on short-term perturbation experiments. Recent work has suggested that growth rates are an important proxy for coral reef health as factors such as OA are thought to negatively impact both growth and calcification rates (Herler & Drinwöber 2011). It can be assumed that a reduction in growth rate can be attributed to increased metabolic costs elsewhere within the energy budget of an individual coral.

Estimations of growth in aquaria can be established on the scale from single branches to entire colonies. Initial reference points can be marked on live corals using stains such as Alizarin red-S (Barnes 1970) and the field of new growth beyond the reference point monitored. The technique has, however, been linked with the onset of physiological stress in corals when exposure to the dye exceeds 12 hours, resulting in a significant reduction of calcification rates post treatment (Dodge 1984). In situ laser measurements to determine growth can be conducted (Vago et al. 1997), and have not been linked to the initiation of physiological stress responses. However, laser techniques are difficult to run as they are technically demanding and have a very short duration of observation.

With regards to a more holistic approach where physical attributes, such as growth, would ideally be observed alongside physiological aspects, such as metabolism and energy partitioning, the induction of stress responses should be minimised and therefore it may be prudent to avoid techniques that are known to initiate stress responses. Additionally, while external linear extension in relation to a reference point can be used to measure coral growth, the efficacy and accuracy of utilising this proxy has been questioned (Bak 1973).

6.2.1 Measuring calcification rates

To date most investigations into cold-water coral growth in aquaria have focused on radial and linear extension (Maier et al. 2012). Destructive techniques, such as X-ray examination, will provide relevant information about differences in the microstructure and calcification mechanisms, but yield only one set of results and therefore are not useful for long-term studies (Barnes 1970; Davies 1989). Ideally, a suite of non-destructive techniques should be implemented, facilitating the acquisition of replicate values over a time period. This can include details regarding interspecific and intraspecific factors varying with temperature, pH, coral age, and nutritional state, etc. that will not only provide information on the physiological responses at specific time steps, but also elucidate evidence of any adaptation behaviour over a prolonged period of exposure.

^{45}Ca labelling

The addition of ^{45}Ca to coral aquaria allow the estimation of $CaCO_3$ precipitation over a given time frame (Maier et al. 2009). The corals need to be incubated in the inoculated water for a given time then washed thoroughly in untreated seawater to allow removal of unbound ^{45}Ca present in the coral coelenteron, tissue and skeleton (Tambutté et al. 1996), which would otherwise skew calcification results. The samples then need to be dried and dissolved in acid before the uptake of ^{45}Ca can be determined and the calcification rate extrapolated. ^{45}Ca labelling is a destructive technique requiring the sacrifice of samples to calculate calcification rates, therefore producing only a single set of results. Additionally, while this technique is very sensitive and can be used to assess short exposure times (for example 24 hours, Maier et al. 2009) it does involve the use of radioactive material, which is avoided by using alternative observation techniques.

Buoyant weight determination

Weight increment and buoyant weight measurements of coral species provide a good proxy for growth as calcification rates are taken into consideration (Jokiel et al. 2008). This technique has been used extensively across various scales (whole colonies to branches and nubbins; Herler & Drinwöber 2011) and has been shown to provide very accurate results (Davies 1989).

The buoyant weight technique involves the measurement of coral colonies or fragments while immersed in a fluid. Buoyant weight (BW) depends on the density of the immersion fluid, thus the temperature and salinity need to be closely monitored to account for fluctuations. Care has to be taken when using this technique as inaccuracy issues, related to initial volume determination and density estimation methodologies, have been identified (Herler & Drinwöber 2011). However, more accurate and appropriate techniques have been outlined in the literature (Herler & Drinwöber 2011). NIWA has also developed a very accurate buoyant weight measuring system for use with coralline algae which would work well with deep-sea corals (Nelson et al. 2012).

Alkalinity anomaly technique

This technique allows the rate of calcification to be estimated using the 2:1 stoichiometric relationship between the decrease of total alkalinity (A_T) and the precipitation of $CaCO_3$ (Wolf-Gladrow et al. 2007). However, care needs to be taken to account for the significant amounts of inorganic nutrients produced during the incubation period. A correction factor can be implemented to normalise the data from which the calcification rates can be derived (Maier et al. 2012; Maier et al. 2011). It should be noted that open, rather than closed, circulation systems are preferable for this analysis as a build-up of CO_2 from coral respiration could potentially alter water carbonate chemistry thus obscuring calcification data (Maier et al. 2012). Additionally, water should be pre-filtered (0.2µm) to help minimise bacterial and phytoplankton influence on A_T. This method has been deemed sensitive enough to monitor calcification rates for short-term incubations (Maier et al. 2012) and long-term experiments (Carreiro-Silva et al. University of the Azores, Portugal, unpublished data; Orejas et al. 2013).

6.2.2 Metabolism

Deep-water corals, as with all species, have access to a finite amount of resources, which are partitioned between factors such as basal metabolism, growth and reproduction. Basal metabolism facilitates basic vital requirements while the individual is classed to be 'at rest'. The surplus of energy available from the total energy budget, once basal requirements have been met, is then used for growth and reproduction. With the induction of stress comes an associated metabolic cost, thus leaving less energy available in the budget for growth and other processes. Therefore, observing factors linked to food acquisition and metabolic rate would provide insights into how stresses such as OA will impact the fecundity and survivorship of the species over a long-term basis.

6.2.3 Oxygen consumption rates

Oxygen consumption can be used as a proxy for basal metabolic rates (Cummings et al. 2011). Closed systems, where a probe is used to monitor the levels of dissolved oxygen, have been utilised in a variety of studies to estimate respiration rates (e.g., Portner et al. 1999; Heilmayer & Brey 2003). More recently, deep-water coral studies have utilised optodes and sensor spots (Cornelia Maier, Centre National de la Recherche Scientifique-Institut National des Sciences de l'Univers, Laboratoire d'Océanographie de Villefranche, France, pers comm.). Small sensor spots can be attached to the inside surface of any transparent glass or plastic vessel, and the optode then records the oxygen levels through the transparent vessel wall (www.presens.de). The use of sensor spots and optodes rather than large O_2 probes inside the closed systems mean that there is less chance of damaging fragile coral fragments and they have been shown to be sufficiently sensitive for coral respiration measurements (C. Maier, unpublished data).

6.2.4 Gene expression

Assessments of genetic expression will not only provide information on what might be driving changes in skeleton formation, but will also give insight into the potential extent of compensation in key biomineralization (Hofmann et al. 2008). Microarrays have been used to investigate physiological responses to abiotic factors and could have applications when investigating the implications of elevated CO_2 (Gracey 2007). Genetic techniques that target genes known to be involved in cellular stress responses and metabolism can be targeted utilising mRNA expression-based techniques such as RT-qPCR analysis (Orejas et al. 2013). Calcium channels in the calcioblastic epithelium have been suggested to be a good site to target efforts investigating the expression genes such as carbonic anhydrase (Zoccola et al. 1999, Hofmann et al. 2008).

6.2.5 Food Capture

The ability of filter feeding species to capture and consume prey items is paramount to their survival. Shifts in environmental parameters that cause an increase in sub-optimal conditions can cause heat shock proteins or other stress responses to be produced as the animal attempts self-regulation and self-preservation. The removal rate of food items such as *Artemia salina* nauplii during a set period of time has been used to assess variability in coral feeding success under different environmental conditions (Orejas et al. 2013). Any increase in the corals activity will drive up metabolic requirements and as such the animals will need to feed more (up-regulate) their feeding, to satisfy demand. Up-regulation of feeding could suggest that the specimens were stressed and therefore required more energy to account for stress mediated responses. This can also result in variability of prey capture rates. We might expect to see feeding rates increase to a point then decreasing below normal levels suggesting that the specimens are being seriously impaired due to environmentally induced physiological stress.

6.2.6 Summary and next steps

In summary, it would be prudent to avoid relying solely on assessments of growth to determine the implications of stressors such as OA on deep-sea corals. Length increment studies, when used alone, have been described as a poor proxy for growth (Bak 1973) and it would therefore be advisable to utilise a suite of observations such as such as variations in basal metabolism and oxygen consumption (*sensu* Cummings et al. 2011) to determine the impact of OA on deep-sea corals. Because of the slow growth rate of these corals any length increment study would need to be carried out over a long period.

Observations that are destructive or have been seen to induce physiological stress, such as [45]Ca measurement, X-ray observation and Alizarin red staining, should also be avoided. The corals may well be able to cope with a degree of fluctuation in water pH and appear to calcify at a 'normal' rate (Form & Riebesell 2012). However, by implementing a suite of observations, variations in basal

metabolism, for example, could reveal otherwise undetected ramifications of sub-optimal environmental factors. These concealed responses may be more detrimental to the corals in the long-term as up-regulation of stress responses and basal metabolic costs will impinge upon the resource partitioning capabilities of these species. Thus, long-term effects may include reduced survivorship, fecundity and reproductive capacity.

In terms of a small scale, experimental laboratory set up, studies using buoyant weight or alkalinity anomaly techniques would appear to yield satisfactory results with regards to the determination of calcification rates. The analysis of O_2 consumption at various times during and at the termination of the experiment using optodes and O_2 sensors (or similar) would be beneficial to monitor respiration in order to assess whether any acclimation was occurring or to identify increased metabolic costs associated with non-optimal environmental conditions. Tissue samples could be preserved upon culmination of the experiment to allow PCR and microarray analysis, to further elucidate potential physiological changes as a result of a low pH environment.

Chapter 7:   DEEP-SEA CORAL IN-AQUARIA FEASIBILITY TRIALS

Di Tracey, Neill Barr, Sarah Allen, Philip Heath, Vonda Cummings (NIWA)

Figure 7.1: Live *Solenosmilia variabilis* (bottom left colony in image) and potentially live *Enallopsammia rostrata* (middle colony in image), in deep-sea corals aquaria, Mahanga Bay Hatchery, October, 2012. Image Dave Allen (NIWA)

In this Chapter, we provide results of our investigations into the feasibility of at-sea sampling, and maintaining deep sea habitat-forming corals alive in the laboratory. Live corals were sampled to evaluate the feasibility of successfully collecting live specimens at sea and maintaining them in the laboratory, as a precursor to conducting laboratory trials on these organisms. Live corals were collected on two *Tangaroa* voyages. The initial set up was trialled during the Chatham Rise Fisheries Oceanography II voyage (TAN1116) in November 2011 and improved for a subsequent trip in April 2012 (Vulnerable Deep-sea Communities voyage, TAN1205) to the Bay of Plenty region and southern end of Kermadec Arc. One live colony of the reef–forming scleractinian coral (*S. variabilis*) is currently alive at Mahanga Bay (Figure 7.1), 14 months after it was collected.

7.1   Methods

7.1.1   At-sea equipment and collection

A small aquaria kit, comprising two holding tanks, an air pump, and chiller, was prepared to maintain live corals at sea during the Chatham Rise Fisheries Oceanography II voyage. Tanks were covered to keep out any light. During the voyage, no live branching stony corals were sampled but stony cup corals from the same order, *Flabellum* spp. (Flabellum cup coral) and *Stephanocyathus platypus* (solitary bowl coral), were retained to test the tank set up.

During this voyage, it was challenging to keep the tank system's circulating sea water sourced from a re-circulating salt water intake pipe from sub-surface waters to an optimum temperature ($7–8^{\circ}$C). Nevertheless at the end of the voyage, seven cup coral specimens remained alive and these were transferred to the NIWA Mahanga Bay Aquaculture Facility. Unfortunately, the specimens died three days later. This first trial provided valuable information to help refine our methods for keeping corals alive in aquaria at sea before transferring to a land-based aquarium.

A new tank system with a more sophisticated aeration and cooling system was developed and the tank system set up on board *Tangaroa* (Figure 7.2a), in readiness for the April Vulnerable Deep-sea

Communities voyage. Based on data from previous fish community voyages in the Bay of Plenty/Kermadec Arc regions, it was anticipated that live stony branching corals would be present and able to be sampled.

From footage collected along transects lines by NIWA's Deep towed imaging system (DTIS), stony corals were observed on various seamounts during the voyage (Figure 7.2b). On Clark's seamount at the southern end of Kermadec Arc (Figure 7.3a), several live colonies of *Enallpsammia rostrata* were collected using the benthic sled (Figure 7.3b) in 840–872 m. An additional small colony of branching stony coral (*S. variabilis*) and one cup coral (*Caryophyllia* spp.) were also collected.

Environmental data were collected at the site (station 95) using a conductivity, temperature, and density (CTD) profiler. The temperature at the sample depth was 6.7^{o}C and the environment within which the corals were sampled had a relatively high current velocity (Phil Sutton, NIWA unpublished data). The red dots in Figure 7.3a show the position of the CTD station, adjacent to station 95; sled and DTIS tow and transect lines are in yellow.
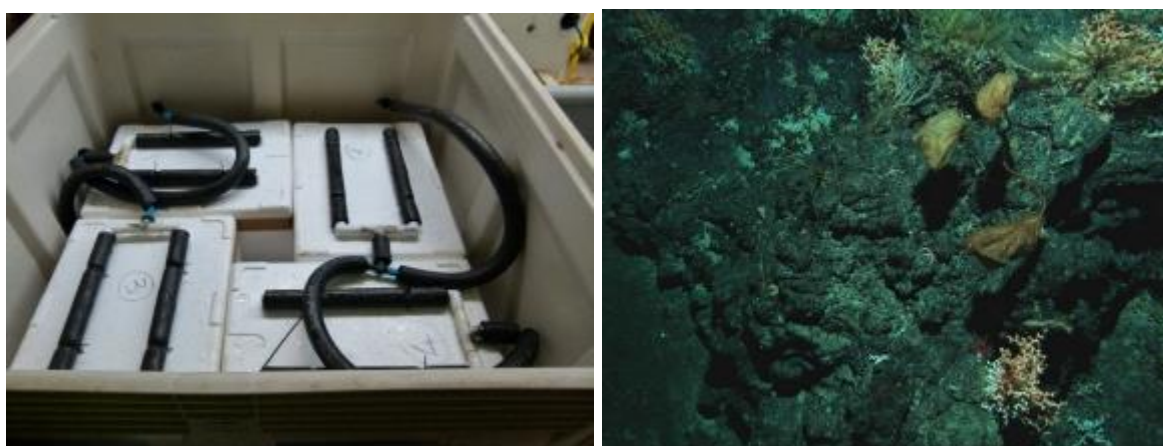
Figure 7.2a: Tank system set-up with a water circulation and temperature control system on board *Tangaroa*, TAN1205, (left). Image Rob Stewart (NIWA). Figure 7.2b: Live stony branching corals in situ Bay of Plenty region (right), (NIWA Image captured from DTIS).

Figure 7.3a (left image): DTIS Transect lines and benthic sled tow lines (in yellow) on Clark Seamount, southern end of Kermadec Arc. Red dot marks the position of the CTD, adjacent to station 95 where live corals were sampled. Figure 7.3b (right image): Benthic sled invertebrate sampling tool. Both images taken during voyage, TAN1205 (Images Malcolm Clark (NIWA).

All live coral specimens obtained were immediately placed into the on-board tank system. On advice from experts, no feeding took place at sea (Ron Thresher, CSIRO, pers. comm,). The corals were left

to settle and recover from the barotrauma effect of being brought to the surface from such a high pressure environment. There was good flow rate in the tanks (50 L/hr, equal to a turnover of about 1 system volume per hour) and temperatures were optimal based on the sample site CTD data. After two weeks of being kept alive at-sea, the corals were transferred from the vessel to tanks at Mahanga Bay.

7.1.2   Mahanga Bay in-aquaria set up

Several colonies of the live *E. rostrata* colonies were held in a dark environment with branch pieces held in 24 separate chambers in optimal temperature conditions and under two flow rates, 120 mL/min and 240 mL/min. The tank configuration is shown in Figure 7.4. The one live *S. variabilis* colony was placed in one chamber (Figure 7.4, bottom right) as was the live cup coral *C.* spp. The flow rate was turning over the volume of the chambers every 15 minutes. Environmental conditions were maintained to match the in situ sample site environmental data as closely as possible.

The corals were fed four times a week – initially with a combination of *Artemia* (brine shrimp) and a liquid coral food (KorallFluid) that comprises marine plankton and added vitamins (e.g., B_{12}, C) but then with only KorallFluid. It was decided that the commercial coral food might provide a more balanced diet, and help overcome the potential problem of the coral feeding polyp soaking up dissolved organic carbon (DOC) when fed due to the corals not being in their normal state. Seawater temperature can affect normal behaviour and key physiological processes, such as growth (i.e., calcification), respiration, and dissolved organic carbon (DOC) flux, (Gori et al. 2012)), and dissolved organic matter (DOM) may be an important carbon and nitrogen source for corals (Gori et al. 2012).

Knowledge of basic biology for deep-sea corals is limited; however, other species of deep-sea corals, such as *L. pertusa*, feed on copepods, krill, fish and detritus (e.g., see Mortenson in Baussant et al. 2010), indicating that the food supplement for the corals was appropriate in the experiments that were conducted.
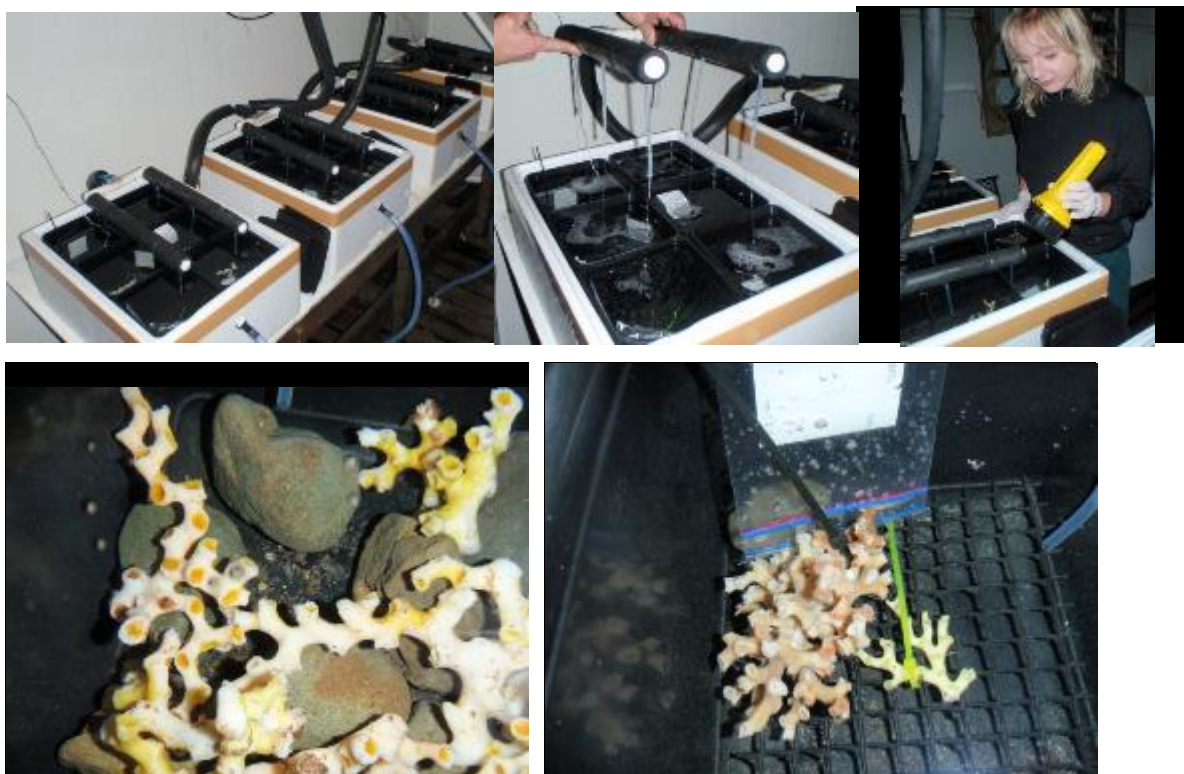
Figure 7.4: Deep-sea corals aquaria, Mahanga Bay Hatchery. Top row: Images show the tank configuration, normally in darkness, with 24 separate chambers (left and middle) under two flow rates at optimal temperatures, and hatchery expert Sarah Allen (previously NIWA) working in the dark experimental environment observing corals post feeding (right). Bottom row: Potentially live *Enallopsammia rostrata* (left), (note yellow pigmentation on coral colony skeleton), and live *Solenosmilia variabilis* colony (right). A small branch of *E. rostrata* is in the chamber with the one *S. variabilis* colony. All corals were collected during TAN1205. Images Rob Stewart, (NIWA).

7.2   Results

As time progressed it was unclear whether the *E. rostrata* colonies were alive in the aquaria. The yellow pigment was clearly visible on the skeleton of the *E. rostrata* colonies and appeared bright for several months, there was no sign of colony degradation or decay, and there was no excessive mucus visible in the holding tank chambers. However, live polyps were not observed and polyp tentacles remained retracted on all branchlets. Often, there can be a period of 'sulking' post-capture, so the feeding regime and optimal environmental conditions were maintained in the hope that polyp activity would be observed at a later date. However, it is recognised that deep-sea species can die when brought to the surface due to pressure change or barotrauma.

In May 2013, one year after their collection, all *E. rostrata* colonies were dead. The yellow pigment tissue had dulled, contracted, and disappeared from some of the branches and no live polyps had presented during the period that the corals had been observed in the aquaria. The *E. rostrata* specimens were removed from the tanks and frozen.

In contrast, the *S. variabilis* colony held in-aquaria at Mahanga Bay survived for 14 months and is still alive at time of writing. We believe that this is a world first. Since the date of capture, live polyp tentacles have regularly been observed extended from some colony branchlets. In May 2013, close up images were made of the colony (Figure 7.5), and these clearly show live polyps with tentacles both extended and retracted (Figure 7.5 bottom images). We note that the proportion of the live (pink) polyps visible on the colony has reduced since date of capture (see image of colony in Figure 5.1.5 compared to the bottom right image in Figure 7.4).

The results of this study show that it is feasible to successfully collect deep-sea branching stony corals from depth and to keep them alive in the laboratory. We are restrained by funding but are currently keeping the *S. variabilis* colony alive using a portable water chiller.
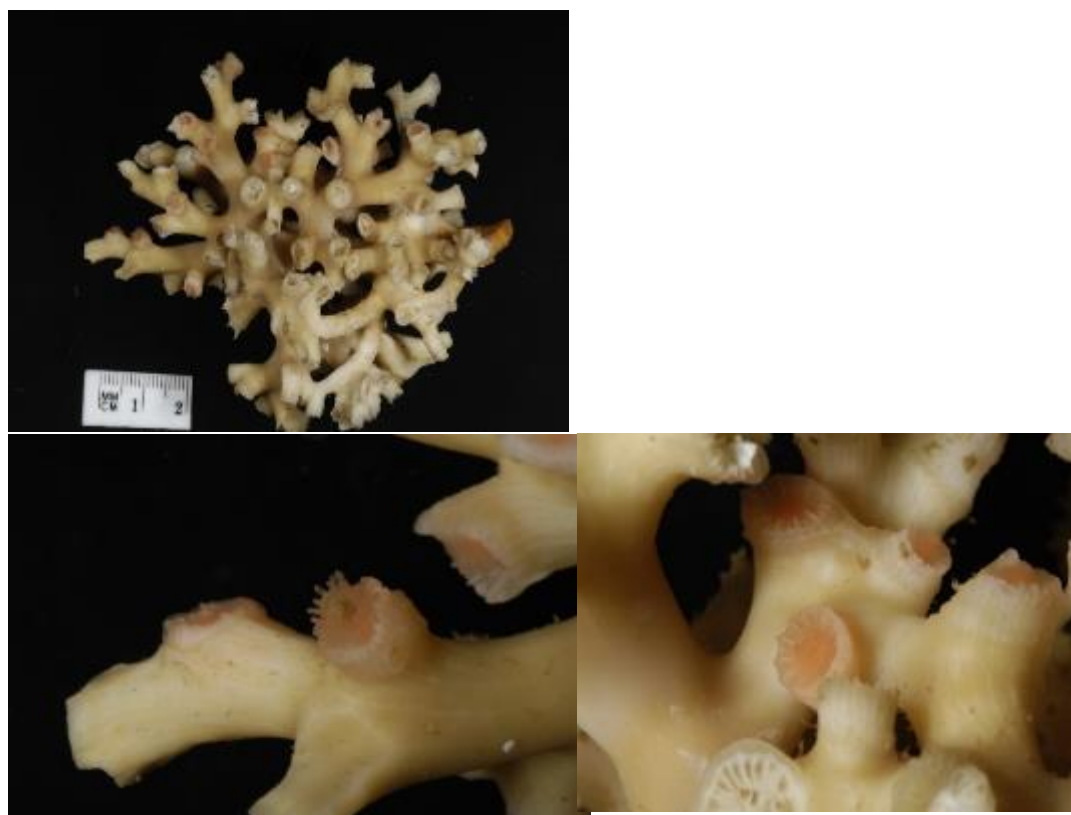
Figure 7.5: Live *Solenosmilia variabilis colony* (top) and close up of live pink polyps showing tentacles extended (left) and retracted (right), as at May 2013. Images Peter Marriott (NIWA).

7.3   Summary

We successfully sampled a live (*S. variabilis* colony at-sea and maintained the specimen alive in the laboratory for 14 months, illustrating the potential for using deep-sea, habitat-forming corals in laboratory-based studies (e.g., to investigate growth and/or ocean acidification impacts). While we were able to successfully sample *E. rostrata*, we could not maintain it alive in the laboratory longer term. The cup coral appeared to be an easy species to maintain alive in aquaria, but was not the focus of our studies.

The work with *E. rostrata* highlights some of the complexity in bringing deep-sea corals into the laboratory. *E. rostrata,* appears to be a difficult species to keep alive in-aquaria and more research is required to help understand its physiology. For example, the tissue of some living *Enallopsammia* spp. is typically yellow, red, or purple. Information on this colour pigmentation is lacking, and we are unsure what role it plays with respect to the functioning of the coral. The color difference could be polymorphism, it is not of taxonomic value, and most likely not biofilm (Steve Cairns Smithsonian Institute, Washington DC, pers comm.).

In contrast, *S. variabilis* appears a robust species for in-aquaria studies. This species survived for a long period in environmental conditions that reasonably represented its natural environment – dark, optimal temperature, flow rate based on current velocity data for the region, feeding using commercial food, and reasonably minimal husbandry (e.g., regular cleaning of the tank).

7.4 Conclusions and future work

Further research is required to improve our understanding of the impacts of ocean acidification on deep-sea coral growth. Clearly, different species have different tolerances for changes in temperature and other environmental parameters and more effort needs to be put into understanding and researching coral groups that commonly occur in New Zealand waters.

Internationally, there has been little experimental work on either of the feasibility of studying deep-sea coral species (e.g. Orejas et al. 2013), and there is little information in the literature to aid our understanding of the stony coral group's physiology and ecology. *S. variabilis* was collected at sea by CSIRO scientists using an ROV and kept alive in the laboratory for about one year (Ron Thresher, CSIRO, pers. comm.). Scientists measured some behavioural responses (e.g., percentage of polyps 'out' or extended), but no physiological responses were assessed.

In contrast, more effort has gone into in-aquaria research and measuring ocean acidification impacts in both the United Kingdom and Europe on stony cup coral species and other stony branching forms such as research on the well-studied, habitat-forming scleractinian corals *L. pertusa* and *M. oculata*. Only the latter species, *M. oculata*, is found in New Zealand waters, although *S. variabilis* and *G. dumosa* resemble the coral genus *Lophelia* (Tracey et al. 2011a).

In the literature search and analysis, some key questions with regard to our understanding of a specific species age and growth, and assessing the best approach to in situ or in-aquaria experiments to measure acidification of these key fauna are highlighted.

At a recent European workshop (Baussant et al. 2010), the current knowledge status, gaps, and research needs for cold-water corals, particularly in relation to anthropogenic impacts including OA, were summarised. These included:

1. What is the chemical and biological variability of their natural habitat?
2. What are the physiological responses of deep-sea corals to ocean acidification, temperature rise, and other multiple stressors such as changes in DIC, salinity, and the combination thereof?
3. How can we examine this group adequately in aquaria, to reflect the natural environment?

Our in-aquaria feasibility study was able to replicate aspects of the natural environment and keep the corals alive; however, the scope of the study was such that no experimental manipulations were carried out.

Future studies could investigate the interaction between factors, such as acidification, temperature, food and oxygen availability (the multiple stressors focus), so that we can better predict the consequences of global climate change on deep-sea corals. Research support would be required to:

- support environmental multiple stressor experiments on deep-sea corals (e.g., manipulate pH, temperature, and other important environmental stressors);
- improve our knowledge on the understanding coral growth patterns particularly in understanding the impacts of OA; and
- continue with age-growth and mineralogy studies (e.g., measure the growth increments, observe changes in morphology and colony weight), as well as understanding the calcification and the $CaCO_3$ mineralogy and structure of deep-sea branching stony corals). We stress that any length increment studies would need to be undertaken for a several years.

Chapter 8: OVERALL RECOMMENDATIONS FOR FUTURE WORK

Additional sampling will always improve the accuracy of estimates and models. Below, in no order of priority, we list recommendations for future work to help understand the potential impact of ocean acidification on deep-water fisheries habitat associated with deep-sea corals.

8.1   Coral mineralogy

Further mineralogical analyses of deep-sea corals will help provide an understanding of the compositional variability between and within species and establish if differences are due to depth, region, or colony age, and inform on a species' likely resilience under future OA conditions. To improve our knowledge of coral mineralogy, particularly in understanding the impacts of OA on the composition, morphology and calcification, we propose to:

- Continue with mineralogy analyses, analysing not only the growing tips, but also the crystal structure within the coral skeletons to ascertain whether some parts of the skeleton may be more vulnerable to dissolution than others.
- Carry out more analyses on the Primnoid corals, as well as on different species, to see whether carbonate mineralogy varies within species.
- Analyse additional samples of the gorgonians to help ascertain the variability in Mg content and determine if this is related to temperature or other environmental variables.
- Carry out research on the solitary scleractinian stony cup corals that appear to live at considerable depths, well below the ASH, to determine how this group has adapted to survive in waters undersaturated with respect to aragonite.

8.2.   Coral distribution

Ongoing support to update the coral database, to help refine our understanding of the spatial distribution data, including local variation, and improve our understanding of the association between deep-sea corals and deep-water fisheries. Improved knowledge of the spatial variability of corals within specific areas, e.g., shallower habitat-forming species' distributions on the top of the Chatham Rise, is required. Certain species may continue to thrive in isolated areas and the various potential refugia need to be defined. This could provide managers with options to manage (close) areas with high density coral regions where associated fisheries and invertebrate habitats co-exist.

Effort is required to update and maintain the deep-sea coral database and datasets and improve the identification of coral species from around New Zealand (e.g., from Science and Capability Group, DOC funding (DOC12303); and as part of the U.S. - New Zealand (NZ) Joint Committee Meeting (JCM) on Science and Technology Cooperation Theme 2.4: Marine and Ocean Research (MBI13303)). Support is required to ensure that we understand the relationship between coral habitat and associated fisheries. Spatial relationships between coral communities and fish species or fish populations have been clearly determined in the North Pacific and North Atlantic and could well be expected in the South Pacific region, although direct observations required to document such associations have not yet been made. We propose support be given to:

- Continuation of sample collection, identification and dataset updates of deep sea coral species in the New Zealand region.
- Determine the level of association between fish and coral distribution, and potential use of coral habitat by fish, by analysing fisheries data over coral habitat and non-coral habitat regions.
- Investigate local variations in coral distribution.
- Define areas that may provide coral refugia in the future and indicate protection of these benthic habitats from manageable anthropogenic impacts.

8.3.   Ocean chemistry

Dissolved organic carbon (DIC) will change with increasing CO_2 uptake by the ocean. To obtain a fuller understanding of the ocean's chemistry and OA impacts, opportunistic water sampling for alkalinity and DIC around the New Zealand region needs to continue. This will enable the monitoring of changes in the carbonate chemistry of the ocean waters. Dedicated sampling programmes may be required, particularly in presently poorly sampled areas and highly variable coastal regions. The sampling would be aided by the development of algorithms to estimate carbonate saturation states in the surface and coastal waters (less than 200 m). We propose it would be opportune to:

- Continue at-sea water sampling to measure the carbonate parameters DIC and alkalinity over time.
- Develop regional/localised surface and coastal algorithms (less than 200 m) to estimate carbonate saturation states in the upper ocean where some corals (*O. virgosa*) live together with other carbonate organisms.

8.4. Modelling of carbonate saturation state

The ASH and CSH depths for the New Zealand region produced from this research will greatly aid the modelling of the distribution of protected corals and add to the available environmental layers used in previous New Zealand predictive habitat modelling studies. Application of the new and detailed ASH and CSH for the New Zealand region would be advantageous in future benthic habitat models. Upcoming government projects will have access to this new environmental layer to help improve understanding and prediction of the distribution of vulnerable marine ecosystem (VME) taxa, including protected corals, within the New Zealand EEZ and High Seas regions.

Outputs from new global climate models should be interrogated to determine the estimated depths of the ASH and CSH for the New Zealand region in 2100. This will aid the identification of potential refugia for deep-sea corals in the New Zealand region and help managers define regions that could be protected. This work has been started by our international collaborators with whom we will continue to liaise.

Future modelling needs to include:

- Calculation of the high Mg calcite saturation horizons, as many organisms are made of this mineral.
- Use of carbonate saturation states when looking at the habitat-forming, deep-sea corals and fish. We suggest that future work using benthic habitat models should include carbonate saturation states, along with other more typical environmental variables, such as temperature, depth, slope, and rugosity.
- Modelling coral distribution at sub-regional level or for specific areas of interest (e.g. Chatham Rise, Benthic Protected Areas (BPAs)) since modelling at smaller spatial scales allows for the use of actual data rather than modelled data for environmental variables.
- A high priority will be to compare the modern saturation horizons derived from the regional algorithms to ground-truth the modelled output for the present-day and use the best models to look at future shoaling of the ASH and CSH by 2100. These models should also be combined with other stressors such as temperature. Use these models to forecast the depth and spatial habitats for deep-sea corals in the future and identify refugia that could be protected.

8.5.   Coral biology

Opportunities to continue to age, and validate the ages, of deep-sea coral species to estimate their longevity and resilience is required. We recommend that this be carried out in tandem with in-aquaria, multiple stressor experiments (manipulating ocean acidification, temperature, age, growth, diet), to determine how these deep-sea corals might tolerate and respond to future climate change.

The age and growth work can be two-fold, using direct ageing, an important first step to obtain longevity data, and also in-aquaria experiments. We recommend:

- Age additional deep-sea corals species to add to currently sparse regional knowledge of growth and longevity, and therefore recovery potential of individual coral species.
- Apply tools to age and measure the effects of ocean acidification on deep-sea, habitat-forming corals, and recommend the best approach for future assessments of the direct effects of changes in ocean pH on these key fauna.
- Measure growth increments, observe changes in morphology and colony weight, as well as improve our understanding of calcification (form and structure) of deep-sea branching stony corals. We stress that any length increment studies need to be long term due to the episodic or allometric growth behaviour of corals.

8.6.   Ocean acidification (OA) experimental research

Future studies need to investigate the interaction between acidification, temperature, food and oxygen availability so that we can better predict the consequences of global climate change on deep-sea corals. In addition, there is a need for more studies investigating the effects of naturally occurring changes in pCO$_2$ on our coral species in situ, including other calcifying (e.g. stony branching corals with a shallower minimum distribution and so within easy access for sampling, e.g., *O. virgosa*; *G. dumosa* and gorgonians) and non-calcifying species (e.g., the black coral Antipatharia) with important roles as habitat-builders. We propose;

- OA and temperature experiments on live corals be undertaken using the NIWA OA experiment set up to look at the physiological and physical responses to lower pH and higher temperatures. It is expected that some species may be more tolerant to lower carbonate saturation than others.
- Investigate the interaction between factors, such as acidification with temperature, food and oxygen availability (the multiple stressors focus), so that we can better predict the consequences of global climate change on deep-sea corals.
- Carry out experiments investigating the effects of naturally occurring changes in pCO$_2$ on deep-sea corals in situ, including other calcifying and non-calcifying species.

9. ACKNOWLEDGEMENTS

10. REFERENCES

Adkins, J.F.; Henderson, G.M.; Wang, S.L.; O'Shea, S.; Mokadem, F. (2004). Growth rates of deep sea scleractinia *Desmophyllum cristigalli* and *Enallopsammia rostrata. Earth Planetary Science Letters 227*:481–490.

Anderson, O.F. (2011). Descriptions of the black oreo and smooth oreo fisheries in OEO 1, OEO 3A, OEO 4, and OEO 6 from 1977–78 to 2009–10. *New Zealand Fisheries Assessment Report 2011/55*. 90 p.

Anderson, O.F.; Dunn M.R. (2007). Descriptive analysis of catch and effort data from New Zealand orange roughy fisheries in ORH 1, 2A, 2B, 3A, 3B and 7B to the end of the 2004–05 fishing year. *New Zealand Fisheries Assessment Report 2007/29.* 71 p.

Andersson, A.J.; Mackenzie, F.T.; Bates, N.R. (2008). Life on the margin: implications of ocean acidification on Mg-calcite, high latitude and cold-water marine calcifiers. *Marine Ecology Progress Series 373*: 265–273.

Andrews, A.H.; Cailliet, G.M.; Kerr, L.A. (2005). Investigations of age and growth for three deep-sea corals from the Davidson Seamount off central California. *In:* Freiwald, A.; Roberts, J.M. (Eds.) *Cold-water corals and ecosystems*. Springer, Berlin, pp 1021–1038.

Andrews, A.H.; Cordes, E.E.; Mahoney, M.M.; Munk, K.; Coale, K.H.; Cailliet, G.M.; Heifetz, J. (2002). Age, growth and radiometric age validation of a deep-sea, habitat-forming gorgonian (*Primnoa resedaeformis*) from the Gulf of Alaska. *Hydrobiologia, 471*:101–110.

Archer, D.E. (1996). An atlas of the distribution of calcium carbonate in sediments of the deep sea. *Global Biogeochemical Cycles 10*: 159–174.

Aumont, O. (2003). An ecosystem model of the global ocean including Fe, Si, P colimitations. *Global Biogeochemical Cycles 17(2)*: doi: 10.1029/2001GB001745.

Aumont, O.; Bopp, L. (2006). Globalizing results from ocean in situ iron fertilization studies. *Global Biogeochemical Cycles 20(2)*: doi: 10.1029/2005GB002591.

Auster, P.J.; Moore, J.; Heinonen, K.B.; Watling, L. (2005). A habitat classification scheme for seamount landscapes: assessing the functional role of deep-water corals as fish habitat. *In:* Freiwald, A., Roberts, J.M. (Eds.), Cold-Water Corals and Ecosystems. Springer-Verlag, Berlin, Heidelberg.

Baillon, S.; Hamel, J-F.; Wareham, V.E.; Mercier, A. (2012). Deep cold-water corals as nurseries for fish larvae. Theme 1. ABSTRACT and PROGRAM BOOK International Deep-Sea Coral Symposium, Amsterdam, The Netherlands, 1–6 April.

Baird, S.J.; Tracey, D.; Mormede, S.; Clark, M. (2013). The distribution of protected corals in New Zealand waters. *NIWA Client Report WLG2012-43*. 93 p. (Report prepared for Department of Conservation).http://www.doc.govt.nz/Documents/conservation/marine-and-coastal/marine-conservation-services/pop-2011-06-coral-distribution.pdf

Bak, R.P.M. (1973). Coral weight increment in-situ. A new method to determine coral growth. *Marine Biology 20(1):* 45–49.

Barnes, D.J. (1970). Coral skeletons: an explanation of their growth and structure. *Science 170(3964)*: 1305–1308.

Baussant, T.; Nilsen, M.; Godal, B.F.; Kaland, T.; Hedegaard, M. (2010). Report from the Coral Workshop 31st May – 1st June 2010 Cold-water coral ecosystems: knowledge status, gaps, research needs and strategy related to oil and gas operations. Report of International Research Institute of Stavanger (IRIS) 2011/054. 51 p.

Bayer, F.M.; Macintyre, I.G. (2001). The mineral component of the axis and holdfast of some gorgonacean octocorals (Coelenterata: Anthozoa), with special reference to the family Gorgoniidae. *Proceedings of the Biological Society of Washington 114*: 309–345.

Bell, N.; Smith, J. (1999) Coral growing on North Sea oil rigs. *Nature 402:*601.

Biber, M.F.; Duineveld, G.C.A.; Lavaleye, M.S.S.; Davies, A.J.; Bergman, M.J. Nvan den Beld, I.M.J. (2013). Investigating the association of fish abundance and biomass with cold-water corals in the deep Northeast Atlantic Ocean using a generalized linear modelling approach. *Deep Sea Research II: In press.*

Bischoff, W.D.; Mackenzie, F.T.; Bishop, F.C. (1987). Stabilities of synthetic magnesian calcites in aqueous solution: comparison with biogenic minerals. *Geochimica et Cosmochimica Acta, 51*: 1413–1423.

Bostock, H.C.; Hayward, B.W.; Neil, H.L.; Currie, K.I.; Dunbar, G.B. (2011). Deep-water carbonate concentrations in the southwest Pacific. *Deep-Sea Research I 58*:72–85.

Bostock, H.C.; Sutton, P.J.; Williams, M.J.M.; Opdyke, B.N. (2013). Reviewing the circulation and mixing of Antarctic Intermediate Water in the South Pacific using evidence from geochemical tracers and Argo float trajectories. *Deep-Sea Research I 73*: 84–98.

Brewer, P.G.; Glover, D.M.; Goyet, C.; Shafer, D.K. (1995). The pH of the North Atlantic Ocean: Improvements to the global model for sound absorption in seawater. *Journal of Geophysical Research 100*: 8761–8776.

Brewer, P.G.; Goyet, C.; Friederich, G. (1997). Direct observation of the oceanic CO_2 increase revisited. *Proceedings of the National Academy of Science of USA 94*: 8308–8313.

Brooke, S.; Young, C.M. (2009). In situ measurement of survival and growth of *Lophelia pertusa* in the northern Gulf of Mexico. *Marine Ecology Progress Series 397*:153–161, doi: 10.3354/meps08344.

Bryan, T.L.; Metaxas, A. (2006). Distribution of deep-water corals along the North American continental margins: relationships with environmental factors. *Deep-Sea Research I 53*: 1865–1879.

Buckley, B.A.; Szmant, A.M. (2004). RNA/DNA ratios as indicators of metabolic activity in four species of scleractinian corals. *Marine Ecology Progress Series 282*, 143–149.

Buddemeier, R.W.; Kinzie, R.A. (1976). Coral growth. *Oceanography and Marine Biology Annual Review 14*: 183–225.

Buhl-Mortensen, L.; Mortensen, P.B. (2005). Distribution and diversity of species associated with deepsea gorgonian corals off Atlantic Canada. Cold-Water Corals and Ecosystems. Springer Publishing House, Heidelberg, Germany, pp. 849–879.

Butschli, O. (1908). Untersuchungen über organische Kalkgebilde: K. Gesell. *Wiss. Gottingen, Abh* 6: 1–164.

Cairns, S.D. (1995). The Marine Fauna of New Zealand: Scleractinia (Cnidaria: Anthozoa). *New Zealand Oceanographic Institute Memoir 103*:210 p.

Cairns S.D. (2012). The Marine Fauna of New Zealand: New Zealand Primnoidae (Anthozoa: Alcyonacea). Part 1. Genera *Narella*, *Narelloides*, *Metanarella*, *Calyptrophora*, and *Helicoprimnoa. NIWA Biodiversity Memoir 126*: 71 p.

Cairns, S.D.; Macintyre, I.G. (1992). Phylogenetic implications of calcium carbonate mineralogy in Stylasteridae (Cnidaria: Hydrozoa). *Palaios 7*:96–107.

Caldeira, K.; Wickett, M.E. (2003). Anthropogenic carbon and ocean pH. *Nature 425*: 365.

Canadell, J.G.; Le Quéré, C.; Raupach, M.R.; Field, C.B.; Buitenhuis, E.T.; Ciais, P.; Conway, T.J.; Gillett, N.P.; Houghton, R.A.; Marland, G. (2007). Contributions to accelerating atmospheric CO_2 growth from economic activity, carbon intensity, and efficiency of natural sinks. *Proceedings of the National Academy of Sciences of USA, 104(47).*

Carreiro-Silva, M.; Purser, A. (2012). Report on decreasing seawater pH effects on coral growth as assessed from experiments. HERMIONE, Hotspot Ecosystem Research and Man's impact on European Seas FP7 Collaborative Project, Deliverable 4.4, 27 p.

Carter, L.; McCave, I.N. (1997). The sedimentary regime beneath the deep western boundary current inflow to the SW Pacific Ocean. *Journal of Sedimentary Research 67*: 1005–1017.

Carton, J.A.; Giese, B.S. (2008). A reanalysis of ocean climate using simple ocean data assimilation (SODA). *Monthly Weather Review 136*: 2999–3017.

Chave, K.E. (1954). Aspects of the biogeochemistry of magnesium: 1. Calcareous marine organisms. *Journal of Geology 62*: 266–283.

Cheng, H.; Adkins, J.; Edwards, R.L.; Boyle, E.A. (2000). U-Th dating of deep sea corals. *Geochimica et Cosmochimica Acta 64*: 2401–2416.

Chiswell, S.M.; Sutton, P.J.H. (1998). A deep eddy in the Antarctic Intermediate Water north of the Chatham Rise. *Journal of Physical Oceanography 28*: 535–540.

Clark, M.R. (1999). Fisheries for orange roughy (*Hoplostethus atlanticus*) on seamounts in New Zealand. *Oceanologica Acta 22(6):* 593–602.

Clark, M.; O'Driscoll, R. (2003). Deepwater fisheries and aspects of their impact on seamount habitat in New Zealand. *Journal of Northwest Atlantic Fishery Science 31*: 441–458.

Clark, M.R.; Rowden, A.A. (2009). Effect of deepwater trawling on the macro-invertebrate assemblages of seamounts on the Chatham Rise, New Zealand. *Deep Sea Research I 56*: 1540–1554.

Clark, M.R.; Tittensor, D.P. (2010). An index to assess the risk to stony corals from bottom trawling on seamounts. *Marine Ecology 31*:200–211.

Clark, M.R., Dunn, M.R. (2012). Spatial management of deep-sea seamount fisheries: balancing sustainable exploitation and habitat conservation. Environmental Conservation 39: 204–214.

Clarke, F.W.; Wheeler, W.C. (1917). The inorganic constituents of marine invertebrates. *U.S. Geological Survey Professional Papers 102*: 56 p.

Consalvey, M.; MacKay, K.; Tracey, D. (2006). Information review for protected deep-sea coral species in the New Zealand region. NIWA Client Report prepared for Department of Conservation. WLG2006-85. 60 p.

Correge, T. (2006). Sea surface temperature and salinity reconstruction from coral geochemical tracers. *Palaoegeography, Palaeoclimatology, Palaeoecology*, 232, 408–428.

Costello, M.J.; McCrea, M.; Freiwald, A.; Lundalv, T.; Jonsson, L.; Bett, B.J.; van Weering, T.C.E.; de Haas, H.; Roberts, J.M.; Allen, D. (2005). Role of cold-water *Lophelia pertusa* coral reefs as habitat in the NE Atlantic. *In:* Freiwald, A; Roberts, J.M. (Eds.), *Cold-Water Corals and Ecosystems*. Berlin: Springer-Verlag, 771–805.

Cummings, V.; Hewitt, J.; Van Rooyen, A.; Currie, K.; Beard, S.; Thrush, S.; Norkko, J.; Barr, N.; Heath, P.; Halliday, N.J.; Sedcole, R.; Gomez, A.; McGraw, C.; Metcalf, V. (2011). Ocean acidification at high latitudes: Potential effects on functioning of the Antarctic bivalve *Laternula elliptica. PLoS ONE 6(1):* e16069.

Damour, A. (1852). Note sur la composition des millepores et de quelque corallinées. *Academie of Sciences, Paris, Comptes Rendus 32*: 253–255.

Davies, P.S. (1989). Short-term growth measurements of corals using an accurate buoyant weighing technique. *Marine Biology 101*: 389–395.

Davies, A.J.; Guinotte, J.M. (2011). Global habitat suitability for framework-forming cold-water corals. *PLoSONE, 6*: e18483.

Dickson, A.G.; Millero, F.J. (1987). A comparison of the equilibrium constants for the dissociation of carbonic acid in seawater media, *Deep Sea Research I 34*: 1733–1743.

Dickson, A.G.; Sabine, C.L.; Christian, J.R. (2007). Guide to Best Practices for Ocean CO2 Measurements, *PICES Special Publication, 3*, 191 pp., North Pacific Marine Science Organisation, Sidney, B. C., Canada.

Dodge, R.E.; Wyers, S.C.; Frith, H.R.; Knap, A.H.; Smith, S.R.; Cook, C.B.; Sleeter, T.D. (1984). Coral calcification rates by the buoyant weight technique: Effects of alizarin staining. *Journal of Experimental Marine Biology and Ecology 75(3)*:217–232.

Doney, S.C.; Balch, W.M.; Fabry, V.J.; Feely, R.A. (2009). Ocean acidification: A critical emerging problem for the ocean sciences. *Oceanography* 22(4):16–25. http://dx.doi.org/10.5670/oceanog.2009.93

D'Onghia, G.; Maiorano, P.; Sion, L.; Giove, A.; Capezzuto, F.; Carlucci, R.; Tursi, A. (2010). Effects of deep-water coral banks on the abundance and size structure of the megafauna in the Mediterranean Sea. *Deep Sea Research II 57*:397–411.

Druffel, E.R.M.; Griffin, S.; Witter, A.; Nelson, E.; Southon, J.; Kashgarian, M.; Vogel, J. (1995). *Gerardia*: bristlecone pine of the deep sea? *Geochimica et Cosmochimica Acta, 59*:5031–5036.

Druffel, E.R.M.; King, L.L.; Belastock, R.A.; Buesseler K.O. (1990). Growth rate of a deep-sea coral using ^{210}Pb and other isotopes. *Geochimica et Cosmochimica Acta 54*:1493–1500.

Duncan, P.M. (1877). On the rapidity of growth and variability of some *Madreporaria* on an Atlantic cable with remarks on the rate of accumulation of foraminiferal deposits. *Proceedings of the Royal Society of London 26*:133–137.

Echevin, V.; Aumont, O.; Ledesma, J.; Flores, G. (2008). The seasonal cycle of surface chlorophyll in the Peruvian upwelling system: A modelling study. *Progress in Oceanography 79(2–4)*: 167–176.

Etnoyer, P.; Morgan. L.E. (2005). Habitat forming deep-sea corals in the Northeast Pacific Ocean. *In:* Freiwald, A.; Roberts, J.M. (eds) Cold-water corals and ecosystems. Springer-Verlag Berlin, p 332–343

Fabry, V.J. (2008). Marine calcifiers in a high-CO_2 ocean. *Science 320:*1020–1022.

Feely, R.A.; Sabine, C.L.; Byrne, R.H.; Millero, F.J.; Dickson, A.G.; Wanninkhof, R.; Murata, A.; Miller, L.A.; Greeley, D. (2012). Decadal changes in the aragonite and calcite saturation state of the Pacific Ocean. *Global Biogeochemical Cycles, 26*: GB3001, doi:10.1029/2011GB004157.

Feely, R.A.; Sabine, C.L.; Hernandez-Ayon, J.M.; Ianson, D.; Hales, B (2008). Evidence for upwelling of corrosive "acidified" water onto the continental shelf. *Science 320*:1490–1492.

Feely, R.A.; Sabine, C.L.; Lee, K.; Berelson, W.; Kleypas, J.; Fabry, V.J.; Millero, F.J. (2004). Impact of anthropogenic CO_2 on the $CaCO_3$ system in the oceans. *Science, 305:* 362–366.

Fine, M.; Tchernov, D. (2007). Scleractinian coral species survive and recover from decalcification. *Science 315*: 1811.

Forchammer, G. (1852). Beiträge zur Bildungsgeschichte des Dolomits. *Neues Jahrbuch für Mineralogie, Jahrg*. 854–858.

Form, A.U.; Riebesell, U. (2012). Acclimation to ocean acidification during long-term CO_2 exposure in the cold water coral *Lohelia pertusa. Global Change Biology, 18*: 843–853, doi: 10.1111/j.1365-2486.2011.02583.x

Försterra, G.; Häussermann, V. (2008). Unusual symbiotic relationships between microendolithic phototrophic organisms and azooxanthellate cold-water corals from Chilean fjords. *Marine Ecology Progress Series 370*: 121–125.

Fosså, J.H.; Kutti, T.; Helle, K.; Bergstad, O.A. (2012). Associations and functional links between tusk and cold water coral and sponge habitats examined by experimental long-line fishing. Theme 1. ABSTRACT and PROGRAM BOOK International Deep-Sea Coral Symposium, Amsterdam, The Netherlands, 1–6 April.

Freiwald, A.; Fosså, J.H.; Grehan, A.; Koslow, T.; Roberts, J.M. (2004). Cold-water coral reefs. UNEP-WCMC, Cambridge, UK.

Freiwald, A.; Henrich, R.; Pätzold, J. (1997). Anatomy of a deepwater coral reef mound from Stjernsund, West-Finnmark, northern Norway. *SEPM, Special Publication, 56,* pp. 141–161.

Gagan, M.K.; Ayliff, L.K.; Hopley, D. (1998). Temperature and surface-ocean water balance of the mid-Holocene tropical Western Pacific. *Science, 279*: 1014–1018.

Gass, S.E.; Roberts, J.M. (2006). The occurrence of the cold water coral *Lophelia pertusa* (Scleractinia) on oil and gas platforms in the North Sea: colony growth, recruitment and environmental controls on distribution. *Marine Pollution Bulletin 52*:549–559.

Goreau, T.F. (1959). The physiology of skeleton formation in corals I. A method for measuring the rate of calcium deposition by corals under different conditions. *The Biological Bulletin 116*:59–75.

Gori, A.; Orejas, C.; Ferrier-Pagès, C. (2012). Uptake rates of dissolved organic matter by four cold-water coral species from the Cap de Creus canyon (northwestern Mediterranean). Theme II. 5th International Symposium on Deep-Sea Corals 2012, April 2–6. *In*: van Weering, T., Mienis, F., de Raad, I., Nieuwenhuizen, J. *Program and Abstracts,* 128 p. www.deepseacoral.nl

Gracey, A.Y. (2007). Interpreting physiological responses to environmental change through gene expression profiling. *Journal of Experimental Biology 209*:1584–1592.

Grange, K.R. (1985). Distribution, standing crop, population structure, and growth rates of black coral in the southern fiords of New Zealand. *New Zealand Journal of Marine and Freshwater Research 19*:467–475.

Grange, K.R.; Singleton, R.J.; Richardson, J.R.; Hill, P.J.; Main, W. de L. (1981). Shallow rock wall biological associations of some southern fiords of New Zealand. *New Zealand Journal of Zoology 8*:209–227.

Griffin, S.; Druffel, E.R.M. (1989). Sources of carbon to deep-sea coral skeletons. *Radiocarbon 31*:533–542.

Gruber, N.; Gloor, M.; Mikaloff Fletcher, S.E.; Doney, S.C.; Dutkiewicz, S.; Follows, M.J.; Gerber, M.; Jacobson, A.R.; Joos, F.; Lindsay, K.; Menemenlis, D.; Mouchet, A.; Müller, S.A.; Sacramento, J.L.; Takahashi, T. (2009). Oceanic sources, sinks, and transport of atmospheric CO_2. *Global Biogeochemical Cycles, 23 (1)*, doi:10.1029/2008GB003349.

Gruber, N.; Hauri, C.; Lackhar, Z.; Loher, D.; Frölicher, T.L.; Plattner, G.-K. (2012). Rapid Progression of Ocean Acidification in the California Current System. *Science 337*: 220–223.

Guinotte, J.M.; Orr, J.; Cairns, S.; Freiwald, A.; Morgan, L.; George, R. (2006). Will human-induced changes in seawater chemistry alter the distribution of scleractinian bioherms? *Frontiers in Ecology and the Environment 4*: 141–146.

Hadfield, M.G.; Rickard, G.J.; Uddstrom, M.J. (2007). A hydrodynamic model for Chatham Rise, New Zealand. *New Zealand Journal of Marine and Freshwater Research 41*:239–264.

Haidvogel, D.B.; Arango, H.G.; Hedström, K.S.; Beckmann, A.; Malanotte-Rizzoli, P.; Shchepetkin, A.F. (2000). Model evaluation experiments in the North Atlantic Basin: simulations in nonlinear terrain-following coordinates. *Dynamics of Atmospheres and Oceans 32:* 239-281.

Hamilton, L.J. (2006). Structure of the Subtropical Front in the Tasman Sea. *Deep-Sea Research I, 53*:1989–2009.

Häussermann, V.; Försterra, G. (2007). Large assemblages of cold-water corals in Chile—a summary of recent findings and their implications. *In:* George, R.Y.; Cairns, S.D. (Eds.) Conservation and adaptive management of seamount and deep-sea coral ecosystems. Rosenstiel School of Marine and Atmospheric Science, University of Miami, Miami, FL, 195–207.

Heilmayer, O.; Brey, T. (2003). Saving by freezing? Metabolic rates of *Adamussium colbecki* in a latitudinal context. *Marine Biology, 143 (3):*477–484.

Henry, L.A.; Roberts, J.M. (2007). Biodiversity and ecological composition of macrobenthos on cold-water coral mounds and adjacent off-mound habitat in the bathyal Porcupine Seabight, NE Atlantic. *Deep Sea Research 1 54:* 654–672.

Herler, J.; Drinwöber, M. (2011). A simple technique for measuring buoyant weight increment of entire, transplanted coral colonies in the field. *Journal of Experimental Biology and Ecology 407*: 250–255.

Hobgom, A.G. (1894). Über Dolomitbildung und dolomitische Kalkorganismen. *Neues Jahrbuch für Mineralogie, Jahrg. 1*: 262–274.

Hofmann, G.E.; O'Donnell, M.J.; Todgham, A.E. (2008). Using functional genomics to explore the effects of ocean acidification on calcifying marine organisms. *Marine Ecology Progress Series 373*: 219–225.

Huehnerbach, V.; Blondel, P.; Huvenne, V.; Freiwald, A. (2007). Habitat mapping on a deep-water coral reef off Norway, with a comparison of visual and computer-assisted sonar imagery interpretation. *In:* Todd, B.; Greene, G. (Eds.), Mapping the Seafloor for Habitat Characterization. *Geological Association of Canada Special Paper 47:* 297–308.

Husebø, A.; Nøttestad, L.; Fosså, J.H., Furevik, D.M., Jørgensen, S.B. (2002) Distribution and abundance of fish in deep-sea coral habitats. *Hydrobiologia 471*: 91–99.

(IPCC) Intergovernmental Panel on Climate Change (2007). http://www.ipcc.ch/publications_and_data/publications_and_data_reports.shtml.

Jantzen, C.; Laudien, J.; Häussermann, V.; Försterra, G.; Richter, C. (2012). Cold water corals grow under future pH conditions in situ. 5th International Symposium on Deep-Sea Corals 2012, April 2-6. *In:* van Weering, T., Mienis, F., de Raad, I., Nieuwenhuizen, J. *Program and Abstracts*, 128 p. www.deepseacoral.nl

Jensen, A.; Frederikson, R. (1992). The fauna associated with the bankforming deepwater coral *Lophelia pertusa* (Scleractinaria) on the Faroe shelf. *Sarsia 77*: 53–69.

Jokiel, P.L.; Rodgers, K.S.; Kuffner, I.B.; Andersson, A.J.; Cox, E.F.; Mackenzie, F.T. (2008). Ocean acidification and calcifying reef organisms: a mesocosm investigation. *Coral Reefs 27(3)*: 473–483.

Kalnay, E.; Kanamitsu, M.; Kistler, R.; Collins, W.; Deaven, D.; Gandin, L.; Iredell, M.; Saha, S.; White, G.; Woollen, J.; Zhu, Y.; Leetmaa, A.; Reynolds, R.W.; Chelliah, M.; Ebisuzaki, W.; Higgins, W.; Janowiak, J.; Mo, K.C.; Ropelewski, C.; Wang, J., Jenne, R.; Joseph, D. (1996). The NCEP/NCAR 40-Year Reanalysis Project. *Bulletin of the American Meteorological Society 77*:437–471.

Lagenbuch, M.; Pörtner , H.O. (2003). Energy budget of hepatocytes from Antarctic fish (Pachycara brachycephalum and Lepidonotothen kempi) as a function of ambient CO_2: pH-dependent limitations of cellular protein biosynthesis? *Journal of Experimental Biology 206*: 3895–3903.

Lahkar, Z.; Gruber, N. (2013). Response of biological production and air-sea CO2 fluxes to upwelling intensification in the California and Canary Current Systems. *Journal of Marine Systems*, 109: 149–160.

Lewis, E.; Wallace, D.W.R. (1998). Program developed for CO_2 system calculations, Rep. 105, 33 pp., Oak Ridge Natl. Lab., Oak Ridge, Tenn. [Available at http://cdiac.esd.ornl.gov/oceans/co2rprt.html]

Lundälv, T.; Guihen, D.; Jonsson, L.; White, M. (2012). Long-term time-lapse observations in situ in a cold-water coral habitat. 5th International Symposium on Deep-Sea Corals 2012, April 2–6. *In:* van Weering, T., Mienis, F., de Raad, I., Nieuwenhuizen, J. *Program and Abstracts*, 128 p. www.deepseacoral.nl

Lunden, J.J.; Georgian, S.E.; McNicholl, C.; Sears, C.; El-Ashry, S.; Cordes, E.E. (2012) Carbonate Dynamics and Calcification of *Lophelia pertusa* in the Northern Gulf of Mexico 5th International Symposium on Deep-Sea Corals 2012, April 2-6. *In:* van Weering, T., Mienis, F., de Raad, I., Nieuwenhuizen, J. *Program and Abstracts*, 128 p. www.deepseacoral.nl

Maier, C. (2012). Response of cold-water corals to ocean acidification. 5th International Symposium on Deep-Sea Corals 2012, April 2–6. *In:* van Weering, T., Mienis, F., de Raad, I., Nieuwenhuizen, J. *Program and Abstracts*, 128 p. www.deepseacoral.nl

Maier, C.; Hegeman, J.; Weinbauer, M.G.; Gattuso, P. (2009). Calcification of the cold-water coral *Lophelia pertusa* under ambient and reduced pH. *Biogeosciences 6:* 1671–1680, doi:10.5194/bg-6-1671-2009.

Maier, C.; de Kluijver, A.; Agis, M.; Brussaard, C.P.D.; Van Duyl, F.C.; Weinbauer, M.G. (2011). Dynamics of nutrients, total organic carbon, prokaryotes and viruses in onboard incubations of cold-water corals. *Biogeosciences 8*: 2609–2620, doi:10.5194/bg-8-2609-2011.

Maier, C.; Watremez, P.; Taviani, M.; Weinbauer M.G.; Gattuso, J.P. (2012). Calcification rates and the effect of ocean acidification on Mediterranean cold-water corals. *Proceedings of the Royal Society B-Biological Sciences 279(1734):* 1716–1723. doi: 10.1098/rspb.2011.1763.

Marchesiello, P.; McWilliams, J.C.; Shchepetkin, A.F. (2003). Equilibrium structure and dynamics of the California Current System. *Journal of Physical Oceanography 33*:753–783.

Marschal, C.; Garrabou, J.; Harmelin, J.G.; Pichon, M. (2004). A new method for measuring growth and age in the precious red coral *Corallium rubrum* (L.). *Coral Reefs 23*:423–432.

Matsumoto, A.K. (2007). Effects of low water temperature on growth and magnesium carbonate concentrations in the cold-water gorgonian *Primnoa pacifica. Bulletin of Marine Science 81:* 423–435.

McCloskey, L.R., (1970). The dynamics of the community associated with a marine scleractinian coral. *Internationale Revue der gesamten Hydrobiologie und Hydrographie 55*: 13–81.

McCulloch, M.; Trotter, J.; Montagna, P.; Falter, J.; Dunbar, R.; Freiwald, A.; Forsterra, G.; Lopez-Correa M.; Maier, C.; Ruggerberg, A.; Taviani, M. (2012). Resilience of cold-water scleractinian corals to ocean acidification: Boron isotopic systematics of pH and saturation state up-regulation. *Geochimica et Cosmochimica Acta 87:* 21–34.

Mehrbach, C.; Culberson, C.H.; Hawley, J.E.; Pytkowicz R.M. (1973). Measurement of the apparent dissociation constants of carbonic acid in seawater at atmospheric pressure, *Limnology and Oceanography 18:* 897–907, doi:10.4319/lo.1973.18.6.0897

Meigen, W. (1903). Beiträge zur Kenntnis des kohlensäuren Kalk. *Naturwiss. Gesell. Freiburg Ber. (Journal of the Royal Microscopical Society) 13*: 1–55.

Mikkelsen, N.; Erlenkauser, H.; Killingley, J.S.; Berger, W.H. (1982). Norwegian corals: radiocarbon and stable isotopes in *Lophelia pertusa. Boreas 5:*163–171.

Millero, F.J. (1995). Thermodynamics of the carbon dioxide system in the Oceans. *Geochimica et Cosmochimica Acta 59:* 661–677, doi:10.1016/0016-7037(94)00354-O

Milliman, J.D. (1974). *Recent sedimentary carbonates*. New York, Springer-Verlag.

Ministry for Primary Industries (2012). Report from the Fisheries Assessment Plenary, May 2012: stock assessments and yield estimates. Compiled by the Fisheries Science Group, Ministry for Primary Industries, Wellington, New Zealand. 1194 p. (Unpublished report held by the Ministry for Primary Industries, Wellington.)

Moore, J.; Auster, P.; Calini, D.; Heinonen, K.; Barber, K.; Hecker, B. (2008). The false boarfish *Neocyttus helgae* in the western North Atlantic. *Bulletin of the Peabody Museum of Natural History 49*: 31–41.

Morse, J.W. ; Andersson, A.J. ; Mackenzie, F.T. (2006). Initial responses of carbonate rich shelf sediments to rising atmospheric pCO_2 and ocean acidification: role of high Mg-calcites. *Geochimica et Cosmochimica Acta 70*: 5814–5830.

Mortensen, P.B. (2000). *Lophelia pertusa* (Scleractinia) in Norwegian waters. Distribution, growth, and associated fauna. Unpublished PhD thesis, University of Bergen.

Mortensen, P.B. (2001). Aquarium observations on the deepwater coral *Lophelia pertusa* (L., 1758) (Scleractinia) and selected associated invertebrates. *Ophelia 54*:83–104.

Mortensen, P.B.; Buhl-Mortensen, L., (2004). Distribution of deep-water gorgonian corals in relation to benthic habitat features in the Northeast Channel (Atlantic Canada). *Marine Biology 144:*1223–1238.

Mortensen, P.B.; Buhl-Mortensen, L. (2005). Morphology and growth of the deep-water gorgonians *Primnoa resedaeformis* and *Paragorgia arborea. Marine Biology 147*:775–788.

Mortensen, P.B.; Rapp, H.T. (1998). Oxygen and carbon isotope ratios related to growth line patterns in skeletons of *Lophelia pertusa* (L) (Anthozoa: Scleractinia): implications for determination of linear extension rates. *Sarsia 83*: 433–446.

Mucci, A. (1983). The solubility of calcite and aragonite in seawater at various salinity's, temperatures and one atmospheric total pressure. *American Journal of Science 283:* 780–799.

Munday, P.L.; Donelson, J.M.; Dixon, D.L.; Endo, G.G.K. (2009). Effects of ocean acidification on the early life history of a tropical marine fish. *Proceedings of the Royal Society B-Biological Sciences 276:* 3275–3283.

Naumann, M.S.; Orejas, C.; Ferrier-Pagès, C. (2013). Species-specific physiological response by the cold-water corals *Lophelia pertusa* and *Madrepora oculata* to variations within their natural temperature range, *Deep-Sea Research II,* http://dx.doi.org/10.1016/j.dsr2.2013.05.025

Neil, H.; Clark, M.; Tracey, D.; Marriott, P. (in review). Age and growth of habitat-forming *Solenosmilia variabilis* – information to assess recovery potential from bottom trawling. *New Zealand Journal of Marine and Freshwater Research.*

Nelson, W.A.; Neill, K.; Farr, T.; Barr, N.; D'Archino, R.; Miller, S.; Stewart, R. (2012). Rhodolith beds in northern New Zealand: characterisation of associated biodiversity and vulnerability to environmental stressors. *New Zealand Aquatic Environment and Biodiversity Report. 99.* 106 p.

Nichols, H.W. (1906). New forms of concretions. *Field Columbian Mus. Pub. 111 Geology series, 3:* 25–54.

Nodder, S.D.; Boyd, P.W.; Chiswell, S.M.; Pinkerton, M.H.; Bradford-Grieve, J.M.; Greig, M.J.N. (2005). Temporal coupling between surface and deep ocean biogeochemical processes in contrasting subtropical and subantarctic water masses, southwest Pacific Ocean. *Journal of Geophysical Research, 110:* C12017, doi:10.1029/2004JC002833.

Noé, S.U.; Lembke-Jene, L.; Dullo, W.C. (2008). Varying growth rates in bamboo corals: sclerochronology and radiocarbon dating of a mid-Holocene deep-water gorgonian skeleton (*Keratoisis* sp.: Octocorallia) from Chatham Rise (New Zealand). *Facies 54*:151–166.

Orejas, C.; Ferrier-Pages, C.; Reynaud, S.; Gori, A.; Beraud, E.; Tsounis, G.; Allemand, D.; Gili, J. M. (2011a). Long-term growth rates of four Mediterranean cold-water coral species maintained in aquaria. *Marine Ecology Progress Series 429:* 57–65. doi:10.3354/meps09104.

Orejas, C.; Ferrier-Pagès, C.; Reynaud, S.; Tsounis, G.; Allemand, D.; Gili, J.M. (2011b). Experimental comparison of skeletal growth rates in the cold-water coral *Madrepora oculata* Linnaeus, 1758 and three tropical scleractinian corals. *Journal of Experimental Marine Biology and Ecology* doi:10.1016/j.jembe.2011.05.008.

Orejas, C.; Gori, A.; Gili, J.M. (2008). Growth rates of live *Lophelia pertusa* and *Madrepora oculata* from the Mediterranean Sea maintained in aquaria. *Coral Reefs 27*:255.

Orejas, C.; Purser, A.; Roberts, J.M.; Carreiro-Silva, M.; Gori, A.; Gili, J.M.; Madurell, T.; Puig, P.; Braga-Henriques, A.; Thomsen. L. (2013). Report on coral aquaria experiments related to ecophysiology (growth, feeding, respiration, mucus production and reproduction). WP4: Cold water Coral (CWC) Ecosystems. EU DG Research FP7 project Hermione Report 27 p.

Orr, J.; Fabry, V.J.; Aumont, O.; Bopp, L.; Doney, S.C.; Feely, R.A.; Gnanadesikan, A.; Gruber, N.; Ishida, A.; Fortunat, J.; Key, R.M.; Lindsay, K.; Maier-Reimer, E.; Matear, R.; Monfray, P.; Mouchet, A.; Najjar, R.G.; Plattner, G.-K.; Rodgers, K.B.; Sabine, C.L.; Sarmiento, J.L.; Schlitzer, R.; Slater, R.D.; Totterdell, I.J.; Weirig, M.-F.; Yamanaka, Y.; Yool, A. (2005). Anthropogenic ocean acidification over the twenty-first century and its impact on calcifying organisms. *Nature 437*: 681–686. doi:10.1038/nature04095.

Pearse, V.B.; Muscatine, L. (1971). Role of symbiotic algae (Zooxanthellae) in coral calcification. *The Biological Bulletin 141*: 350–363.

Poloczanska, E.S.; Babcock, R.C.; Butler, A.; Hobday, A.J.; Hoegh-Guldberg, O.; Kunz, T.J.; Matear, R.; Milton, D.A.; Okey, T.A.; Richardson, A.J. (2007). Climate change and Australian marine life. *Annual Review on Oceanography and Marine Biology 45:* 407–478.

Pörtner, H.O. (2008). Ecosystem effects of ocean acidification in times of ocean warming: a physiologist's view. *Marine Ecology Progress Series 373*: 203–217.

Pörtner, H.O.; Hardewig, I.; Peck, L.S. (1999). Mitochondrial function and critical temperature in the Antarctic bivalve *Laternula elliptica. Comparative Biochemistry and Physiology A* 124:179–189.

Purser, A.; Orejas C.; Gori, A.; Tong, R.; Unnithan, V.; Thomsen, L. (2013). Local variation in the distribution of benthic megafauna species associated with cold-water coral reefs on the Norwegian margin. *Continental Shelf Research 54*:37–51.

Ramm, K. (2012a). Conservation Services Programme Observer Report: 1 July 2009 to 30 June 2010 Final Report. Conservation Services Programme, Department of Conservation. 130 p.

Ramm, K. (2012b). Conservation Services Programme Observer Report: 1 July 2010 to 30 June 2011. Final Report. Conservation Services Programme, Department of Conservation, November 2012. 121 p.

Reynolds, R.W.; Rayner, N.A.; Smith, T.M.; Stokes, D.C.; Wang, W. (2002). An improved in situ and satellite SST analysis for climate. *Journal of Climate 15:*1609–1625.

Reveillaud, J.; Freiwald, A.; Van Rooij, D.; Le Guilloux, E.; Altuna, A.; Foubert, A.; Vanreusal, A.; Roy K.O.-L.; Henriet, J.P. (2008). The distribution of scleractinian corals in the Bay of Biscay, NE Atlantic. *Facies 54,* 317–331.

Rickard, G.J.; Hadfield, M.G.; Roberts, M.J. (2005). Development of a regional ocean model for New Zealand. *New Zealand Journal of Marine and Freshwater Research 39*:1171–1191.

Riebesell, U.; Zondervan, I.; Rost, B.; Tortell, P.D.; Zeebe, R.E.; Morel, F.M.M. (2000). Reduced calcification of marine plankton in response to increased atmospheric CO2. *Nature* 407: 364–367.

Ries, J.B.; Cohen, A.L.; McCorkle, D.C. (2010). A nonlinear calcification response to CO2-induced ocean acidification by the coral *Oculina arbuscula*. *Coral Reefs 29:* 661–674, doi:10.1007/s00338-010-0632-3.

Risk, M.J.; Heikoop, J.M.; Snow, M.G.; Beukens, R. (2002). Lifespan and growth patterns of two deep sea corals: *Primnoa resedaeformis* and *Desmophyllum cristigalli*. *Hydrobiologia 471:*125–131.

Roark, E.B.; Guilderson, T.P.; Dunbar, R.B.; Fallon, S.J.; Mucciarone, D.A. (2009). Extreme longevity in proteinaceous deep-sea corals. *Proceedings of the National Academy of Science of USA 106(13):* 5204–5208.

Roark, E.B.; Guilderson, T.P.; Dunbar, R.B.; Ingram, B.L. (2006). Radiocarbon-based ages and growth rates of Hawaiian deep-sea corals. *Marine Ecology Progress Series 327:*1–14.

Roark, E.B.; Guilderson, T.P.; Flood-Page, S.R.; Dunbar, R.B.; Ingram, B.L.; Fallon, S.J.; McCulloch, M.T. (2005). Radiocarbon-based ages and growth rates for bamboo corals from the Gulf of Alaska. *Geophysical Research Letters 32:*L04606, doi:04610.01029/02004GL021919.

Roberts, J.M. (2002). The occurrence of the coral *Lophelia pertusa* and other conspicuous epifauna around an oil platform in the North Sea. *Journal of the Society for Underwater Technology, 25*: 83–91.

Roberts, J.M.; Henry, L.A.; Long, D.; Hartley, J.P. (2008). Cold-water coral reef frameworks, megafaunal communities and evidence for coral carbonate mounds on the Hatton Bank, north east Atlantic. *Facies 54:* 297–316

Roberts, J.M.; Wheeler, A.J.; Freiwald, A.; Cairns, S.D. (2009). *Coldwater corals: the biology and geology of deep-sea coral habitats.* Cambridge University Press.

Rodolfo-Metalpa, R.; Houlbreque, F.; Tambutte, E.; Boisson, F.; Patti, F.P.; Jeffre, R.; Fine, M.; Foggo, A.; Gattuso, J-P.; Hall-Spencer, J.M. (2011). Coral and mollusc resistance to ocean acidification adversley affected by warming. *Nature Climate Change 1:* 308–312.

Rodolfo-Metalpa, R.; Martin, S.; Ferrier-Pages, C.; Gattuso, P. (2010). Response of the temperate coral *Cladocora caespitosa* to mid- and long-term exposure to pCO2 and temperature levels projected for the year 2100 AD. *Biogeosciences 7:* 289–300, doi:10.5194/bg-7-289-2010.

Rogers, A.D.; Baco, A.; Griffiths, H.; Hall-Spencer, J.M. (2007). Corals on seamounts. In: Pitcher, T.J.; Morato, T.; Hart, P.J.B.; Clark, M.R.; Haggan, N.; Santos, R.S.; Oxford, M. (Eds.), *Seamounts: Ecology, Fisheries and Conservation.* Blackwell Publishing Fisheries and Aquatic Resources Series, Blackwell Scientific pp. 141–169.

Royal Society (2005). Ocean acidification due to increasing atmospheric carbon dioxide. http://royalsociety.org/policy/publications/2005/ocean-acidification/

Sanchez, J.A. (2005). Systematics of the bubblegum corals (Cnidaria: Octocorallia: Paragorgiidae) with description of new species from New Zealand and the Eastern Pacific. *Zootaxa 1014:* 1–72.

Shchepetkin, A.F.; McWilliams, J.C. (1998). Quasi-monotone advection schemes based on explicit locally adaptive diffusion. *Monthly Weather Review 126*:1541–1580.

Shchepetkin, A.F.; McWilliams, J.C. (2003). A method for computing horizontal pressure-gradient force in an oceanic model with a non-aligned vertical coordinate. *Journal of Geophysical Research 108:*3090, doi:3010.1029/2001JC001047.

Shchepetkin, A.F.; McWilliams, J.C. (2005). The regional oceanic modeling system (ROMS): a split-explicit, free-surface, topography-following-coordinate oceanic model. *Ocean Modelling 9:*347–404.

Silliman, B. (1846). On the chemical composition of the calcareous corals. *American Journal of Science 1:*189–199.

Smith, R.O.; Vennell, R.; Bostock, H.C.; Williams, M.J.M. (2013). Interaction of the subtropical front with topography around southern New Zealand. *Deep Sea Research I 76*: 13–26.

Soffker, M.; Sloman, K.A; Hall-Spencer, J.M. (2011). *In situ* observations of fish associated with coral reefs off Ireland. *Deep Sea Research I 58:* 818–825.

Song, Y.; Haidvogel, D.B. (1994). A semi-implicit ocean circulation model using a generalized topography-following coordinate system. *Journal of Computational Physics 115:*228–244.

Squires, D.F. (1965). Deep-water coral structure on the Campbell Plateau, New Zealand. *Deep Sea Research 12:*785–788.

Stanley, S.M.; Hardie, L.A. (1998). Secular oscillations in the carbonate mineralogy of reef-building and sediment producing organisms driven by tectonically forced shifts in seawater chemistry. *Palaeogeography, Palaeoclimatology, Palaeoecology*, 144: 3–19.

Stone, R.P. (2006). Coral habitat in the Aleutian Islands of Alaska: depth distribution, fine-scale species associations, and fisheries interactions. Coral Reefs 25: 229–238.

Tambutté, É.; Alleman, D.; Mueller, E.; Jaubert, J. (1996). A compartmental approach to the mechanism of calcification in hermatypic corals. *Journal of Experimental Marine Biology 199(5):* 1029–1041.

Thresher, R.E.; Guinotte, J.; Matear R.; Fallon S. (2012). Adapting to the effects of climate change on Australia's deep marine reserves. Fisheries Research and Development Corporation FRDC/NCCARF Report 2010/510, 68 p.

Thresher, R.E.; MacRae, C.M.; Wilson, C.M.; Gurney, R. (2007). Environmental effects on the skeletal composition of deepwater gorgonians (*Keratoisis* spp: Isididae). *Bulletin of Marine Science 81*:409–422.

Thresher, R.E.; Rintoul, S.R.; Koslow, J.A.; Weidman, C.; Adkins, J.; Proctor, C. (2004). Oceanic evidence of climate change in southern Australia over the last three centuries. *Geophysical Research Letters 31*:L07212.

Thresher, R.E.; Tilbrook, B.; Fallon, S.; Wilson, N.C.; Adkins, J. (2011). Effects of chronic low carbonate saturation levels on the distribution, growth and skeletal chemistry of deep-sea corals and other seamount megabenthos. *Marine Ecology Progress Series, 442*: 87–99. doi: 10.3354/meps09400.

Tittensor, D.P.; Baco, A.R.; Brewin, P.E.; Clark, M.R.; Consalvey, M.; Hall-Spencer, J.; Rowden, A.A.; Schlacher, T.; Stocks, K.I.; Rogers, A.D. (2009). Predicting global habitat suitability for stony coral on seamounts. *Journal of Biogeography, 36:* 1111–1128.

Tittensor, D.P.; Baco, A.R.; Hall-Spencer, J.M.; Orr; J.C.; Rogers, A.D. (2010). Seamounts as refugia from ocean acidification for cold-water stony corals. *Marine Ecology 31 (Suppl. 1):* 212–225.

Tracey, D.; Baird, S.J.; Sanders, B.M.; Smith, M.H. (2011a). Distribution of protected corals in relation to fishing effort and assessment of accuracy of observer identification. *NIWA Client Report No: WLG2011-33* prepared for Department of Conservation, Wellington. 74 p. http://www.doc.govt.nz/documents/conservation/marine-and-coastal/marine-conservation-services/draft-coral-report.pdf

Tracey, D.; Neil, H.; O'Shea S.; Gordon, D. (2003). Chronicles of the Deep: Complex steps to ageing deep-sea corals in New Zealand waters. *Water and Atmosphere. 11(2)*:3.

Tracey; D.M.; Neil; H.; Marriott; P.; Andrews, A.H.; Cailliet, G.M.; Sanchez, J.A. (2007). Age, growth, and age validation of two genera of deep-sea bamboo corals (Family Isididae) in New Zealand waters. *Bulletin of Marine Science 81 (3)*:393–408.

Tracey, D.M.; Rowden, A.A.; Mackay, K.A.; Compton, T. (2011b). Habitat-forming cold-water corals show affinity for seamounts in the New Zealand region. *Marine Ecology Progress Series 430:* 1–22.

Turley, C.M.; Roberts, J.M.; Guinotte, J.M. (2007). Corals in deep-water: will the unseen hand of ocean acidification destroy cold-water ecosystems? *Coral Reefs 26:* 445–448.

Vago, R.; Gill, E.; Collingwood, J.C. (1997). Laser measurements of coral growth. *Nature 386:* 30–31.

Wallace, D.W.R. (1995). Monitoring global ocean carbon inventories, Ocean Observing System Development Panel. Texas A&M University, College Station, TX 54 p.

Walter, L.M.; Morse, J.W. (1984). Magnesian calcite stabilities: a re-evaluation. *Geochimica et Cosmochimica Acta, 48*: 1059–1070.

Watling, L.; France, S.C.; Pante, E.; Simpson, A. (2011). Biology of deep-water octocorals. *Advances in Marine Biology 60*: 41–122.

Weinbauer, M.G.; Brandstätter, F.; Velimirov, B. (2000). On the potential use of Magnesium and Strontium concentrations as ecological indicators in the calcite skeleton of red coral (*Corallium rubrum*). *Marine Biology 137:* 801–809.

Wheeler, A.J.; Beyer, A.; Freiwald, A.; de Haas, H.; Huvenne, V.A.I.; Kozachenki, M.; Olu-Le Roy, K.; Opderbecke, J. (2007). Morphology and environment of cold-water coral carbonate mounds

on the NW European margin. *International Journal of Earth Sciences (Geologisch Rundschau) 96:*37–56.

Williams, A.; Schlacher, T.A.; Rowden, A.A.; Althaus, F.; Clark, M.R.; Bowden, D.A.; Stewart, R.; Bax, N.J.; Consalvey, M.; Kloser, R.J. (2010) Seamount megabenthic assemblages fail to recover from trawling impacts. *Marine Ecology 31(suppl. 1)*: 183–199.

Wilkin, J.L.; Arango, H.G.; Haidvogel, D.B.; Lichtenwalner, C.S.; Glenn, S.M.; Hedström; K.S. (2005). A regional ocean modeling system for the Long-term Ecosystem Observatory. *Journal of Geophysical Research 110*:C06S91, doi:10.1029/2003JC00221.

Wilson, J.B. (1979). Patch development of the deep-water coral *Lophelia pertusa* (L.) on Rockall Bank. *Journal of the Marine Biology Association UK 59*:165–177.

Wolf-Gladrow, D.A.; Zeebe, R.E.; Klass, C.; Körtzinger, A.; Dickson, A. (2007). Total alkalinity: the explicit conservative expression and its application to biogeochemical processes. *Marine Chemistry 106*:287–300.

World Ocean Atlas (2009) http://www.nodc.noaa.gov/OC5/WOA09/pr_woa09.html

Yesson, C.; Taylor, M.L.; Tittensor, D.P.; Davies, A.J.; Guinotte, J.; Baco, A.; Black, J.; Hall-Spencer, J. M.; Rogers, A.D. (2012). Global habitat suitability of cold-water octocorals. *Journal of Biogeography* doi:10.1111/j.1365-2699.2011.02681.x.

Zoccola, D.; Tambutté, E.; Senegas-Balas, F.; Michiels, J.F.; Failla, J.P.; Jaubert, J.; Allemand, D. (1999). Cloning of a calciumchannel α1 subunit from the reef-building coral, *Stylophora pistillata. Gene 227(2):* 157–167.

11. APPENDICES

Appendix 1. Table of corals analysed for trace element analyses, Mg/Ca, Sr/Ca, U/Ca

Appendix 2. Skeletal carbonate mineralogy of deep-water primnoid corals from east of New Zealand. Report from Abigail Smith, University of Otago, 26 April 2013

Appendix 3. Table of opportunistic water sample data analysed for alkalinity and DIC since 2011.

Appendix 1: Table of corals analysed for trace element analyses, Mg/Ca, Sr/Ca, U/Ca. Orange text denotes duplicates where the reproducibility is not very good; red text - there was a calculation error - these numbers have changed; green text - new data; blue text - checked outlier data.

Genera/Species	NIWA #	Latitude	Longitude	Depth	Temp	Region	An#	Run#	Mg/Ca	Sr/Ca	U/Ca
Primnoa sp.	53325	-42.809500	-179.516333	1251.0	4.3	2	M1_1	Mg CC 2	18.00	8.74	0.000126
Primnoa sp.	42636	-49.851670	175.321700	781.0	4.6	4	M2_1	Mg CC 3	6.90	9.11	0.000110
Primnoa sp.	11293	-48.001500	166.084800	940.0	5.4	5	M5_1	Mg CC 3	6.70	8.45	0.000080
Primnoa sp.	42618	-50.086670	165.938300	1004.0	4.5	5	M6_1	Mg CC 3	7.30	8.76	0.000093
Primnoa sp.	42634	-49.936670	163.811700	780.0	6.8	5	M7_1	Mg CC 3	8.80	8.68	0.000073
Primnoa sp.	42613	-44.517500	175.783333	600.0	6.0	3A	M8_1	Mg CC 3	5.00	9.69	0.000141
Primnoa sp.	42613	-44.517500	175.783333	600.0	6.0	3A	M8_1	Mg CC 4	6.00	9.54	0.000150
Primnoa sp.	62704	-44.517500	175.783333	600.0	6.0	3A	M9_1	Mg CC 3	5.00	9.58	0.000139
Primnoa sp.	62704	-44.517500	175.783333	600.0	6.0	4A	M9_1	Mg CC 4	5.05	9.57	0.000152
Primnoa sp.	49230	-44.496667	-174.821667	1283.0	4.4	3B	M10_1	Mg CC 3	10.50	8.65	0.000109
Primnoa sp.	49230	-44.496667	-174.821667	1283.0	4.4	3B	M10_1	Mg CC 4	10.50	8.88	0.000121
Primnoa sp.	42628	-44.510000	-174.825000	1300.0	4.1	3A	M11_1	Mg CC 5	30.00	8.37	0.000129
Keratoisis spp.	41553	-40.171699	177.3049927	951	6.67	1	M12a_1	Mg CC 3	85.00	3.10	0.000014
Keratoisis spp.	41553	-40.171699	177.3049927	951	6.67	1	M12b_1	Mg CC 3	90.00	3.09	0.000015
Keratoisis spp.	41553	-40.171699	177.3049927	951	6.67	1	M12c_1	Mg CC 3	90.00	3.12	0.000025
Keratoisis spp.	41553	-40.171699	177.3049927	951	6.67	1	M12_1	Mg CC 2	86.00	3.09	0.000015
Keratoisis spp.	27583	-43.357666	179.5828333	409	8.45	2	M13_1	Mg CC 5	93.00	3.12	0.000024
Keratoisis spp.	27583	-43.357666	179.5828333	409	8.45	2	M13node_1	Mg CC 5	94.00	3.36	0.000047
Keratoisis spp.	28307	-42.7325	-179.8985	1076	5.55	2	M14_1	Mg CC 6	90.00	3.05	0.000015
Keratoisis spp.	41843	-48.813333	175.37	740	4.64	4	M17_1	Mg CC 6	87.00	3.01	0.000026
Keratoisis spp.	41843	-48.813333	175.37	740	4.64	4	M17node_1	Mg CC 6	92.00	2.97	0.000178
Keratoisis spp.	17972	-48.0335	166.1002	935	5.38	5	M18_1	Mg CC 6	89.00	3.02	0.000019
Keratoisis spp.	41856	-49.945	163.8316667	835	5.76	5	M19_1	Mg CC 6	87.00	3.00	0.000023
Keratoisis spp.	41856	-49.945	163.8316667	835	5.76	5	M19node_1	Mg CC 7	91.00	3.03	0.000054
Keratoisis spp.	26596	-35.916999	165.6001587	1118	4.86	6	M20_1	Mg CC 7	84.00	3.00	0.000018
Keratoisis spp.	26588	-32.241699	170.2366943	2340	2.11	7	M23_1	Mg CC 7	84.00	2.97	0.000011
Keratoisis spp.	66242	-33.683333	167.733333	907	6.27	7	M24_1	Mg CC 7	88.00	3.00	0.000018
Keratoisis spp.	14375	-44.27283	178.9005	1063	3.69	3A	M25_1	Mg CC 7	85.00	3.05	0.000023

Genera/Species	NIWA #	Latitude	Longitude	Depth	Temp	Region	An#	Run#	Mg/Ca	Sr/Ca	U/Ca
Lepidisis spp.	28368	-39.446701	178.333298	1000.0	6.2	1	M28_1	Mg CC 2	81.00	3.07	0.000029
Lepidisis spp.	28368	-39.446701	178.333298	1000.0	6.2	1	M28_1	Mg CC 3	84.00	3.06	0.000032
Lepidisis spp.	26598	-42.715557	-179.906113	1181.0	4.5	2	M29_1	Mg CC 9	81.82	3.00	0.000020
Lepidisis spp.	41838	-42.723833	-179.690333	860.0	6.4	2	M30_1	Mg CC 9	88.62	3.05	0.000016
Lepidisis spp.	45305	-46.766000	166.153667	956.0	5.2	5	M31_1	Mg CC 9	86.05	2.92	0.000029
Lepidisis spp.	41827	-44.618333	-175.145000	1016.0	5.5	3B	M32_1	Mg CC 9	84.66	2.95	0.000022
Lepidisis spp.	28279	-31.980333	174.264500	1680.0	2.8	7B	M35_1	Mg CC 9	91.00	2.92	0.000021
Paragorgia spp.	42001	-44.496667	-174.821667	1283	4.36	3B	M37_1	Mix 3	87.00	3.16	0.000017
Paragorgia spp.	42001	-44.496667	-174.821667	1283	4.36	3B	M38_1	Mg CC 2	89.00	2.94	0.000025
Paragorgia spp.	42001	-44.496667	-174.821667	1283	4.36	3B	M38_1	Mg CC 3	96.00	2.92	0.000025
Paragorgia spp.	3308	-33.926667	167.918333	1225	4.29	7	M42_1	Mg CC 10	98.00	2.92	0.000042
Paragorgia spp.	42003	-34.821667	169.855000	780	7.32	7	M43_1	Mg CC 11	99.26	2.97	0.000061
Paragorgia spp.	66273	-47.296667	177.300000	577	7.81	4	M44_1	Mg CC 11	99.41	2.82	0.000088
Paragorgia spp.	66159	-49.298333	176.320000	1248	2.78	4	M45_1	Mg CC 11	101.45	3.00	0.000073
Paragorgia spp.	25527	-42.829166	177.421829	826	6.51	2	M46_1	Mg CC 11	102.00	2.95	0.000069
Paragorgia spp.	28154	-43.345001	178.658295	427	8.45	2	M47_1	Mix 3	109.00	3.09	0.000053
Madrepora oculata	26972	-41.295200	176.556198	731.0	7.6	1	A1_1	Arag 1	2.92	10.72	0.00240
Madrepora oculata	27572	-40.039799	178.142502	760.0	7.7	1	A2_1	Arag 2	3.13	10.64	0.00043
Madrepora oculata	3941	-42.792830	-179.981000	950.0	5.9	2	A3_1	Arag 1	2.52	11.28	0.00200
Madrepora oculata	4027	-42.786200	-179.985300	900.0	6.1	2	A4_1	Arag 1	2.75	11.03	0.00190
Madrepora oculata	47810	-42.750000	-179.980000	1112.0	5.0	2	A5_2	Arag 2	2.40	10.81	0.00223
Madrepora oculata	46495	-47.525000	177.923333	870.0	3.8	4	A6_1	Arag 2	2.36	11.07	0.00232
Madrepora oculata	47901	-50.078333	174.748333	916.0	3.9	4	A7_1	Arag 2	2.56	11.00	0.00214
Madrepora oculata	16019	-36.5732	177.2	1080	5.26	8	A9_1	Mix 3	2.69	6.01	0.00211
Madrepora oculata	65514	-44.461667	178.586667	730.0	5.1	3A	A11_1	Arag 2	2.78	10.51	0.00203

Genera/Species	NIWA #	Latitude	Longitude	Depth	Temp	Region	An#	Run#	Mg/Ca	Sr/Ca	U/Ca
Madrepora oculata	42406	-44.515000	-175.290000	709.0	7.1	3B	A12_1	Arag 3	2.60	11.33	0.00230
Madrepora oculata	42406	-44.515000	-175.290000	709.0	7.1	3B	A12 rep	Arag 5	2.60	11.46	0.00225
Madrepora oculata	47936	-44.278333	-174.605000	1099.0	5.1	3B	A14_1	Arag 3	2.31	10.68	0.00245
Madrepora oculata	47936	-44.278333	-174.605000	1099.0	5.1	3B	A14 rep	Arag 5	2.30	11.09	0.00247
Madrepora oculata	47958	-44.198300	-174.460000	1198.0	4.6	3B	A15_1	Arag 3	2.70	11.26	0.00240
Madrepora oculata	47957	-44.198000	-174.455000	1198.0	4.6	3B	A16_1	Arag 3	2.81	11.32	0.00229
Madrepora oculata	J185 TAN0307/79						A17_1	Arag 3	2.29	10.91	0.00222
Solenosmilia variabilis	26971	-41.295200	176.556198	731.0	7.6	1	A18_1	Arag 4	2.36	10.96	0.00224
Solenosmilia variabilis	3938	-42.795502	179.987167	1009.0	5.6	2	A19_1	Arag 4	3.00	10.74	0.00144
Solenosmilia variabilis	3939	-42.804001	179.987839	1013.0	5.6	2	A20_1	Arag 4	2.70	10.70	0.00187
Solenosmilia variabilis	25099	-42.717700	-179.904800	1025.0	5.6	2	A22_2	Arag 4	2.60	10.24	0.00161
Solenosmilia variabilis	47953	-50.051670	175.243300	960.0	3.4	4	A23_1	Arag 4	2.66	10.40	0.00141
Solenosmilia variabilis	47953	-50.051670	175.243300	960.0	3.4	4	A23 rep	Arag 5	2.77	10.81	0.00150
Solenosmilia variabilis	47921	-50.075000	174.761700	910.0	3.9	4	A24	Arag 5	2.30	11.08	0.00219
Solenosmilia variabilis	42506	-50.325000	163.420000	952.0	4.8	5	A26	Arag 5	2.80	11.10	0.00188
Solenosmilia variabilis	39839	-50.097167	163.474167	1070.0	3.9	5	A28	Arag 6	2.50	10.04	0.00193
Solenosmilia variabilis	39711	-50.090500	163.482167	1077.0	3.9	5	A29	Arag 6	2.50	10.05	0.00193
Solenosmilia variabilis	44150	-34.815000	169.853333	820.0	6.6	7	A31	Arag 6	2.48	10.18	0.00211
Solenosmilia variabilis	42546	-44.175000	-174.386700	894.0	4.3	3B	A34	Arag 6	2.60	9.91	0.00189
Solenosmilia variabilis	42501	-44.618333	-175.145000	1016.0	5.1	3B	A36	Arag 6	2.60	9.80	0.00162
Solenosmilia variabilis	42503	-44.171670	-174.466700	1113.0	5.1	3B	A37	Arag 6	2.60	10.23	0.00175
Solenosmilia variabilis	Z9794 TAN9901/67						A38_1	Mix 3	2.69	10.59	0.00158
Goniocorella dumosa	3934	-42.798170	179.981800	1000.0	5.59	2	A40_1	Arag 7	2.84	10.49	0.00157

Genera/Species	NIWA #	Latitude	Longitude	Depth	Temp	Region	An#	Run#	Mg/Ca	Sr/Ca	U/Ca
Goniocorella dumosa	47399	-43.560501	179.675995	386.0	8.5	2	A41_1	Arag 7	2.65	10.64	0.00192
Goniocorella dumosa	46485	-50.130000	174.868333	1000.0	3.1	4	A43_1	Arag 7	2.90	10.49	0.00170
Goniocorella dumosa	47973	-47.571670	177.908300	873.0	3.9	4	A44_1	Arag 7	2.65	10.72	0.00188
Goniocorella dumosa	41283	-50.942667	164.609167	1140.0	4.0	5	A45_1	Arag 7	2.40	10.65	0.00238
Goniocorella dumosa	47975	-50.250000	163.490000	1043.0	4.4	5	A46_1	Arag 9	2.76	10.93	0.00180
Goniocorella dumosa	28732	-38.207500	168.585000	512.0	9.6	6	A47_1	Arag 9	2.58	10.42	0.00219
Goniocorella dumosa	32485	-38.023830	168.447000	570.0	8.8	6	A48_1	Arag 9	3.00	10.06	0.00149
Goniocorella dumosa	54119	-44.149833	-174.768167	830.0	6.5	3B	A51_1	Arag 9	2.23	10.57	0.00224
Goniocorella dumosa	45327	-44.214833	-179.300500	414.0	7.8	3B	A53_1	Arag 9	2.90	10.21	0.00158
Enallopsammia rostrata	26935	-40.040298	178.144501	749	7.6	1	A54_1	Arag 10	2.70	10.76	0.00205
Enallopsammia rostrata	27571	-40.039799	178.142502	760	7.57	1	A56_1	Arag 10	2.27	10.77	0.00216
Enallopsammia rostrata	3933	-42.804001	179.987839	1013	5.59	2	A58_1	Arag 10	2.70	10.61	0.00183
Enallopsammia rostrata	42829	-50.043333	174.698333	857	4.1	4	A60_1	Arag 10	5.30	11.03	0.00223
Enallopsammia rostrata	65467	-35.606667	165.178333	931	5.78	6	A63_1	Arag 10	2.80	10.64	0.00166
Enallopsammia rostrata	65478	-35.430000	165.303333	935	5.78	6	A64_1	Arag 11	2.75	11.06	0.00218
Enallopsammia rostrata	42404	-44.751667	173.723333	940	4.02	3A	A68_1	Arag 11	1.99	11.34	0.00278
Enallopsammia rostrata	42405	-44.751667	173.723333	940	4.02	3A	A69_1	Arag 11	2.50	11.52	0.00281
Enallopsammia rostrata	42735	-44.490000	-174.751667	1267	4.36	3B	A70_1	Arag 11	2.57	11.40	0.00279
Oculina virgosa	63020	-41.671167	175.625000	640.0	8.63	1	A71_1	Arag 12	4.57	9.90	0.00151
Oculina virgosa	47393	-35.146700	174.351700	70.0	16.6	7	A72_1	Arag 12	7.60	9.94	0.00197
Oculina virgosa	57523	-34.978800	173.998000	85.0	16.6	7	A73_1	Arag 12	2.62	10.42	0.00197
Oculina virgosa	73123	-34.157167	172.100667	54.0	16.4	7	A75_1	Arag 12	3.27	10.06	0.00157
Oculina virgosa	15654	-37.213500	177.100000			8	A76_1	Arag 12	2.63	10.87	0.00222

Note: Mix3 data is in italics - not the best analytical run, errors will be higher on these values.

M12_1a-c indicates same sample digestion at three very different dilutions to test matrix loading affects. M12_1a and M12_1 were much more concentrated than the calibration standard, and Pulse/Analog detector calibration uncertainties may have affected particularly the Mg for these. M12b_1 was the best matched to the standard for Ca, and M12c_1 was best matched for the Mg. Hence, I would take M12b and M12c to give the more accurate Mg/Ca. Sr would not have been similarly affected.

Appendix 2: Skeletal carbonate mineralogy of deep-water primnoid corals from east of New Zealand

To Di Tracey, NIWA
From Abby Smith, University of Otago
26 April 2013

Six specimens of primnoid (Alcyonacea: Primnoidae) deep-water corals were provided by NIWA. They belonged to the species *Primnoa* sp. They are from localities in deep water around New Zealand. Table 1 shows the data provided along with the specimens.

Table 1. Locality data

NIWA Number	Area	Latitude (°S)	Longitude (°E)	Depth (m)
42613 PRI	3A	-44.5175	175.7833	600
42628 PRI	3A	-44.5100	185.1750	1300
42634 PRI	5	-49.9367	163.8117	780
42636 PRI	4	-49.8517	175.3217	781
62704 PRI	3A	-44.5175	175.7833	600
66128 PRI	4	-47.3733	178.0917	904

In order to carry out X-ray diffractometry (XRD), organic material must be removed, and we thus carried out some light bleaching of the specimens. There was consequent dissociation of the skeleton and we were able to identify three discrete components in the skeletons.

Larger pieces had a brown central "stem" which was very hard and difficult to pulverize. This material was surrounded by a shiny white layer that dissociated into a very fine powder. In thinner branches the entire "stem" was made of this shiny white material. The "bubbles" around the stem dissociated into brittle grey flakes, somewhat coarser and harder than the white powder. Having noted these skeletal elements, we decided to run our XRDs on each type of material, rather than on whole skeletal samples. In cases where there was enough material, we ran replicate scans.

Table 2 shows the twenty-one subsamples that were scanned. There is a wide range of mineral types in these specimens. Calcite content ranges from 0 to 100% (mean = 37.2, SD = 42.2, N = 21). Seven specimens were 100% aragonite, and six were 100% calcite. Wt% $MgCO_3$ in calcite also varies, with nine

samples containing moderate Mg-calcite, ranging from 5 to 7 wt% $MgCO_3$, and five samples containing high-Mg calcite in the range of 10-13 wt% $MgCO_3$. In all specimens with calcite, mean wt% $MgCO_3$ was 8.0 (SD = 2.6, N = 14).

Table 2. Mineralogy Data

Otago Sample number	NIWA No	Skeletal layer	Wt% Calcite	Wt% MgCO3 in calcite
PC-42613-1-bs	42613	brown	0	
PC-42613-1-gf	42613	grey	100	6.1
PC-42613-1-wf	42613	white	0	
PC-42628-1-bs	42628	brown	3	11.6
PC-42628-1-gf	42628	grey	100	6.3
PC-42628-1-wf	42628	white	0	
PC-42634-1-bs	42634	brown	3	13.4
PC-42634-2-bs	42634	brown	6	10.4
PC-42634-1-gf	42634	grey	100	5.7
PC-42634-1-wf	42634	white	0	
PC-42636-1-gf	42636	grey	100	6.5
PC-42636-2-gf	42636	grey	100	6.3
PC-42636-1-wf	42636	white	0	
PC-42636-2-wf	42636	white	0	
PC-62704-1-gf	62704	grey	100	6.5
PC-62704-1-wf	62704	white	0	
PC-66128-2-bs	66128	brown	38	11.1
PC-66128-1-bs	66128	brown	39	10.5
PC-66128-3-wf	66128	white	10	5.9
PC-66128-1-wf	66128	white	40	6.4
PC-66128-2-wf	66128	white	43	5.6
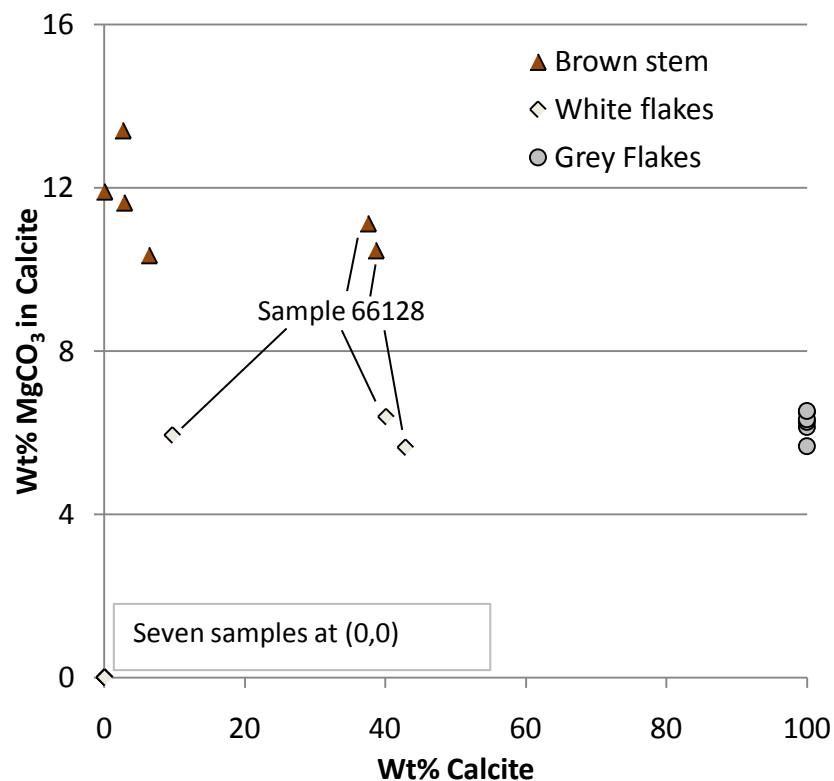
Figure 1. Skeletal carbonate mineralogy of some primnoid corals.

These data show two obvious trends: that the three skeletal components are mineralogically distinct in most of the samples, and that the sample labelled 66128 is different from the others (Figure 1).

In the five similar specimens, the brown stem material is dominantly aragonite (mean = 3% calcite, N =4) with small amounts of very high-Mg calcite (11.8 wt% $MgCO_3$, N = 4). Sample 66128, on the other hand, contains almost 40% high-Mg calcite in the mixture (N = 2).

The shiny white material that surrounds the stems is entirely aragonitic in most specimens (N = 7). In specimen 66128, however, it is very much like the adjacent stem material, containing 10 to 40% calcite, though the Mg content of the calcite is lower (about 6 wt% $MgCO_3$, N = 3). One possibility is that in that particular specimen we were unable to distinguish the layers and inadvertently mixed them. Another possibility is that it is a different taxon from the others.

Finally, the grey material that makes "bubbles" on the outside of the corals is different again – in all samples it was 100% calcite, with a consistent Mg content of about 6 wt% $MgCO_3$ (mean = 6.2, SD = 0.29, N = 6). There was none of this material present on sample 66128.

Most octocorals limit their mineralisation to spicules, but these primnoids are unusually capable mineralisers. To find distinct minerals in different parts of a skeleton is not abnormal in controlled mineralizing phyla like echinoderms and molluscs, but it is unusual in groups like corals, considered to be "passive" mineralisers, strongly influenced by sea water chemistry.

A brief trawl though the literature suggests that most people have characterised deep-water corals as being exclusively Mg-calcite. The specimens contained here have been shown to contain at least three distinct minerals, including pure aragonite. It would be instructive to carry out an ontogenetic series, sampling from older to younger parts of the same colony to look for within-colony variability. Another really interesting study would be to carry out detailed ultra-structural analysis of the crystalline structure of the three skeletal components. The most obvious take-home message from these data is that samples should be examined carefully before replicate analyses are carried out; a single measurement of a homogenized sample of one of these corals would be both misleading and uninformative.

These skeletons are clearly worthy of further investigation and we would be delighted to be part of any further study on these fascinating creatures. Thanks very much for letting us have a look at them.

Dr Abby Smith and Mr Marc Riedi
Department of Marine Science
University of Otago

Appendix 3: Table of opportunistic water sample data analysed for alkalinity and DIC since 2011.

TAN1113

CTD #	Date	Time	Latitude	Longitude	Depth	Salinity	Temp	At µmol/kg	Ct µmol/kg	pH Calc (in situ temp)	[CO₃²⁻] µmol/kg	Ωcalcite	Ωaragonite
U7407	29-Sep-11	2:54	-46.5902	178.4320	2539	34.730	1.9	2354.7	2255.0	7.854	80.5	1.155	0.750
U7407	29-Sep-11	2:54	-46.5902	178.4320	2023	34.679	2.3	2352.5					
U7407	29-Sep-11	2:54	-46.5902	178.4320	1515	34.570	2.6	2343.9	2256.1	7.851	76.3	1.346	0.863
U7407	29-Sep-11	2:54	-46.5902	178.4320	1418	34.545	2.8	2345.9	2255.3	7.861	78.0	1.403	0.899
U7407	29-Sep-11	2:54	-46.5902	178.4320	1318	34.516	3.0	2342.5					
U7407	29-Sep-11	2:54	-46.5902	178.4320	1213	34.476	3.2	2334.4	2242.1	7.869	79.2	1.486	0.950
U7407	29-Sep-11	2:54	-46.5902	178.4320	1113	34.434	3.4	2325.1	2233.4	7.869	78.8	1.511	0.964
U7407	29-Sep-11	2:54	-46.5902	178.4320	1007	34.381	3.6	2314.7	2217.9	7.888	81.4	1.594	1.016
U7408	29-Sep-11	11:02	-46.6348	178.5833	756	34.324	4.8	2294.1	2188.1	7.909	86.7	1.788	1.138
U7408	29-Sep-11	11:02	-46.6348	178.5833	506	34.318	6.5	2281.0	2152.7	7.955	99.6	2.162	1.375
U7408	29-Sep-11	11:02	-46.6348	178.5833	300	34.376	7.4	2280.2	2136.0	7.990	109.3	2.468	1.567
U7408	29-Sep-11	11:02	-46.6348	178.5833	202	34.384	7.7	2282.0	2130.7	8.007	113.7	2.618	1.661
U7408	29-Sep-11	11:02	-46.6348	178.5833	149	34.341	7.9	2280.4	2114.8	8.042	122.3	2.844	1.804
U7408	29-Sep-11	11:02	-46.6348	178.5833	99	34.336	8.1	2279.4	2108.8	8.054	125.4	2.944	1.867
U7408	29-Sep-11	11:02	-46.6348	178.5833	77	34.335	8.4	2280.7	2113.4	8.041	123.6	2.914	1.848
U7408	29-Sep-11	11:02	-46.6348	178.5833	49	34.335	8.4	2277.2	2110.4	8.042	123.4	2.925	1.854
U7408	29-Sep-11	11:02	-46.6348	178.5833	21	34.336	8.4	2281.0	2106.4	8.060	128.1	3.052	1.935
U7408	29-Sep-11	11:02	-46.6348	178.5833	9	34.336	8.4	2277.1	2106.6	8.051	125.6	3.000	1.902
U7419	1-Oct-11	0:12	-43.4045	178.4948	352	34.427	7.8	2279.2	2137.7	7.975	107.8	2.412	1.534
U7419	1-Oct-11	0:12	-43.4045	178.4948	153	34.575	9.5	2281.9	2104.7	8.041	129.8	3.013	1.917
U7419	1-Oct-11	0:12	-43.4045	178.4948	11	34.651	10.3	2277.6	2065.9	8.110	151.3	3.604	2.292
U7423	1-Oct-11	21:49	-41.2263	178.5018	1415	34.475	4.0	2328.3	2228.4	7.873	82.8	1.498	0.961
U7423	1-Oct-11	21:49	-41.2263	178.5018	1311	34.417	4.4	2312.7	2214.0	7.869	82.2	1.520	0.973
U7423	1-Oct-11	21:49	-41.2263	178.5018	1210	34.392	4.9	2303.1	2196.6	7.889	86.4	1.633	1.045
U7423	1-Oct-11	21:49	-41.2263	178.5018	1110	34.387	5.5	2294.5	2185.3	7.891	88.1	1.699	1.087
U7423	1-Oct-11	21:49	-41.2263	178.5018	1011	34.384	6.0	2289.0	2167.6	7.923	94.9	1.867	1.194
U7423	1-Oct-11	21:49	-41.2263	178.5018	910	34.396	6.6	2286.0	2156.7	7.940	99.5	2.000	1.278

TAN1116

CTD #	Date	Time	Latitude	Longitude	Depth	Salinity	Temp	At µmol/kg	Ct µmol/kg	pH Calc (in situ temp)	[CO$_3^{2-}$] µmol/kg	Ωcalcite	Ωaragonite
U7454	11-Nov-11	3:30	-44.2125	178.8918	1008	34.317	10.4	2294.502	2190.1	7.81	87.84	1.75	1.13
U7454	11-Nov-11	3:30	-44.2125	178.8918	762	34.316	11.8	2289.886	2166.6	7.85	98.90	2.07	1.33
U7454	11-Nov-11	3:30	-44.2125	178.8918	307	34.457	8.6	2283.763	2117.4	8.02	122.76	2.77	1.76
U7454	11-Nov-11	3:30	-44.2125	178.8918	152	34.514	9.8	2286.975	2110.7	8.03	129.53	3.01	1.91
U7454	11-Nov-11	3:30	-44.2125	178.8918	6	34.585	11.6	2277.942	2033.2	8.16	172.49	4.11	2.62
U7455	13-Nov-11	10:12	-43.8292	178.5358	469	34.388	13.5	2285.068	2137.4	7.90	113.77	2.51	1.61
U7455	13-Nov-11	10:12	-43.8292	178.5358	301	34.463	13.8	2284.767	2117.7	7.95	125.45	2.85	1.83
U7455	13-Nov-11	10:12	-43.8292	178.5358	148	34.461	5.8	2281.555	2115.8	8.07	121.42	2.82	1.79
U7455	13-Nov-11	10:12	-43.8292	178.5358	40	34.553	7.3	2285.169	2113.4	8.07	125.88	2.99	1.89
U7455	13-Nov-11	10:12	-43.8292	178.5358	5	34.605	10.7	2274.53	2016.6	8.20	180.23	4.30	2.74
U7456	14-Nov-11	14:20	-42.8523	177.9365	494	34.553	12.7	2284.667	2138.8	7.90	112.26	2.46	1.58
U7456	14-Nov-11	14:20	-42.8523	177.9365	310	34.683	14.4	2288.179	2127.6	7.92	121.88	2.76	1.78
U7456	14-Nov-11	14:20	-42.8523	177.9365	149	34.862	7.6	2291.291	2127.3	8.04	121.22	2.81	1.78
U7456	14-Nov-11	14:20	-42.8523	177.9365	31	34.968	8.4	2303.435	2097.5	8.12	147.28	3.49	2.21
U7456	14-Nov-11	14:20	-42.8523	177.9365	5	34.997	9.0	2301.528	2053.8	8.20	173.46	4.13	2.62
U7457	16-Nov-11	6:36	-42.7158	178.0700	1001	34.427	12.4	2299.219	2181.8	7.81	95.72	1.92	1.24
U7457	16-Nov-11	6:36	-42.7158	178.0700	757	34.467	12.6	2286.674	2149.9	7.87	106.64	2.23	1.44
U7457	16-Nov-11	6:36	-42.7158	178.0700	300	34.825	11.7	2293.198	2127.7	7.97	123.69	2.79	1.79
U7457	16-Nov-11	6:36	-42.7158	178.0700	153	35.041	11.8	2306.947	2091.3	8.08	154.59	3.58	2.29
U7457	16-Nov-11	6:36	-42.7158	178.0700	5	35.105	11.8	2310.861	2053.8	8.17	180.92	4.30	2.75
U7458	18-Nov-11	9:34	-43.4162	178.9595	386	34.410	11.8	2283.262	2133.4	7.93	114.38	2.55	1.63
U7458	18-Nov-11	9:34	-43.4162	178.9595	283	34.515	1.5	2288.681	2139.2	8.10	109.98	2.49	1.57
U7458	18-Nov-11	9:34	-43.4162	178.9595	151	34.520	1.9	2282.158	2110.4	8.15	123.22	2.86	1.80
U7458	18-Nov-11	9:34	-43.4162	178.9595	41	34.676	2.5	2300.123					
U7458	18-Nov-11	9:34	-43.4162	178.9595	6	34.682	3.7	2289.384	2036.7	8.30	173.90	4.16	2.62

TAN1205

CTD #	Date	Time	Latitude	Longitude	Depth	Salinity	Temp	At µmol/kg	Ct µmol/kg	pH Calc (in situ temp)	[CO$_3^{2-}$] µmol/kg	Ωcalcite	Ωaragonite
U7610	26-Mar-12	7:44	-37.6505	176.8008	199.6	35.077	12.4	2305.1	2138.7	7.96	124.94	2.87	1.84
U7610	26-Mar-12	7:44	-37.6505	176.8008	102.0	35.301	14.6	2313.4	2116.7	8.00	144.39	3.37	2.17
U7610	26-Mar-12	7:44	-37.6505	176.8008	10.4	35.447	19.5	2322.6	2045.0	8.08	197.50	4.70	3.05
U7617	27-Mar-12	0:39	-36.2335	177.7365	2228.4	34.64	2.3	2393.0	2304.8	7.83	76.35	1.17	0.75
U7617	27-Mar-12	0:39	-36.2335	177.7365	1010.8	34.433	5.5	2304.8	2192.8	7.90	89.98	1.77	1.13
U7617	27-Mar-12	0:39	-36.2335	177.7365	502.7	34.663	9.1	2283.6	2146.8	7.93	105.43	2.29	1.46
U7617	27-Mar-12	0:39	-36.2335	177.7365	202.5	35.203	13.5	2313.3	2138.6	7.96	130.53	3.00	1.92
U7617	27-Mar-12	0:39	-36.2335	177.7365	101.1	35.38	16.8	2322.8	2077.6	8.06	175.65	4.11	2.65
U7617	27-Mar-12	0:39	-36.2335	177.7365	51.2	35.506	19.9	2324.4	2045.8	8.07	198.21	4.68	3.05
U7617	27-Mar-12	0:39	-36.2335	177.7365	10.1	35.506	19.9	2329.0	2044.7	8.08	202.06	4.81	3.13
U7623	27-Mar-12	22:23	-34.4015	178.8340	2750.5	34.645	2.2	2389.5	2298.7	7.81	76.66	1.06	0.69
U7623	27-Mar-12	22:23	-34.4015	178.8340	2027.4	34.619	2.4	2380.8	2286.9	7.85	79.28	1.26	0.81
U7623	27-Mar-12	22:23	-34.4015	178.8340	1009.7	34.375	5.7	2288.7	2180.5	7.89	87.67	1.72	1.10
U7623	27-Mar-12	22:23	-34.4015	178.8340	758.3	34.47	7.4	2287.2	2152.1	7.95	103.43	2.14	1.37
U7623	27-Mar-12	22:23	-34.4015	178.8340	506.8	34.647	9.1	2288.8	2140.3	7.96	112.19	2.44	1.56
U7623	27-Mar-12	22:23	-34.4015	178.8340	305.6	35.111	12.8	2301.2	2120.9	7.98	133.05	3.00	1.93
U7623	27-Mar-12	22:23	-34.4015	178.8340	203.7	35.366	15.0	2314.5	2114.2	7.99	146.54	3.37	2.17
U7623	27-Mar-12	22:23	-34.4015	178.8340	101.2	35.48	17.2	2320.3	2071.2	8.06	178.11	4.17	2.69
U7623	27-Mar-12	22:23	-34.4015	178.8340	49.3	35.626	20.8	2327.0	2043.6	8.07	201.57	4.77	3.11
U7623	27-Mar-12	22:23	-34.4015	178.8340	8.4	35.656	21.1	2321.3	2048.5	8.04	194.77	4.63	3.02
U7667	6-Apr-12	5:06	-34.3285	173.1282	183.3	35.308	15.2	2302.6	2098.1	8.00	148.87	3.43	2.21
U7667	6-Apr-12	5:06	-34.3285	173.1282	106.5	35.537	19.6	2317.5	2050.4	8.05	190.34	4.46	2.90
U7667	6-Apr-12	5:06	-34.3285	173.1282	14.5	35.631	20.6	2320.5	2037.8	8.07	200.91	4.77	3.11
U7673	7-Apr-12	0:17	-33.2663	173.8435	2182.2	34.657	2.1	2395.1	2298.1	7.86	80.76	1.24	0.80
U7673	7-Apr-12	0:17	-33.2663	173.8435	1013.9	34.38	5.6	2290.6	2173.7	7.92	92.31	1.81	1.16

CTD #	Date	Time	Latitude	Longitude	Depth	Salinity	Temp	At µmol/kg	Ct µmol/kg	pH Calc (in situ temp)	[CO$_3^{2-}$] µmol/kg	Ωcalcite	Ωaragonite
U7673	7-Apr-12	0:17	-33.2663	173.8435	511.3	34.871	10.8	2295.2	2138.1	7.95	118.01	2.56	1.64
U7673	7-Apr-12	0:17	-33.2663	173.8435	204.5	35.497	16.7	2321.5	2083.9	8.04	170.46	3.92	2.53
U7673	7-Apr-12	0:17	-33.2663	173.8435	105.4	35.585	18.4	2325.7	2063.4	8.06	187.03	4.37	2.84
U7673	7-Apr-12	0:17	-33.2663	173.8435	56.6	35.65	20.7	2328.8	2036.4	8.08	207.34	4.90	3.19
U7673	7-Apr-12	0:17	-33.2663	173.8435	11.8	35.707	21.7	2331.7	2031.3	8.08	212.99	5.07	3.31
U7679	8-Apr-12	5:32	-31.0970	175.0445	3553.9	34.683	1.9	2408.8	2303.4	7.83	82.85	0.97	0.64
U7679	8-Apr-12	5:32	-31.0970	175.0445	2024.5	34.634	2.3	2383.5	2293.6	7.84	77.31	1.23	0.79
U7679	8-Apr-12	5:32	-31.0970	175.0445	1009.9	34.393	5.6	2299.4	2178.3	7.93	94.79	1.86	1.19
U7679	8-Apr-12	5:32	-31.0970	175.0445	755.2	34.442	7.1	2285.4	2151.0	7.95	102.88	2.13	1.36
U7679	8-Apr-12	5:32	-31.0970	175.0445	501.8	34.792	10.3	2296.8	2135.2	7.97	120.49	2.62	1.68
U7679	8-Apr-12	5:32	-31.0970	175.0445	303.5	35.305	14.8	2312.5	2105.1	8.01	150.56	3.40	2.19
U7679	8-Apr-12	5:32	-31.0970	175.0445	201.6	35.471	16.5	2308.7	2088.3	8.01	159.30	3.66	2.37
U7679	8-Apr-12	5:32	-31.0970	175.0445	100.9	35.594	18.8	2325.2	2059.5	8.06	189.32	4.43	2.88
U7679	8-Apr-12	5:32	-31.0970	175.0445	49.7	35.606	22.6	2329.0	2017.0	8.09	220.72	5.23	3.43
U7679	8-Apr-12	5:32	-31.0970	175.0445	9.7	35.605	22.6	2330.2	2017.3	8.09	221.42	5.28	3.46

TAN1206

CTD #	Date	Time	Latitude	Longitude	Depth	Salinity	Temp	At µmol/kg	Ct µmol/kg	pH Calc (in situ temp)	[CO$_3^{2-}$] µmol/kg	Ωcalcite	Ωaragonite
U7702	24-Apr-12	10:23	-36.4520	177.8393	877	34.480	6.3	2297.7	2178.9	7.91	94.04	1.90	1.21
U7702	24-Apr-12	10:23	-36.4520	177.8393	507	34.743	9.5	2293.3	2146.4	7.95	111.55	2.42	1.55
U7702	24-Apr-12	10:23	-36.4520	177.8393	252	35.141	12.9	2310.9	2118.7	8.01	140.59	3.20	2.05
U7702	24-Apr-12	10:23	-36.4520	177.8393	102	35.359	16.4	2318.9	2090.2	8.03	165.04	3.86	2.49
U7702	24-Apr-12	10:23	-36.4520	177.8393	49	35.577	19.4	2331.3	2046.8	8.09	201.92	4.77	3.10
U7702	24-Apr-12	10:23	-36.4520	177.8393	9	35.606	19.6	2337.4	2043.2	8.10	208.51	4.96	3.22

At - Alkalinity

Ct - DIC

Where pH, $[CO_3^{2-}]$, OmegaC (ΩCalcite) and OmegaA (ΩAragonite) are calculated from the Alkalinity and dissolved inorganic carbon (DIC).

$[CO_3^{2-}]$ - carbonate ion concentration

ΩCalcite - calcite saturation, where this =1 is the CSH

ΩAragonite - aragonite saturation, where this =1 is the ASH